NTNU
Det skapende universitet

The structural and metamorphic evolution of the Averøya eclogite, WGR Norway

Silje Auglænd

Geologi
Innlevert: juni 2017
Hovedveileder: Suzanne McEnroe, IGP

Norges teknisk-naturvitenskapelige universitet
Institutt for geovitenskap og petroleum

Abstract

The Averøya layered eclogite body is located around 35 kilometers northeast of the Svartberget microdiamond locality, presently marking the eastern extent of the Nordøyane Ultra High-Pressure (UHP) domain on the west coast of Norway. This body appears to be a part of the distal Baltican plate that was subducted to eclogite facies conditions at 415 Ma, followed by exhumation and extensive amphibolite facies reworking at 395 Ma.

Previous studies of this large body have included U-Pb zircon geochronology, igneous geochemistry, and a limited study of mineral compositions and metamorphic petrology. The focus of this thesis has been to assign the eclogite and its surroundings to the regional tectonostratigraphy, provide details of the structural setting and a broader understanding of the petrography of the eclogite and surrounding gneisses.

Field studies uncovered five layered eclogite bodies, where the largest body is the Averøya layered eclogite with a maximum thickness of 1.5 km, extending out approximately 3km in a WNW-ESE direction. Four main rock types were characterized and were assigned to either the Baltic basement unit or to the Blåhø Nappe of the Middle allochthon. The Baltic basement consists of a tonalitic to granodioritic migmatite gneiss with local metamorphosed mafic dykes, pegmatites and rare eclogite boudins.

The structurally overlying Blåhø nappe consists of a garnet amphibolite and a garnet and amphibole quartzo-feldspathic gneiss. Both of these rock types wrap around small-scale variously retrogressed and granoblastic eclogite boudins and larger-scale layered eclogite bodies. Detailed mapping coupled with the aid of a gridded magnetic anomaly map, were used to infer and interpolate boundaries between these rock types.

Structural measurements showed predominantly regional parallel NW dipping foliations, ENE-WSW oriented upright- and foliation parallel folds and a pervasive sinistral or top to the W-SW sense of shear. This is consistent with amphibolite stage reworking. Eclogite stage NW-N plunging lineations, NNW plunging folds and NNW oriented fabrics are locally preserved in the layered eclogite bodies and the garnet and amphibole gneiss.

Mineral chemistry and petrography were used to characterize the different metamorphic stages of the study area. Peak metamorphic P-T conditions was estimated to 3GPa + 800°C, applying the phengite geothermobarometers, indicating peak UHP eclogite conditions. Finally the metamorphic evolution and structural data were used to propose a tectonic model.

Sammendrag

En lagdelt eklogitt kropp på Averøya ligger rundt 35 kilometer nordøst fra en mikrodiamant lokalitet på Svartberget, som markerer den østlige enden av Nordøyane Ultra Høyt-Trykk (UHT) domene på vestkysten av Norge. Denne kroppen synes å være en del av den distale baltiske platen som ble subdusert til eklogitt fascies forhold for 415 MA, etterfulgt av ekshumasjon og omfattende amfibolitt fascies omarbeiding for 395 Ma.

Tidligere studier av denne store kroppen har omfattet U-Pb zirkon geokronologi, magmatisk geokjemi, og en begrenset studie av mineralsammensetninger og metamorf petrologi. Fokuset til denne avhandlingen har vært å tildele eklogitten og omliggende bergarter til den regionale tektonostratigrafien, gi informasjon om den strukturelle settingen og en bredere forståelse av petrografien til eklogitter og omliggende gneiser.

Feltstudier avdekket fem lagdelte eklogitt kropper, hvor den største kroppen er den lagdelte eklogitten på Averøya med en maksimal tykkelse på 1,5 km og en utstrekning på ca. 3 km i en VNV-ØSØ retning. Fire hovedbergarter ble karakterisert og angitt som en del av det Baltiske grunnfjellet eller Blåhø Dekket av Midtre allokton, basert på feltobservasjoner og tynnslip petrografi. Det Baltiske grunnfjellet består av tonalittisk til granodiorittisk migmatitt gneis med lokale metamorfoserte mafiske ganger, pegmatitter og sjeldne eclogite boudiner.

Den strukturelt overliggende Blåhø nappe består av en granat-amfibolitt og en granat- og amfibol-kvartsfeltspatisk gneis. Begge disse bergartstypene pakker inn småskala, varierende retrograderte og granoblastiske eklogitt boudiner og større lagdelte eklogitt kropper. Detaljert kartlegging kombinert med bruk av et magnetisk anomalikart, ble brukt til å utlede og interpolere grenser mellom disse bergartene.

Strukturelle målinger viste overveiende regionalt parallelle NV- dyppende foliasjoner, ØNØ orienterte stående- og foliasjonsparallelle folder og en gjennomgående sinistral eller topp til V-SV-skjærsans. Dette samsvarer med amfibolitt fascies omarbeiding. Eklogitt stadiet NV-N stupende lineasjoner, NNV-hellende folder og NNW-orienterte strukturer, er bevart lokalt i de lagdelte eklogitt kroppene og garnet- og amfibol gneiss.

Mineral kjemi og petrografi ble brukt til å karakterisere de forskjellige metamorfe stadiene i studieområdet. Maksimum metamorfe P-T-forhold ble estimert til 3GPa og 800°C, ved bruk av fengitt-geotermobarometeret, som indikerer topp UHT forhold. Til slutt ble den metamorfe utviklingen og strukturdata brukt for å foreslå en tektonisk modell.

Acknowledgements

This thesis was sponsored by the Department of Geology and Mineral Resources Geology at the Norwegian Technical and Science University and was a part of my Master in Geology specializing in Bedrock and Resource Geology.

First I would like to extend a big thanks to my supervisor Suzanne McEnroe for providing me with such an exciting and challenging topic. I am also very grateful that you gave me the opportunity to shape my thesis the way I wanted and for always keeping me on track. To work with you and Peter have been extremely gratifying for me and I am really happy that you both .joined me in the field and helped me tie up some loose ends. I would also like to thank Peter Robinson for all the time and effort he has enthusiastically put into helping me with my thesis. Your knowledge and extensive expertise have really improved and shaped my understanding of the study area and I am thankful for all the constructive criticism you have provided. I would also like to thank Peter and his colleagues Jared Butler and Mike Terry for the help with P-T estimates for the Averøya layered eclogite.

To Geertje, Zeudia, Nathan, Christine and Alex I would like to thank you all for helping me while I was working with the magnetic properties and modelling project. Thank you for always being available to help me when I needed it. I also really appreciate all the help provided by Alex, who assisted me in the field with conducting the ground magnetic survey and afterwards when he and Zeudia taught me how to use ArcGIS and Modelvision. To my other two field assistants Synnøve and Sissel (mom), thank you for keeping me company in the field. The field days were exceedingly more enjoyable and effective having you working alongside with me.

I am thankful for all help with various problems regarding petrography and geochemistry by Bjørn, Anette, Mai Britt, Morten, Hedda and Bergljot. To all other classmates these last couple of years, I am so happy to have worked alongside you and will miss all the great times we have had. Finally I would like to thank my family and friends for always supporting me and being there for me, especially this last year.

Table of Contents

List of figures

List of tables

Abbreviations

Geological terms:

BASZ – Bergen Arc System Zone

EMPA – Electron Probe Micro Analyzer

HP – High Pressure

MTFZ - Møre-Trøndelag Fault Zone

NSD – Nordfjord-Sogn detachment

NTNU – Norwegian Technical and Science University

PP – Plane polarized

UHP – Ultra high Pressure

UHT – ultra høyt trykk

WGC – Western Gneiss Complex

WGR – Western Gneiss Region

XP – Cross polarized

Magnetization:

H – applied field

Mex – exterior field

Min – internal field

Mi – induced magnetization

Mtot – total magnetization

Mr – remanent magnetization

X - susceptibility

Minerals:

Ae - Aegirine

Al – Albite

Alm - Almandine

Am – Amphibole

An - Anorthite

Bt – Biotite

Cal - Calcite

Cpx – Clinopyroxene

Crn - Corundum

Ep - Epidote

Fsp – feldspar

Grs - Grossular

Grt – Garnet

Hem – Hematite

Ilm – Ilmenite

Jd - Jadeite

K-fsp – K-feldspar

Ky - Kyanite

Omp - Omphacite

Or – Orthoclase

Mag – Magnetite

Phn - Phengite

Pl – Plagioclase

Quad – Ca, Mg, Fe Px

Qz – Quartz

Prp – Pyrope

Px - Pyroxene

Rt – Rutile

Scp – Scapolite

Spl - spinel

Ti – Titanite

Zr - Zircon

Chapter 1 - Introduction

1.1. Previous studies

After (Eskola, 1920) provided the first detailed descriptions of eclogites and garnet peridotites, the western gneiss region (WGR) have become the object of numerous studies. Covering an area of >40.000km^2 (Røhr, Bingen, Robinson, & Reddy, 2013) on the west coast of Norway from Bergen to Trondheim, it is known to expose some of the best outcrops worldwide of high-pressure (HP) and ultra-high-pressure (UHP) rocks.

The present day understanding of the WGR and the corresponding deformational history, stems from piecing together a range of structural-, petrological-, geothermobaromethric-, geochronological and geophysical studies from localities dispersed throughout the area. The geometrical relationship between basement rocks and overlying nappes, is generally well established, from amongst others (Gee, 1980; Krill, 1980; T. E. Krogh, Kamo, Robinson, Terry, & Kwok, 2011; Lutro, Robinson, & Solli, 1997; P. Robinson, 1995).

The evolution of the deformational history have been postulated by establishing overprinting relationships between structural features and placing small-scale to larger-scale structural features into a regional context (Hacker et al., 2010; Terry & Robinson, 2003, 2004). Some aspects of the deformational history remains problematic, especially the understanding of the late stage extensional exhumation processes. The following topics are still up for debate: 1. Driving forces of the exhumation, 2. Exhumation as a solely post-orogenic process, 3. Rapid vs slow exhumation and 4. Exhumation as a single crustal unity or as several slabs separated by faults (P. Robinson, Roberts, Gee, & Solli, 2014).

An increase of metamorphic grade from the SE to the NW is well documented, (Hacker et al., 2010; Røhr et al., 2013; Terry & Robinson, 2003) through geothermometry yielding a general gradient of increasing temperature towards the NW. There are however numerous local irregularities to this trend. As there are few dependable geobarometers in the area, the distribution of peak metamorphic pressure is poorly constrained (Cuthbert, Carswell, Krogh-Ravna, & Wain, 2000). Eclogites are generally absent in the SE, making their first appearance just NW of the Jostedalen mountains (Cuthbert et al., 2000), thereafter occurring regularly towards the NW, culminating in three UHP domains on Nordfjord, Sørøyane and Nordøyane.

Chapter 1 - Introduction

The discovery of coesite at various localities in the Nordfjord domain (D. Smith, 1988; D. C. Smith, 1984) demonstrated UHP metamorphic conditions and further increased interest in the area. Later additions to this record were discoveries of coesite in the Sørøyane domain (D. A. Carswell & Cuthbert, 2003; Root et al., 2005) and on Harøy in the Nordøyane domain (Butler, JAMIESON, STEENKAMP, & ROBINSON, 2012). Microdiamonds and polycrystalline quartz (PCQ), interpreted to be relict coesite, are additional feature characterizing UHP conditions. The former have been registered in a peridotite on Fjørtoft(Scambelluri, Van Roermund, & Pettke, 2010) and in a metasomatic garnet peridotite at Svartberget (Vrijmoed, Van Roermund, & Davies, 2006). These UHP domains (Røhr et al., 2013; Terry & Robinson, 2004)

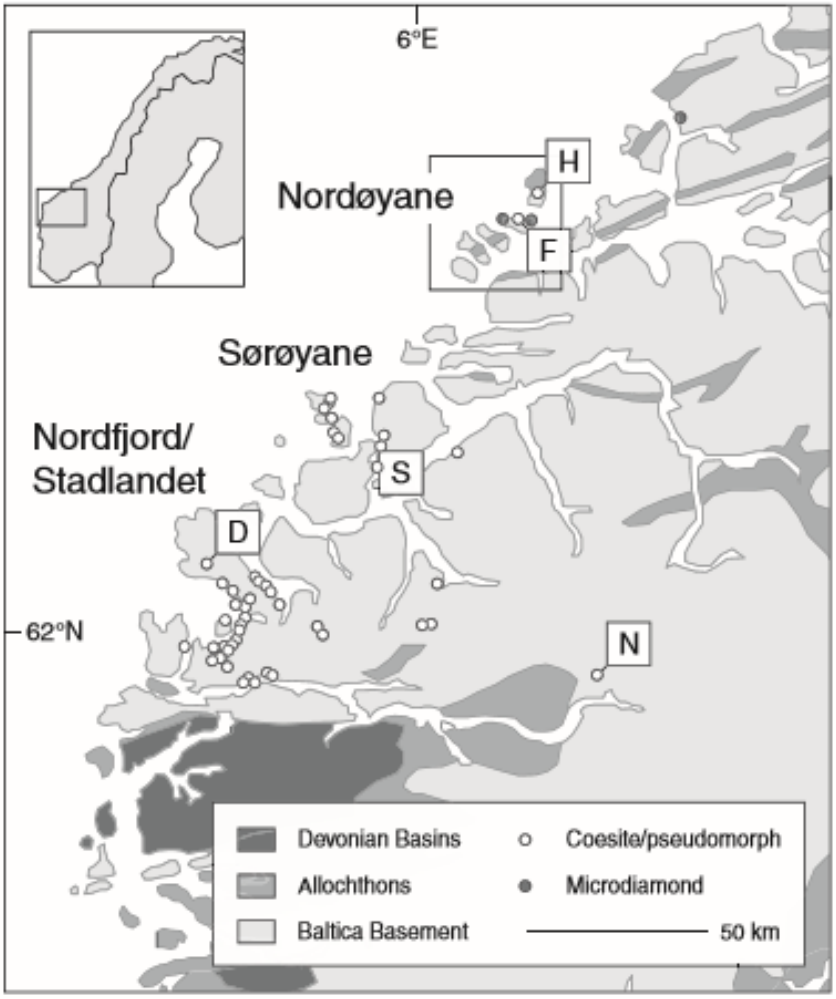

Figure 1.1.1: Nordfjord, Sørøyane and Nordøyane are UHP terranes exposed on the west coast of Norway, reflecting increasing P-T conditions towards the NW. The southwestern tip of Averøya is shown in the upper right corner (Butler et al., 2012).

record peak metamorphic conditions of 3.6GPa and 800°C (Hacker et al., 2010) citing *(Lappin, 1978)*. The furthermost eastern extent of the Nordøyane domain has yet to be established.

1.2. Aim of study

Situated around 35 km NE from documented UHP assemblages in the Nordøyane domain, are two larger bodies and an unknown number of smaller bodies of layered eclogite on the SW coast of Averøya and near the Visnes marble quarry on the mainland. Samples from Averøya shows a homogenously layered and completely eclogitized texture, where whole rock analyses implies a basaltic protolith (Hollocher, Robinson, Terry, & Walsh, 2007; T. E. Krogh et al., 2011). Interstitial quartz-rich zones interlayered within these eclogite bodies, can be interpreted as sedimentary beds formed within a sequence of layered volcanics. U-Pb dating of zircons at the ferry wharf on Tøvika, yields a robust age of 415 Ma for the peak eclogite metamorphism and 395 Ma for a pegmatite that crystallized under amphibolite facies conditions in a late fracture in the eclogite (T. E. Krogh et al., 2011) .

Basing itself on previous studies and maps (Lutro et al., 1997) of the area, this study aims to improve the mapping of rock units and structural features seeking to increase the understanding of the tectonic history in the study area. Because the position of the Averøya eclogite within the tectonostratigraphic order has been inconclusive, mapping of the relationship between the layered eclogite and surrounding rocks on Averøya was emphasized. Lenticular eclogite boudins residing within these domains were thoroughly described and sampled to be compared with the layered eclogites.

Sampling to investigate petrography, geochemistry and the magnetic properties was supplemented to reinforce the accuracy of the inferred field boundaries for the geological map. The magnetic properties were applied to model an E-W trending transect along the main road on the south coast. Textural variations within thin sections record both the prograde and retrograde history of eclogites and a metamorphic evolutionary model will be added. Petrography and electron probe analysis were also applied to search for index minerals like phengite, kyanite and coesite that could be used as geothermobarometers. By compiling and correlating all the information, a complete evolutionary model for the tectonostratigraphic setting and history of the Averøya eclogite should be proposed.

Chapter 2 - Regional Geology

2.1. The Scandian orogeny

The WGR complex and its multiphase deformational history relates to several pre-Scandian orogeny deformational stages and to various stages of the Late Silurian to Early Devonian Scandian Orogeny. The pre-Scandian stages are poorly understood and are typically strongly overprinted by Scandian deformational fabrics (AL Wain, Waters, & Austrheim, 2001). A short summary of the main sequence of events, their corresponding time frame and relation to eclogite formation will be provided in the following section.

One of the few places to study the precursor stages of the Scandian orogeny is at Flatraket and Kråkeneset (Corfu, Gasser, & Chew, 2014). The crystallization of the basement rocks in the area have been dated to 1700-1600 Ma, with two separate stages for intrusion of mafic dykes ranging from 1470 – 1450 Ma and 1260 – 1250Ma (Austrheim, Corfu, Bryhni, & Andersen, 2003; Corfu et al., 2014). These rocks subsequently underwent granulite facies metamorphism during the Sveconorwegian orogeny in 1000-950 Ma. It is estimated that less than 1% of the exposures of these Precambrian granulites escaped the following Scandian overprint (Peterman, Hacker, & Baxter, 2009).

Paleomagnetic dating estimates that the closure of Iapetus Ocean and the initiation of convergence between Baltica and Laurentia, commenced around 430 Ma. (Hacker et al., 2010; Tucker et al., 2004). SE-shortening at rates of 8-10 cm/yr (Terry & Robinson, 2004), resulted in the thrusting of a series of nappe units on top of Baltic basement from 425Ma. (see fig 2.1.1A,B). Coeval subduction of Baltic in a westward direction ensued, reflected by increasing metamorphic grade towards the NW (Cuthbert et al., 2000; Kylander-Clark, Hacker, & Mattinson, 2008).

The following two deformational phases are only preserved sporadically and lack a fixed time reference. Localities in Trollheimen (Krill, 1980) and Surnadal (TUCKER, 1986) record evidence from the first event, a SE directed shear causing the nappe units to be tightly folded into SE oriented recumbent folds(Terry & Robinson, 2003). The second event involves formation of detachments in the hinterland ((Terry & Robinson, 2003) citing (Lutro et al., 1997) and evidence of thinning of individual nappe units.

Towards the final stages of nappe emplacement at around 415 ma, the subducting Baltic slab started reaching UHP conditions. With a maximum duration of 14-20 Ma, eclogite metamorphic

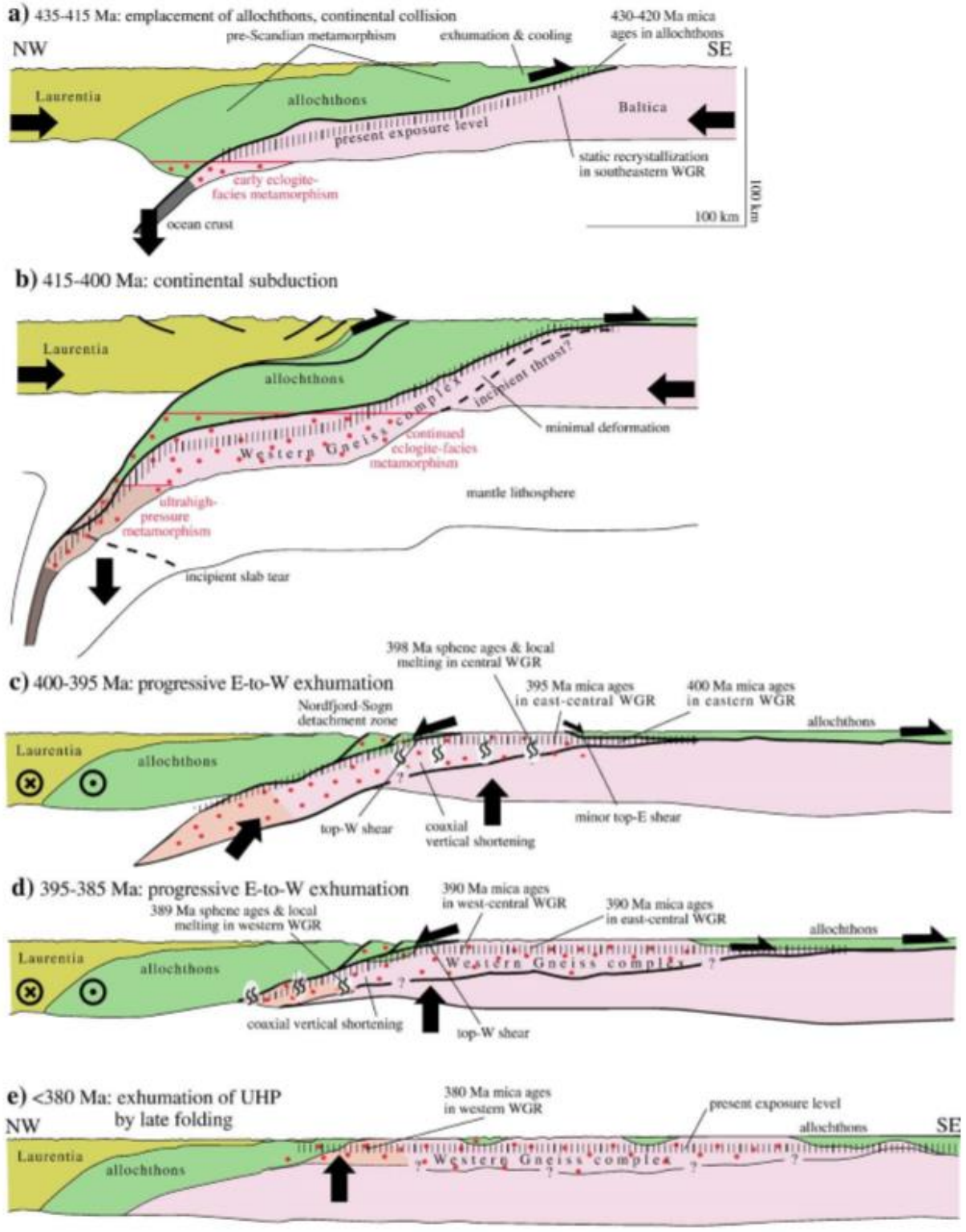

Figure 2.1.1: Stages of the formation and deformational setting for the Scandian Orogeny. (Hacker et al., 2010)

conditions in the WGR are regarded as a short-lived event (T. E. Krogh et al., 2011). The main phase of eclogite metamorphism lasted from 415-410MA from Sørøyane to Nordøyane, whereas eclogite ages in the Nordfjord domain records ages of 400Ma (T. E. Krogh et al., 2011). Based on the age overlap of the deposition of sediments in extensional basins and eclogite metamorphism, many studies argue that syncollisional extension was an important mechanism for exhumation (Labrousse et al., 2004; Terry & Robinson, 2003).

Eventually inverting from an oblique contractional regime into a transtensional regime (fig 2.1.1 C) at around 408 – 402 Ma according to (Fossen, 2000), large scale reactivation of earlier detachments and the basal decollement zone produced a pervasive NE-SW stretch. NW oriented extensional faults and shear zones developed, accommodating the early exhumation of HP and UHP rocks (fig 2.1.1D) up to the lower crust where these were complexly juxtaposed against amphibolite facies rocks obliterating previous metamorphic relationships (P. Robinson, 1995; Røhr et al., 2013) (Labrousse et al., 2004). Late stage exhumation is associated with the formation of orogeny parallel folds and a pervasive top to the W sense of shear (fig 2.1.1 E.

2.2. Fabric development

Except for remnants of a pre-Scandian amphibolite to granulite facies fabrics in the some areas in the southeast, the fabrics in the WGR reflect mainly the early eclogite facies stage of continental subduction or the late amphibolite facies stage of extensional exhumation. The early eclogite facies fabrics formed at depths below 60-70km, related to the subduction and early exhumation phase. A relative motion vector of around 320° to the present day is indicated by many studies (Labrousse et al., 2004). This fabric was induced by a coaxial stretch in a constrictional strain field indicated by the presence of L>S and L>>S tectonites. Lineations are oriented transversely to the orogeny in a N-S to NNE-WSW direction and are solely preserved in isolated eclogite boudins and a few larger bodies. Typical structures from this phase include tubular to mylonitic folds and quartz-rich extensional veins (Andersen, Osmundsen, & Jolivet, 1994; Terry & Robinson, 2004).

A transition into the amphibolite facies regime is set to have occurred depths of 65-45km and around 400 – 390 Ma (Terry & Robinson, 2003). At the onset the early fabric of this phase is characterized by gently plunging ENE –WSW to ESE – WNW lineations and symmetrical

structures like isoclinal folds in the foliation indicating a coaxial and constrictional strain field(Andersen et al., 1994; Hacker et al., 2010). With continued exhumation a steadily more pervasive W-SW sense of shear were imprinted on earlier fabrics, becoming more pervasive towards the NSDZ in the west(Terry & Robinson, 2003).

2.3. Regional Tectonostratigraphy

Classified as a typical Himalayan type Orogeny (Fossen, 2000), a simplified geometrical tripartite division can be inferred for the area. The (para-) autochthonous basement lithologies making up the Western Gneiss Complex (WGC) are of Baltic origins and formed 1750 – 900Ma. Marked with a light brownish color on fig 2.3.1, this tectonic window is constrained geometrically by various extensional and compressional shear zones like the Nordfjord-Sogn

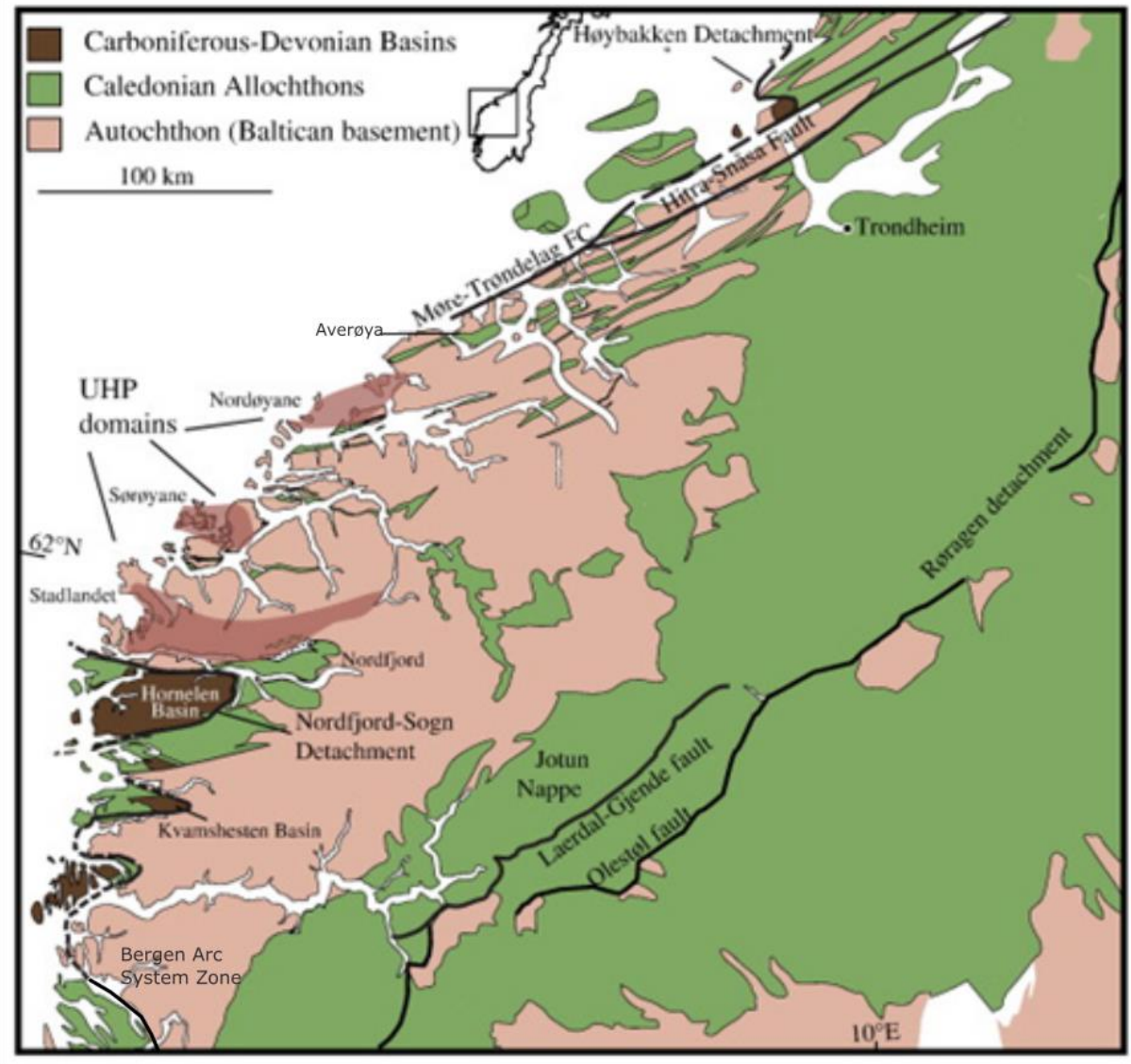

Figure 2.3.1: Overview of the WGR (Walsh, Hacker, Gans, Wong, & Andersen, 2013)

detachment zone (NSDZ) in the west, the Bergen Arc Shear Zone (BASZ) in the south, the Møre Trøndelag Fault Zone (MTFZ) in the north and the Jotun decollement zone with overlying nappes in the east (Labrousse et al., 2004; Røhr et al., 2013).

The WGC is characterized by rocks of varying compositions from tonalitic to granodioritic orthogneisses, locally cut by granitic dykes or variously eclogitized mafic dykes ((Corfu, 1980; Krabbendam & Dewey, 1998; Root et al., 2005). Subordinate rock types include gabbro, eclogite, amphibolite and augen gneiss. Separating the basement from the overlying orogenic wedge, is a mechanically weak basal decollement zone (Fossen & Rykkelid, 1992) (see fig 2.3.2). This zone consist of shales and phyllites, deposited in late Ordovician, enabling the transportation of individual nappes for hundreds of kilometers (Fossen & Rykkelid, 1992; Krabbendam & Dewey, 1998).

The orogenic wedge generally comprises four to five individual nappes, with the following order from lower to upper: The Lower Allochthon, the Middle Allochthon comprising Risberget, Sætra, and Blåhø and the Upper Allochthon comprising of Støren nappe and Skjøtingen in Sweden (P. Robinson, 1995; Terry & Robinson, 2003; Tucker et al., 2004). The Lower Allochthon consists of quartzites, conglomerate and pelites deposited as a sedimentary cover sequence from late Proterozoic to the Cambrian period (P. Robinson et al., 2003). This unit is typically absent or only observed as a thin layers in the field, one of the few areas where it has been described is Trollheimen (P. Robinson, 1995).

The Risberget nappe consists of rapakivi granites and augen gneisses, with subordinate

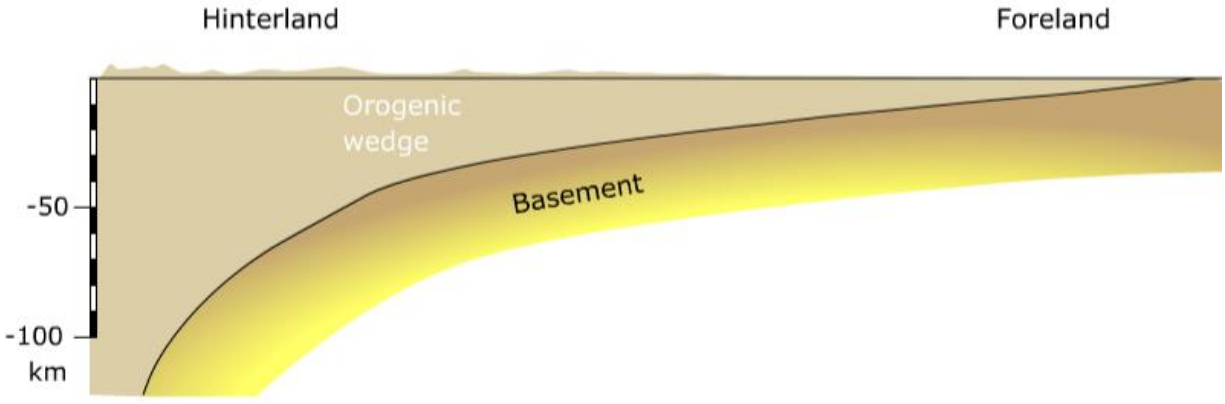

Figure 2.3.2: Idealized sketch of the geometry of Himalayan type orogenies. (Fossen, 2016)

metamorphosed gabbros, anorthosites and undifferentiated granitoids. Age estimations yield two separate age groups, constrained within 1659-1642Ma and 1190-1180 Ma for various localities (P. Robinson et al., 2003). These rocks are interpreted to be derived from a northwestern extension of Baltica basement (Terry & Robinson, 2003).

The Sætra Nappe comprises late Proterozoic intermixed and laminated layers of amphibolite and feldspathic quartzite, interpreted to be sandstones and crosscutting diabase dykes intruded during the rifting forming the Iapetus Ocean(Terry & Robinson, 2003). The thickness of this nappe varies from 2 km across at the nappe front in the east to an average of 10 meters across in the WGR, to as thin as 1 meter across on Nordøyane (P. Robinson et al., 2003).

The main rock types in the Blåhø Nappe are strongly metamorphosed to migmatized schists with a primary assemblage of mica + garnet + feldspar. Subordinate rock types in this nappe include rare eclogite, coarse garnet amphibolite interbedded with schist and pegmatites (P. Robinson, 1995). Both the upper and lower contacts of this nappe is marked by zones of impure marble, with rare quartzite at the base. These assemblages express a volcanic or oceanic arc related origin that suffered extensive metamorphism in close proximity to Baltica during the early Ordovician (P. Robinson, 1995; Terry & Robinson, 2003). Recent whole rock geochemical analysis of Blåhø eclogites indicates a MORB basaltic compositions (Hollocher et al., 2007)

The rock types in the Støren nappe are low grade epidote amphibolites, metamorphosed gabbros and rare tourmaline + biotite + garnet schists (Terry & Robinson, 2003). These rock are geochemically similar to the Løkken ophiolite complex created in the late Cambrian and early Ordovician, later obducted onto the Laurentian margin of Iapetus (Hollocher, Robinson, Kennedy, & Walsh, 2014). The discovery of fossils of early Ordovician age unconformably on the obducted ophiolitic rocks confirm the spatial association to the Laurentian margin (P. Robinson et al., 2003).

According to (P. Robinson et al., 2003) the Risberget and Sætra nappe of the middle Allochthon are present in Moldefjorden and Helleneset synforms, the central segment of Nordøyane and on Midsund. These nappes are otherwise absent in the north, including the study area on Averøya. The main nappe unit in the study area is therefore Blåhø, because Støren have not been observed east of Bolsøy (P. Robinson et al., 2003).

Chapter 2 – Regional Geology

Chapter 3 - Methods

3.1. Field work

Fieldwork was conducted in the course of five weeks in the summer of 2016 on the western part of Averøya, the Atlantic Ocean Road and along roadcuts and in the vicinity of Visnes and Lyngstad on the mainland. Standard equipment in the field included compass, susceptibility meter, north arrow (scale), camera, hammer, phone and notebook. A total of 451 GPs points were marked either as exposures or as localities using a Sony Xperia and the app Theodolite (appendix). A typical locality description contains GPS-coordinates and elevation, day and locality number, lithology, structural data, observations and magnetic susceptibility measurements.

A ground magnetic survey was also conducted, walking with a Total Field Magnetometer along various transects on the main road and smaller roads on Averøya, shown on figure 5.5.1. The resulting signal is a product of averaging the response of five measurements a second to the applied field.

3.2. Processing of structural data

Structural information was collected using a Brunton compass measuring foliation planes, stretching lineations, fold hinges and fold axes, all the time providing detailed notes on the observations made (appendix). Sketches were made of important structures and photographs were taken using Samsung NX1000 and Casio EXZ450. In the aftermath of the fieldwork this information have been compiled to construct lower hemisphere equal area diagrams using the program Dips, structural cross sections and geological maps using ArcGIS.

3.3. Processing of petrological data

3.3.1 Mineral chemistry

Major element analyses were performed on nine carbon coated thin sections using the Electron Microprobe Analyzer (EMPA) at NTNU. Chemical compositions for various minerals were determined for 490 points, using garnet and plagioclase standards. The element list included and their detection limits are shown in table 3.3.1. The focus of the probe work was mainly to identify the compositions of the phases in fine grained symplectites, inclusions and possible core to rim

zoning in garnets. The secondary target was to identify geobarometers like kyanite, coesite and phengite.

Element	Na	F	Cl	V	Mg	P	Cr	Al	K	Mn	Si	Ca	Fe	Ti	Ba
D.L	186	200	106	189	161	426	196	160	157	164	281	164	175	288	464

Table 3.3.1 Element list and detection limit

All compositions were compiled in a spreadsheet, where a number of calculations were conducted:

Equation 3.3-1: $$Oxide = \frac{Number\ of\ oxygen\ atoms\ in\ the\ formula * Weight\ \%\ in\ mineral}{Atomic\ weight}$$

Equation 3.3-2: $$Cation = \frac{Number\ of\ atoms\ of\ element}{Number\ of\ oxygen\ atoms} * Oxide * \frac{Cations\ in\ structural\ formula}{Total\ Oxide}$$

Mineral formulations for garnet (Coleman, Lee, Beatty, & Brannock, 1965), Na-pyroxene (Morimoto, 1988):

Equation 3.3-3: $$Tot.cation\ (garnet) = Fe^{2+} + Ca + Mg + Mn$$

Equation 3.3-4: Garnet Formulae = $$Alm\ \frac{Fe^{2+}}{tot\ cation\ 3.3-3} + Grs\ \frac{Ca}{tot\ cation\ 3.3-3} + Prp\ \frac{Mg}{tot\ cation\ 3.3-3} + Sp\ \frac{Mn}{tot\ cation\ 3.3-3}$$

Mineral formulations for Na-pyroxene (Morimoto, 1988):

Equation 3.3-5: Tot. cation (pyroxene) = Ca + Mg + Fe^{2+} ***+ 2Na***

Equation 3.3-6: Pyroxene formulae: $$Quad\ \frac{Mg+Ca+Fe^{2+}}{tot\ cation\ 3.3-5} + Jd\ \frac{2Na * Al/Fe^{3+}}{tot\ cation\ 3.3-5} + Ae\ \frac{2Na*(1-\ Al/Fe^{3+})}{tot\ cation\ 3.3-5}$$

Mineral formulations for plagioclase:

Equation 3.3-7: Tot cation (plagioclase) = Na + Ca + K

$$\textit{Equation 3.3-8: } Al\ \frac{Ca}{tot\ cation\ 3.3-7} + Al\ \frac{Mg}{tot\ cation\ 3.3-3} + Sp\ \frac{Mn}{tot\ cation\ 3.3-3}$$

$$\textit{Equation 3.3-9: } FM = \frac{Fe2+}{Mg + Fe2+}$$

3.3.2 Petrography

Samples were also collected from the majority of the localities using a hammer, on planes of known foliation. A total of 29 polished thin sections were thereafter prepared at the thin section preparation lab at NTNU. These were cut normal to the foliation and commonly parallel to the lineation and provide a good representation of the eclogites and surrounding lithologies in the field area. The thin sections were described using a polarizing microscope in both transmitted and reflected light. This microscope was also used to take photomicrographs of important textures and structural features. An Epson v600 Scanner was used to scan the handsample as well as the entire section both in plane- and cross polarized light.

3.4. Processing of magnetic data

Oriented blocks were sampled at six different localities, shown in figure 5.4.1. These were then cut to 2.54 cm lengths and used to measure density, remanence and susceptibility.

3.4.1 Density

The samples were left to soak in ionized water for more than 24 hours. After removing excess water from the surface, the samples were placed into the density meter. Measuring the weight of the sample in free air and in water, the Archimedes principle was applied to determine the density and thereafter the volume (Dentith & Mudge, 2014). See formula below

$$\textit{Equation 3.4-1: } \rho\ sample = Weightair\ /\ (Weightair - Weightwater)$$

$$\textit{Equation 3.4-2: } Volume_{sample} = Mass_{sample} / \rho_{sample}$$

3.4.2 Remanence

The six core samples were measured in the spin magnetometer at NTNU and 30 unoriented thin section chips were measured at the magnetometer at NGU.

The local field was found from this site http://www.ngdc.noaa.gov/geomag-web/?model=igrf#igrfwmm, in order find Mj (See formula 1). A latitude of 62.9 and longitude of 7.3, together with the date of acquisition was used to perform the calculation.

3.4.3 Modelling

As the survey was conducted along a non-parallel transect kriging together with a cell size of 50 meters was applied to obtain a grid (Journel & Huijbregts, 1978). This grid was also despiked and a linear regional anomaly was automatically calculated by Modelvision. Modeling was thereafter carried out on the residual anomaly by manually acquiring a best fit for the calculated model to the observed signal. This was conducted by constructing and changing the ends of 2D polygons representing areas with similar susceptibilities and remanence.

Chapter 4 Chapter - Theory

4.1. Eclogite metamorphism

4.2.1 Introduction to metamorphic facies

The definition of metamorphic facies was first introduced by (Eskola, 1915). He would conceptualize that the occurrence of specific mineral assemblages equilibrating together, reflect a specific range of P-T conditions (Smulikowski, Desmons, & Fettes, 2007; Winter John, 2010).

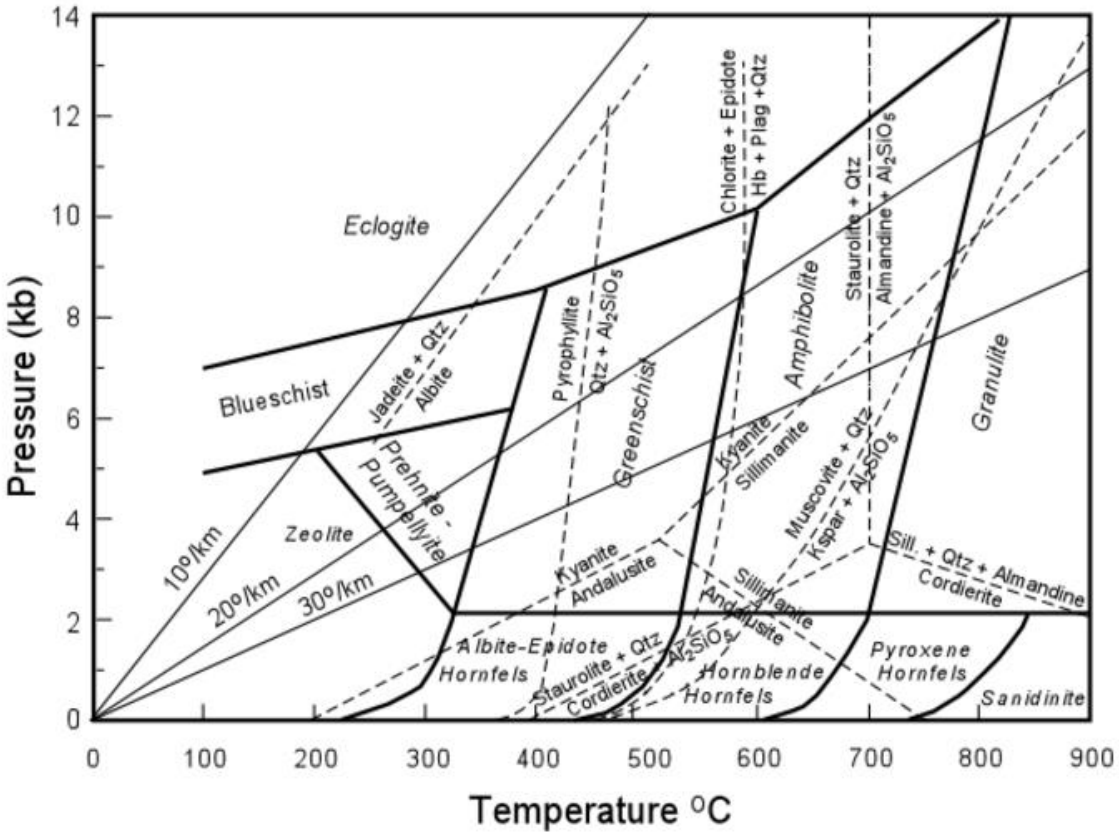

Figure 4.1.1: Metamorphic Facies Diagram (Nelson, 2004)

Later work from (Eskola, 1920) and further improvements by (Turner, 1960), resulted in a classification diagram for metamorphic facies and their corresponding range of stability conditions (see fig 4.1). Solid lines, which in reality reflect transitional boundaries, differentiates eleven facies. Different mineral reactions, showing both reactants and products, are shown with dashed lines in the diagram.

The transition into HP eclogite facies from either blueschist, amphibolite or granulite facies is marked by an increasing pressure component under almost isothermal conditions (Hollocher, 2014; Winter John, 2010). Ranging from 1.2 GPa – 5 GPa in pressure and temperatures 400 – 900°C, the corresponding depths vary from 45 – 150km (Winter John, 2010). When the pressure component exceeds 2.7 GPa, the metamorphic process is termed ultra-high-pressure (UHP). Both HP and UHP metamorphism occurs in deep-seated environments like in subduction zones, continental collisional zones or a combination of these.

4.2.2 Eclogite classification

The established definition of an Eclogite according to IUGS (Fettes, Desmons, & Árkai, 2007) after (Medaris & Carswell, 1990) is:

> *"Plagioclase-free metamorphic rock composed of ≥75% vol. of omphacite and garnet, both of which are present as major constituents, the amount of neither of them being higher than 75% vol. "*

The mineral assemblage is strongly dependent on the composition of the protolith and thereafter the corresponding P-T conditions of formation. Both (Coleman et al., 1965) and (Medaris & Carswell, 1990) worked out classification schemes, characterizing three different types of eclogites based on the wt.% pyrope and temperatures respectively (Winter John, 2010).

Type	T - conditions	Associated rock	Associated minerals
A	900 °C <	Xenoliths in Basalt or kimberlites	Kyanite, coesite and microdiamonds. $Garnet_{Pyrope}$ >55%
B	550 - 900°C	Gneiss	Quartz, zoisite, kyanite and paragonite or Ca-amphibole, scapolite $Garnet_{Pyrope}$: 30 – 55%
C	450 - 550°C	Blueschist	Epidote, zoisite, quartz, amphibole, phengite and paragonite $Garnet_{Pyrope}$: <30 %

Table 4.1.1: Schematic overview of A, B and C type eclogite and their characteristics according to (Winter John, 2010)

4.2.3 Prograde Metamorphism

In the mineral assemblage, the Eclogite facies metamorphism is easily recognizable by the breakdown of plagioclase as a response to higher pressures (Philpotts & Ague, 2009). Separating the Albite-Anorthite endmembers of plagioclase from each other, reactions and reaction products can be described by the use of equations 11.1-11.6 in (Hollocher, 2014):

Equation 4.1-1 $\boldsymbol{Nepheline + Albite \rightarrow Jadeite}$

Equation 4.1-2 $\boldsymbol{Albite \rightarrow Jadeite + Silica}$

Equation 4.1-3 $\boldsymbol{Augite + Jadeite/Albite_{component} \rightarrow Omphacite}$

Equation 4.1-4 $\boldsymbol{Anorthite \rightarrow Grossular \pm Kyanite + Silica}$

Equation 4.1-5 Plagioclase + Orthopyroxene/Olivine → Garnet + Omphacite

Equation 4.1-6 Ilmenite/titanomagnetite → Rutile

All the reactions above are highly simplified and shows the predominantly active elements in the formation of the omphacite and Mg-Fe-Ca garnet. Jadeite is formed at the expense of albite ± nepheline (reaction 4.1-1 and 4.1-2), that in turn forms a solid solution with augite (reaction 4.1-3) from the protolith, producing omphacite (Deer, Howie, & Zussman, 1982).

As anorthite decomposes in equation 4.1-4, the mineral assemblage in the protolith decides whether kyanite forms and also determines the composition of the newly formed garnets. When mafic minerals are present in the source rock, Al will be preferentially incorporated into Mg-Fe garnet over kyanite (Hollocher, 2014). As with omphacite, the garnet also forms a solid solution between the Mg-pyrope, Ca-grossular and Fe-almandine endmembers. From the eclogite classification table, the wt% of pyrope is above 55% for type A, which means that this reaction is strongly pressure dependent(Winter John, 2010). A mafic mineral, typically orthopyroxene or olivine, is required to form eclogites described in equation 4.1-5, favoring eclogite formation when olivine is present in the mineral assemblage.

Rutile is also a common mineral in eclogites, forming either in the matrix due to decomposition of ilmenite or as inclusions within garnet when titanomagnetite breaks down (equation 4.1-6) (Korneliussen et al., 2000).

4.2.4 Retrograde metamorphism

Eclogites are typically found as boudins, in varying shapes and sizes, complexly interwoven within amphibolite, granulite facies rocks and quartzo-feldspathic gneisses. They rarely also occur as larger bodies, extending for up to a couple of kilometers (Hollocher, 2014) (see fig

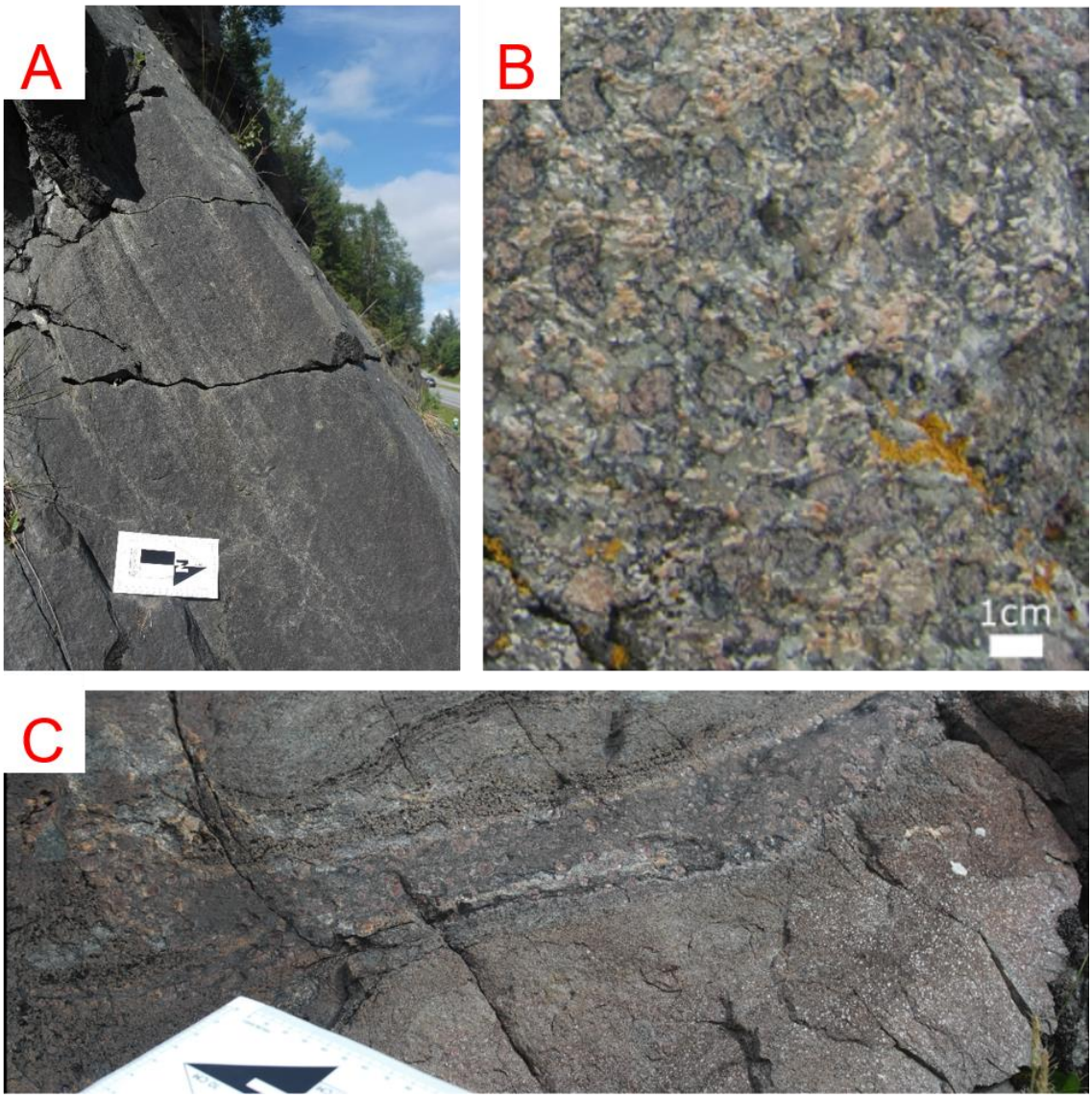

Figure 4.1.2: Typical eclogite geometries, showing: A) Layered eclogite at Visnes, B) Eclogite boudin exhibiting a granoblastic texture, where garnets have amphibole coronas and the greasy green color in the matrix indicates widespread formation of plagioclase + Ca pyroxene symplectite after omphacite on the west coast of Averøya and C) An eclogite boudin in the lower part rimmed by a 20cm wide coarse garnet + amphibole zone.

4.1.2A). One reason for this is that the minerals of the eclogite are extremely resistant to ductile deformation, so they tend to be broken into blocks surrounded by more ductile rock types(D. A. Carswell & Cuthbert, 2003).

Figures 4.1.2A-C, in addition to showing various eclogite geometries, also exhibits textural indications of retrograde metamorphism. These changes are closely linked to exhumation rates, deformation rates and influx of aqueous fluids and thereby reflect whether the mineral assemblages re-equilibrate to continuously lowering P-T conditions before reaching the surface (Hollocher, 2014). On a microscopic level the occurrence of symplectites and corona textures replacing omphacite and garnet respectively, provides definite proof of peak eclogite

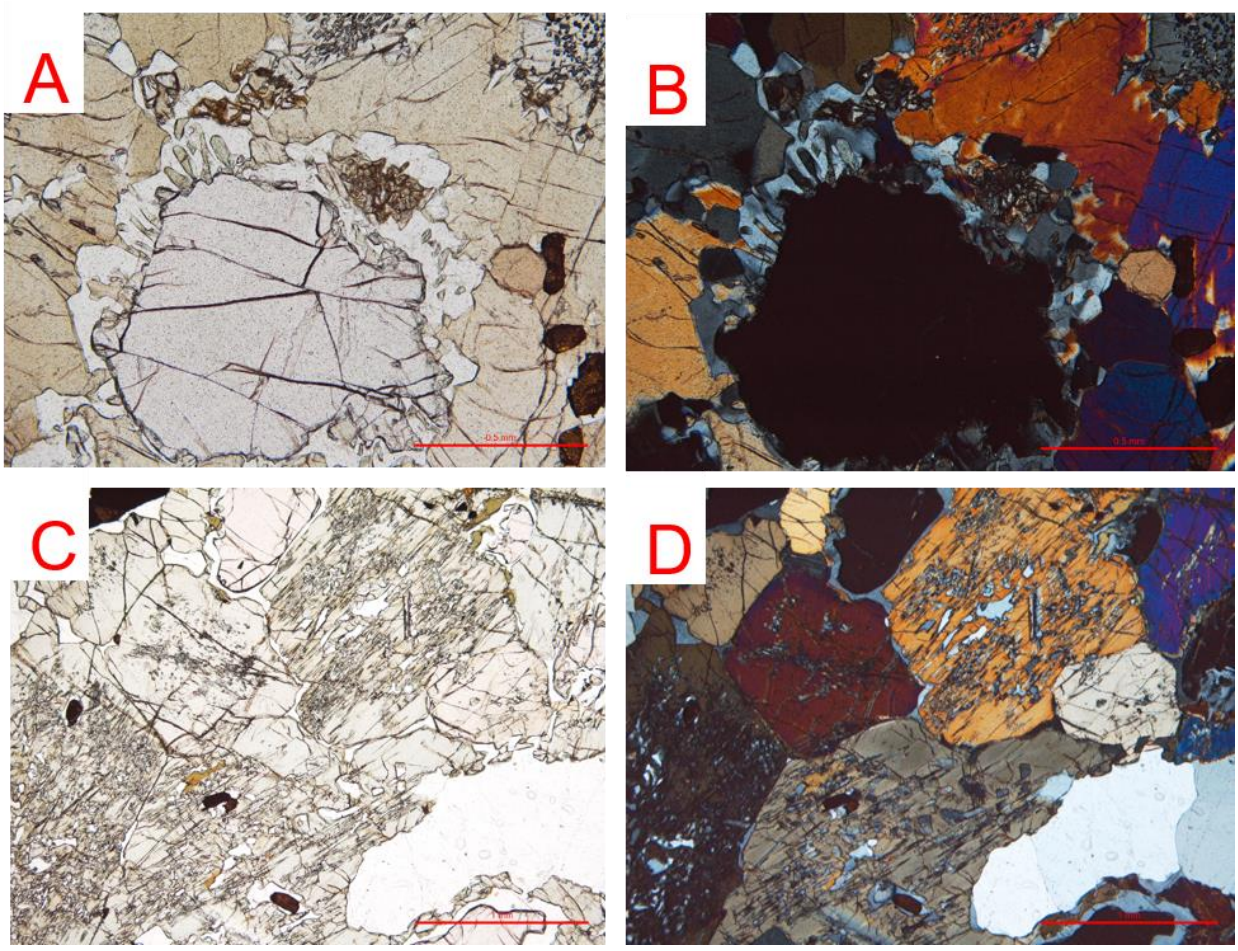

Figure 4.1.3 PP to the left and XP microphotographs to the right, showing: A, B: Garnet rimmed by a plagioclase + amphibole intergrowths. From 37563, width 10X. C, D) Shows variably distributed graphical symplectic intergrowths of plagioclase and Ca-clinopyroxene in relict Omphacite. From 37564, width 5X

metamorphic conditions (see fig 4.1.3A-D). The most common symplectite forming reactions associated with garnet and omphacite decomposition are described by equations 4.1-7-4.1-11.

Symplectites chiefly of plagioclase + Ca clinopyroxene ± amphibole replacing omphacite (Eskola, 1921) are some of the most common textures indicating retrograded eclogite. Additional symplectites that might occur are the formation of orthopyroxene and plagioclase with the decomposition of clinopyroxene and garnet.

Symplectites have become an important field of study for estimating the geobaromethry and associated uplift history of eclogites and surrounding lithologies (Joanny, van Roermund, & Lardeaux, 1991). The process of exsolving clinopyroxene and plagioclase from omphacite, is still not entirely understood, but most studies suggest that this texture is produced through reaction with quartz during decompression (equation 4.1-7 and 4.1-8) (Winter John, 2010). The presence of fluids will further enhance these processes and promote formation of hydrous minerals like amphibole at the expense of pyroxene or plagioclase (Hollocher, 2014).

Equation 4.1-7: Jadeite + quartz → albite

Equation 4.1-7 $\boldsymbol{Omphacite \rightarrow Ca\ pyroxene + Plagioclase \pm Amphibole}$

Equation 4.1-8 Clinopyroxene → Orthopyroxene + Plagioclase

Equation 4.1-9 Mg, Fe, Ca Garnet → Amphibole + Plagioclase + Magnetite

Equation 4.1-10 Mg, Fe, Ca Garnet + Quartz → Plagioclase + Ca-pyroxene ± Amphibole ± Orthopyroxene

Decomposition of garnet involves formation of various corona textures, from merely moats of plagioclase to symplectitc intergrowths of amphibole and plagioclase. Another texture that may form, necessitates the presence of quarts in the sample. Reaction between garnet and most commonly veined to recrystallized sections of quartz leads to the development multiple coronitic rims of ‘moat’s of plagioclase and ‘necklaces’ of clinopyroxene, orthopyroxene and/or amphibole around the garnet (P. Robinson, Daczko, N., Krogh, T.E. & Hollocher, K, 2008).

4.2. Magnetic theory

The Earth's Magnetic field (Mobs) is a result of the combined influence from an exterior - , internal - and a crustal field. The largest contribution originates from the internal field, generated by convection of charged, Fe-rich particles in the outer liquid core. This field is acting like a self-induced and self-sustainable magnet, (Dentith & Mudge, 2014; Nabighian et al., 2005) varying in strength from 30.000-60.000 nT, increasing towards higher latitudes. Charged particles emitted from the sun produces the exterior field in the earth's atmosphere, varying from 0-2000nT.

Magnetic minerals only makes up a small portion of the total mineralogical volume of rocks in the crust and produces the crustal field (Dentith & Mudge, 2014). Rock magnetization can provide valuable information concerning subsurface petrological characteristics, possible alteration processes and implications for geological history. To investigate these properties, it is necessary to first remove the response from the internal field and exterior field, leaving only the crustal response (eq. 4.2.1 and 4.2.2).

Equation 4.2-1 $M_{OBS} = M_{tot} + M_{int} + M_{Ex}$

Equation 4.2-2 $Mtot = Mi + Mr$

Equation 4.2-3 $M_j = \chi * H$

Equation 4.2-4 $Q\text{-}value = M_R / Mi$

Magnetism in a material is dependent on two fundamental properties, induced and remanent magnetization (see eq. 4.9(McEnroe, Fabian, Robinson, Gaina, & Brown, 2009). Induced magnetization is the ability a material has to become magnetized, dependent on the susceptibility of the material and the strength of the applied field (eq 4.2.3). As soon as this external field is removed the magnetization returns to zero (Dentith & Mudge, 2014). Remanent magnetization reflects the ability a material has to retain a magnetization from an ancient field. This is controlled by the direction and strength of the ancient field, the amount of magnetic minerals in the rock, together with magnetic grain size and microstructures (Dentith & Mudge, 2014). The ratio of induced and remanent magnetization is given by the Q-value (eq 4.2.4), where Q-values of >>1 indicates that remanence dominates, and Q-values of <<1 indicates that induced magnetization dominates.

Chapter 5 - Theory

Chapter 5 – Results

5.1. Field and textural relationships of the different rock types

The majority of the fieldwork was concentrated on mapping the layered eclogite body on Averøya and surrounding gneisses, with all outcrops shown in figure 5.1.1. A rectangle shaped area was covered, stretching from Hjertvikbukta in the NW to Nasvika in the SE. The west coast of Averøya is dominated by gentle topography and excellent rounded coastal exposures, whereas steep topography made certain sections of the southern coast inaccessible to map. Steep topography was occasionally also a problem when mapping the middle section of the island, further augmented by dense vegetation and marshy landscape. Inferred boundaries along the northern and eastern edges of the bodies are therefore less reliable.

Four days were also spent mapping two layered eclogite bodies around Visnes and Lyngstad, road cuts both on the main land, on the southwestern side of Averøya and on the Atlantic Ocean Road. Because the area around Lyngstad is densely populated and close to a quarry with restricted access, exposures were few and scattered. Exposures along the roads were fresh and easily available, especially on the Atlantic Ocean Road. A two-day return trip was undertaken in the end of March 2017 to look at outcrops further NW on Averøya and tie up some loose ends.

Field observations together with thin section petrography forms the foundation for classifying the area into seven different rock types, which in turn will be assigned to the Baltican basement or to the Blåhø Nappe of the Middle Allochthon. The rock types will be presented and described consecutively according to the tectonostratigraphic order. According to figure 5.1 the dominating rock types are a granodioritic to tonalitic migmatite gneiss, garnet amphibolite, garnet and amphibole gneiss and eclogite. Subordinate rock types observed on a few localities, includes amphibolite gneiss, mylonite, quartzite, marble and gabbro.

The applied color scheme on the map have been chosen based on the color scheme used on previous maps provided by NGU of the area (from ArcGIS file). Changes that will be made to the previous map of the study area in this thesis, include differentiating between garnet and amphibole gneiss and garnet amphibolite previously labelled paragneisses/amphibolite, adjusting the inferred boundaries between rock types and marking localities highly abundant in granoblastic eclogite boudins within the different rock types.

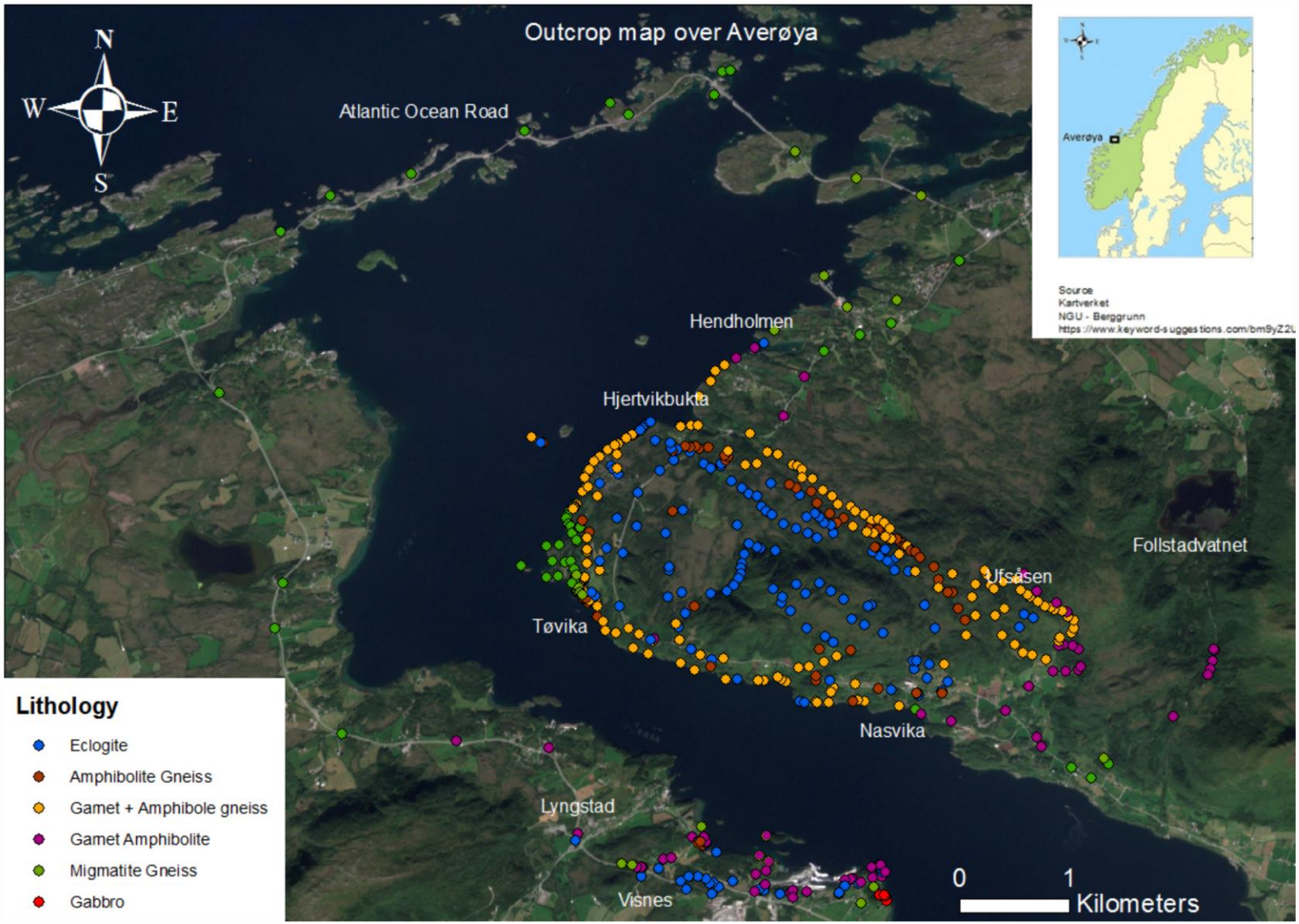

Figure 5.1.1: Outcrop map of Averøya and the mainland.

5.1.1 Granodioritic to tonalitic migmatite gneiss

The most dominating rock type in the study area is a granodioritic to tonalitic migmatite gneiss. Tonalitic assemblages dominate on the Atlantic Ocean road, in the vicinity of Lyngstad and roadcuts on the NW of Averøya. Granodioritic assemblages occurs on the west coast of Averøya, along roadcuts on the mainland and south of Nasvika. Outcrop photographs from selected field localities of this rock type, can be seen in figure 5.1.2 A-E.

This rock type alternates between a strongly undulating foliation, caused by folding and truncating pegmatitic or metamorphosed mafic dykes and a more planar foliation. Three compositionally different bands are defined, based on color variations in the field (see figure 5.1.3 A, B, C). Applying the migmatite classification (Hollocher, 2014) leucosome is the term for the lightest white to pinkish layer, melanosome for the darkest bluish grey layer and mesosome for any intermediate phase, which in this case is a light grey color. The leucosome is predominantly composed of quartz + plagioclase ± feldspar, whereas the dark melanosome reflects high amounts of biotite and amphibole. The mesosome consists of an intermediate plagioclase + biotite assemblage and is the most common type together with the leucosome.

On the west coast of Averøya the migmatite gneiss locally grades into an augen gneiss close to the boundary of the overlying nappe units (figure 5.1.3 D). The augen gneiss is characterized by a fine-grained greyish matrix containing coarse grained, irregular to sigmoidal and somewhat adjointly connected K-feldspar porphyroclasts ranging in sizes from 0.1 – 5cm. An additional accessory mineral here is garnet, which is commonly observed associated with the k-feldspar.

The boundary between this lithology and the garnet and amphibole gneiss along the west coast is generally well established, with the contact witnessed at several outcrops. On the eastern side of the layered eclogite the boundary to the garnet amphibolite remains poorly constrained. An about 4 meter wide zone of the migmatite gneiss were found pinching into the garnet amphibolite at Nasvika, the continuation of this zone in the eastern direction remains uncertain. Contacts between the migmatite gneiss and the garnet amphibolite at the mainland were off lesser priority and were given less time to investigate in the field.

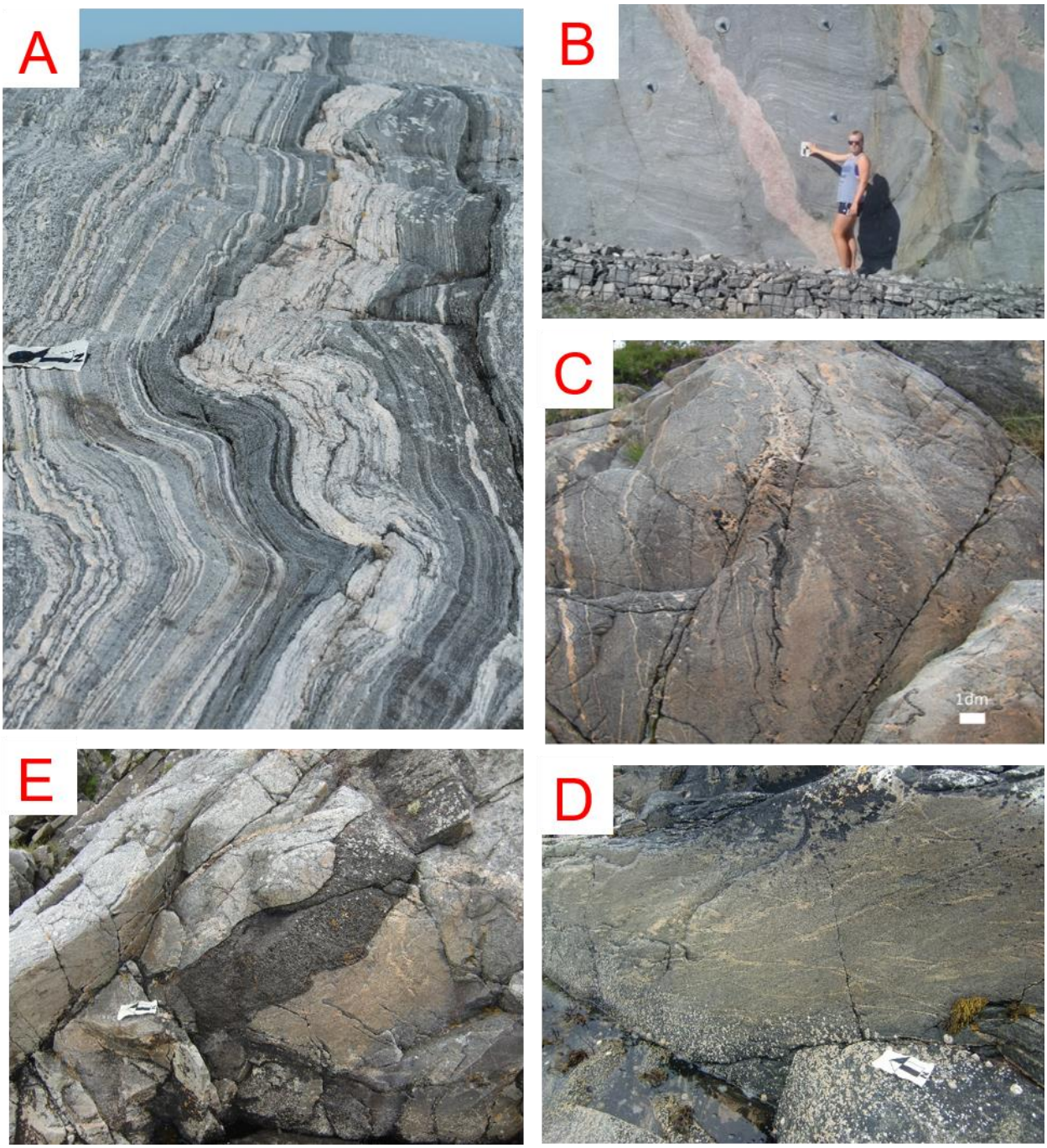

Figure 5.1.2: Photographs from migmatite gneiss localities in the study area, from A) Layered migmatite at the Atlantic Ocean Road, where the dark layer probably is a mafic dyke, B) Another locality at the Atlantic Ocean road, looking in at a surface parallel to the sub-horizontal lineation with crosscutting pegmatites. C, D and E are all from localities on the west coast of Averøya, showing C) Complex small scale passively folded layers, D) The formation of thin < 30cm granitic leucosomes and E) A crosscutting amphibolitic dyke.

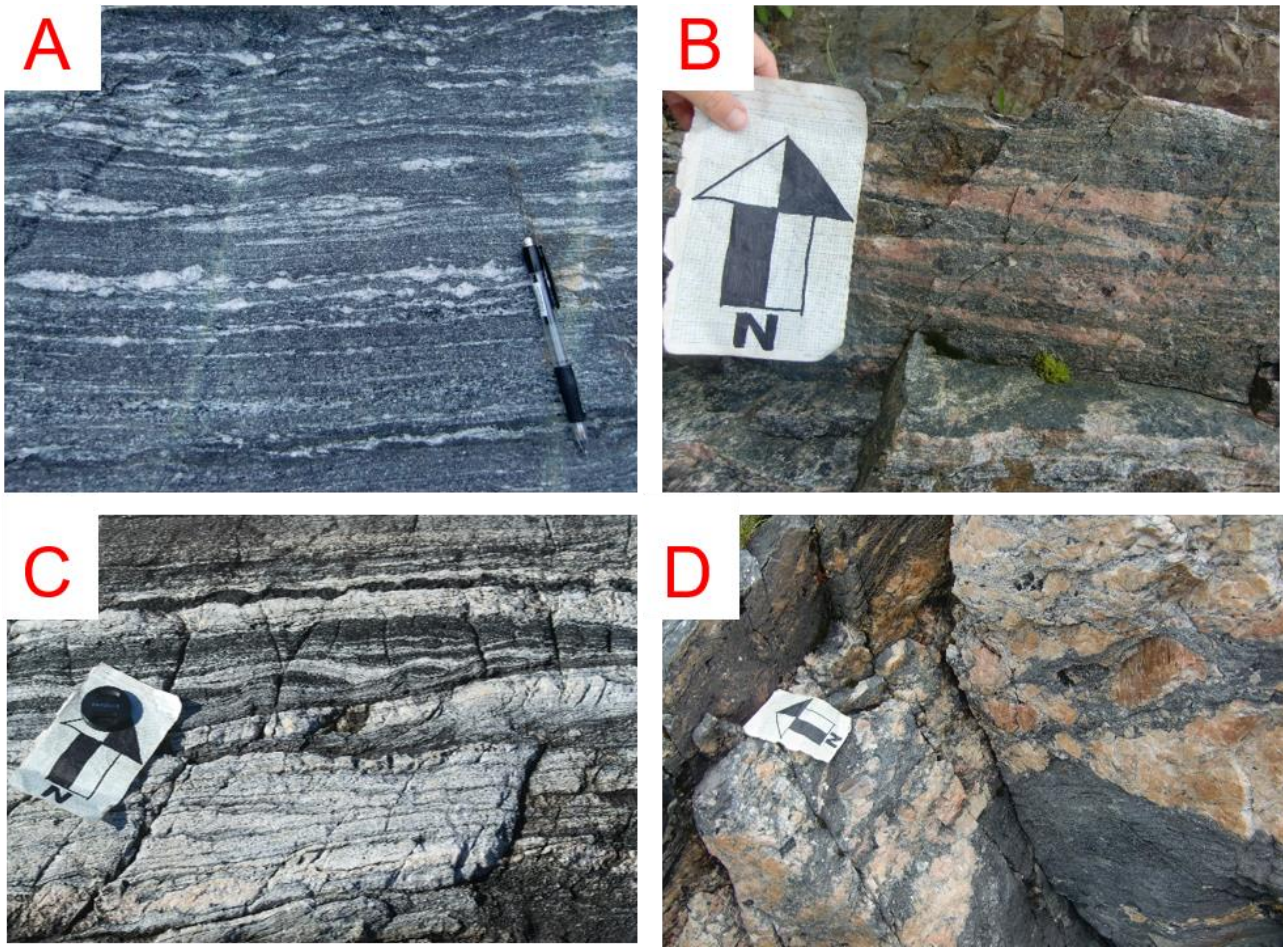

Figure 5.1.3: Close up photographs showing textural variations within the migmatite gneiss, where A) A dark matrix containing thin foliation parallel veins and interstitial plagioclase porphyroclasts, crosscut by two small epidote veins. B) Small scale layers of K-feldspar tightly folded within a light grey matrix. Notice the phaneritic garnets dispersed throughout. C) Undulating dark and white layers at the Atlantic Highway D) Layers of coarse porphyroclasts of K-feldspar set in a fine-grained greyish matrix.

5.1.2 Garnet amphibolite

This rock type displays a chiefly planar foliation with high amounts of quartz, feldspar and garnet porphyroclasts set in a dark amphibole-rich matrix. Localized zones of anastomosing foliation occur when the porphyroclasts and metamorphic mafic boudin content is especially high (figure 5.1.4 B, C). In some of these localities the garnet amphibolite is situated within shear zones, thereby grading into mylonitic assemblages. Thin, light colored recrystallized layers of quartz are commonly observed within the matrix, typically wrapping around the porphyroclasts showing enhanced recrystallization in the pressure shadows. At Lyngstad intersection on the mainland this rock type contains higher amounts of mica, thereby grading locally into a more schistose variety.

The porphyroclasts come in a range of sizes depending on rock compositions, where

Figure 5.1.4: Outcrop photographs of the garnet amphibolite depicting A) Steeply dipping layers along a contact with migmatite gneiss at Nasvika and B, C) Clearly layered texture with interspersed boudins at Hendholmen.

porphyroclasts with feldspathic compositions range from 0.05 – 4cm and garnets range from 0.2 - 2 cm. With the exception of the irregular shaped K-feldspar grains in fig 5.1.5A), the majority of the feldspar porphyroclasts displays either a sigmoidal or ovoid shape. Garnet commonly exhibit rounded to subhedral shapes as shown in figure 5.1.5B. Both types show a progressive development of tails, where the full extent of this growth is more easily recognizable around the garnets due to the difference in color (figure 5.1.5 B, C and D).

Easily accessible outcrops of this rock type have been found on coastal sections close to Nasvika, Hendholmen and Lyngstad. The contact between this rock type and the garnet and amphibole gneiss have not been observed in the field and could be either transitional or tectonic.

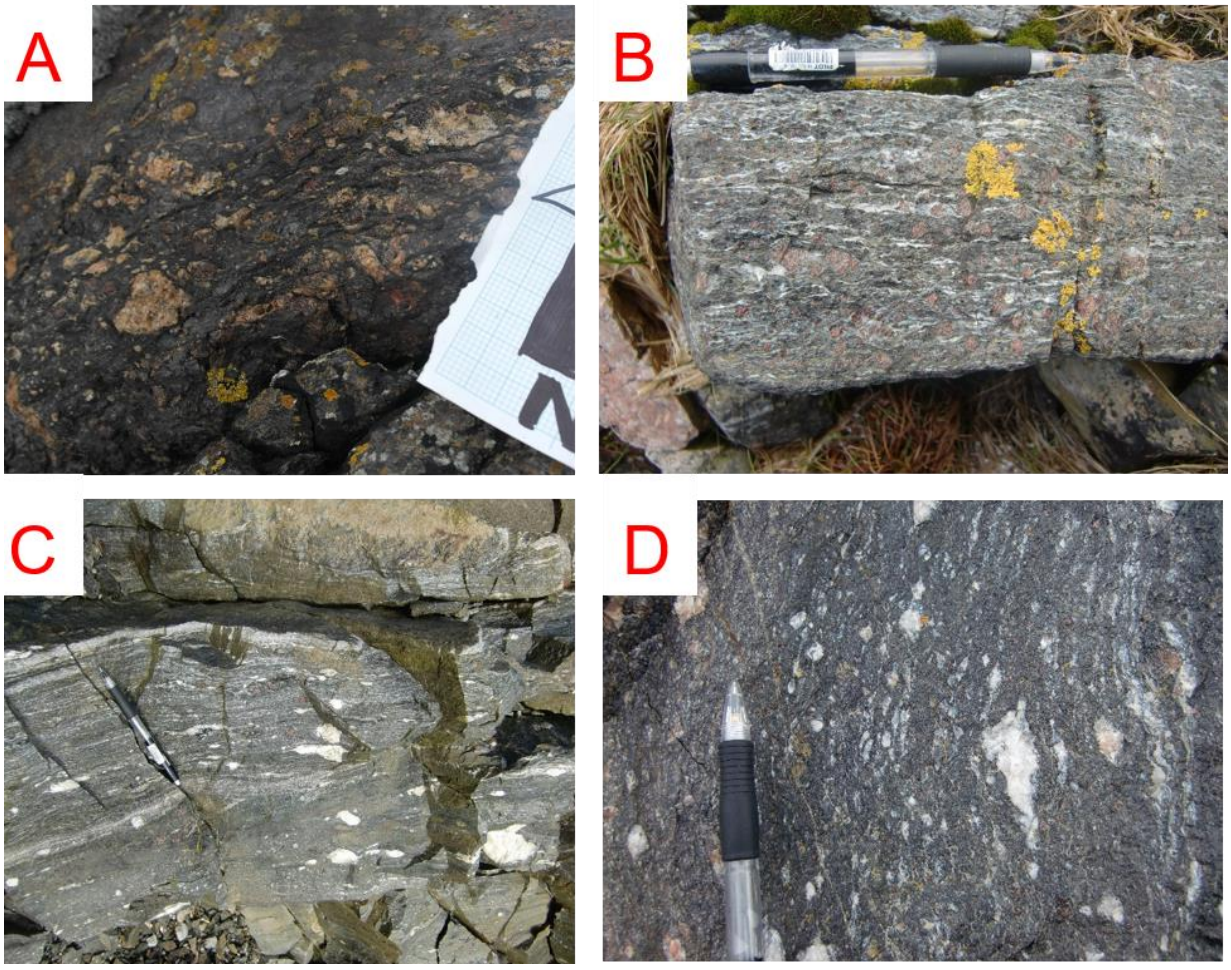

Figure 5.1.5: Showing different textural variations within the garnet amphibolite at A,B) Nasvika, C) Lyngstad and D) Hendholmen.

5.1.3 Garnet and amphibole gneiss

This rock type comprises of a highly heterogeneous mix of a predominantly amphibole and garnet rich quartzo-feldspathic gneiss with interlayered boudins of eclogite and pegmatite veins. Outcrops shows a moderately foliated and layered lithology, alternating between garnet and

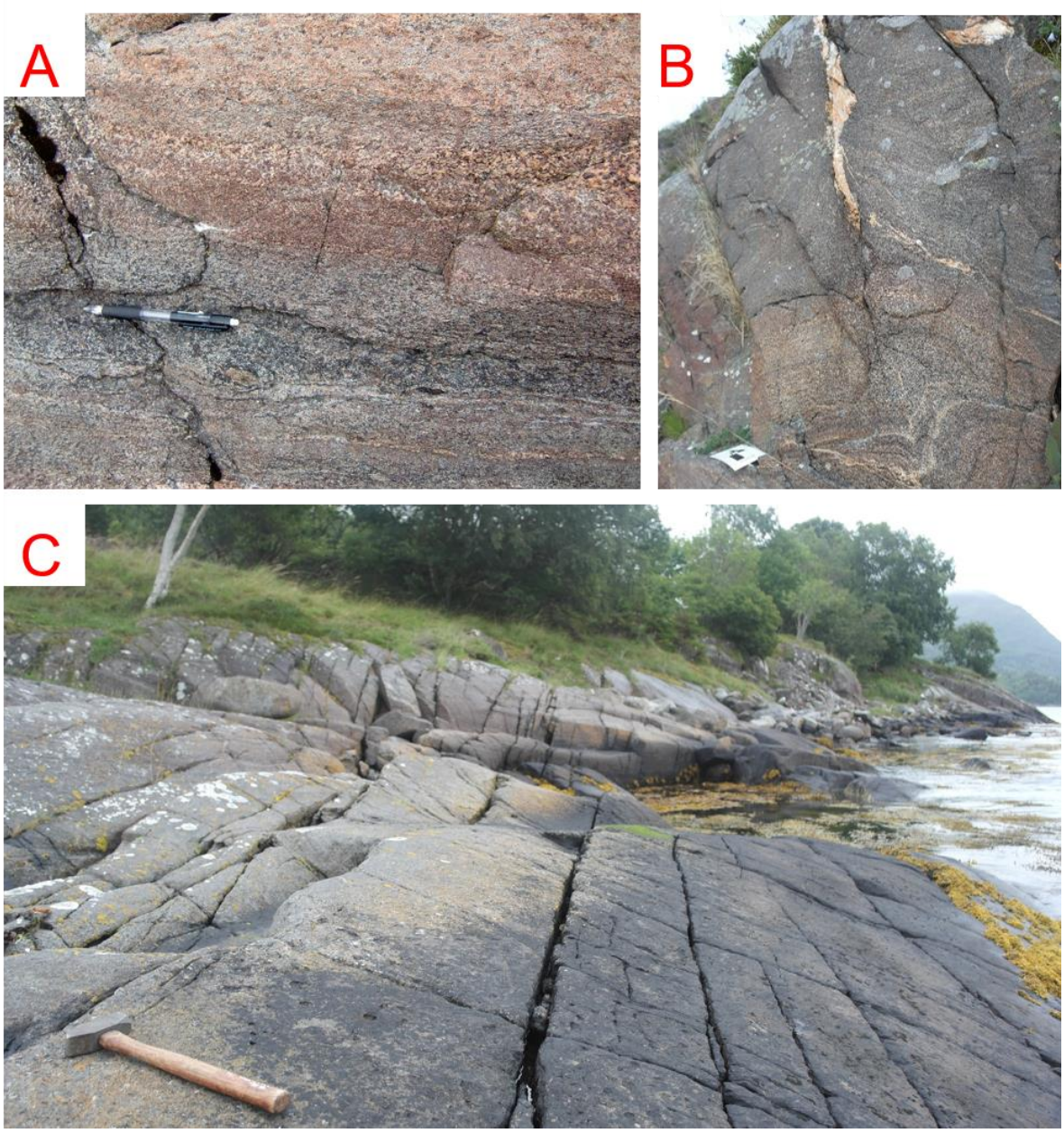

Figure 5.1.6: Photographs of outcrops A, B) on the various localities on the west coast of Averøya, showing the distinct alternating layered texture in and C) an overview of the exposure on the southern coast, with SE dipping layers.

amphibole-enriched layers, as seen in figure 5.1.6 A and B. Variously retrogressed eclogite boudins frequently perturbs the foliation, resulting in a more undulating foliation that wraps around the edges of the individual boudins.

The mineral assemblage is dominated by biotite + quartz + feldspar + amphibole + garnet, with possible kyanite observed in one outcrop on the northwestern coast of Averøya. This assemblage is demonstrated at various field localities shown in figure 5.1.7 A –D. Fine- to medium-grained and equigranular plagioclase and K-feldspar are the dominating minerals in the matrix with a highly variable amount of garnet and amphibole depending on the individual layers. The preferred orientation of elongated biotite and amphibole define a gneissose foliation.

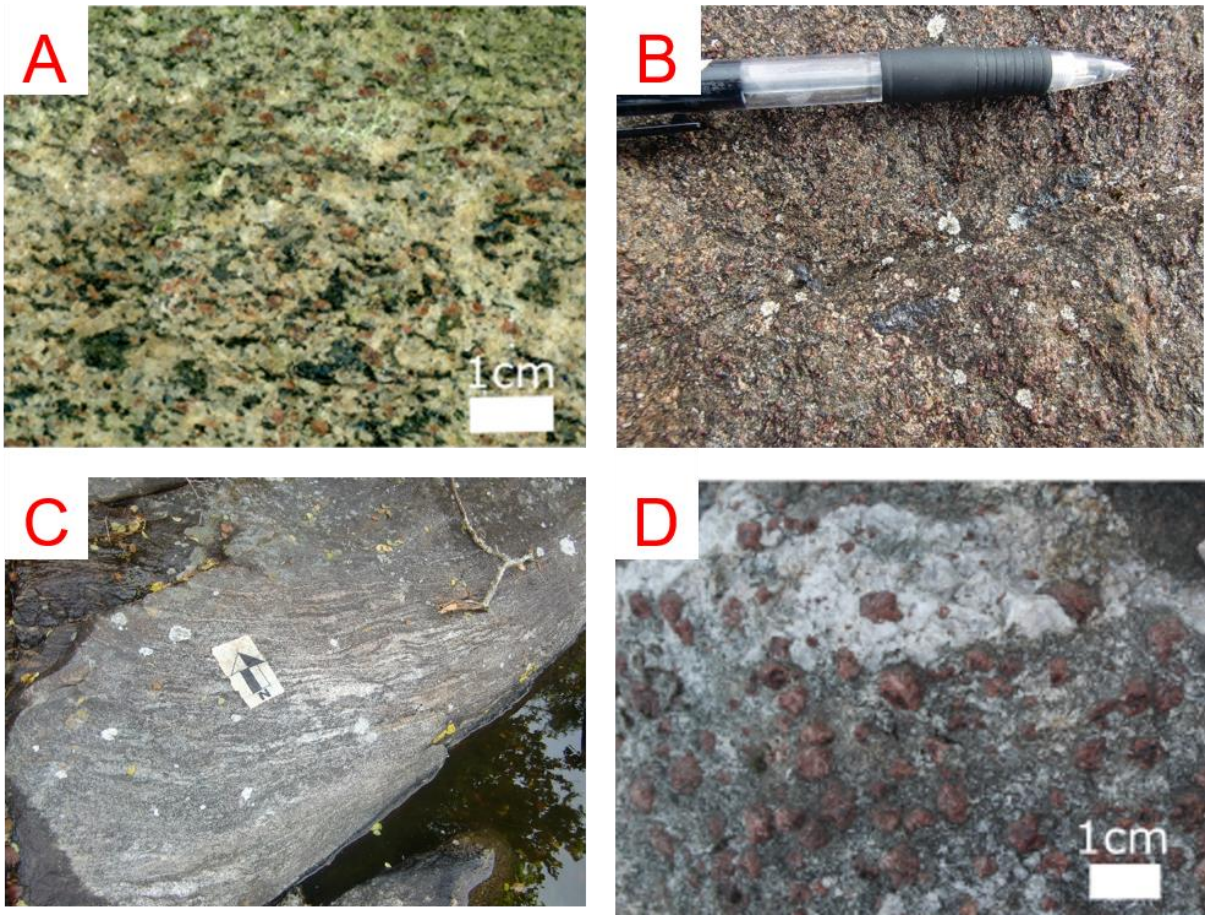

Figure 5.1.7: Textural variations, where A) A fresh sample, showing the typical texture and B) the field equivalent, notice the brown weathering and the possible presence. C) Local zone on the south coast of Averøya where the gneiss contains about 10 cm long granitic leucosomes. D) Coarse garnets in a quartz vein adjacent to garnet and amphibole gneiss

Some of the garnet enriched and amphibole depleted zones contain substantially more coarse-grained and equant garnet, ranging in sizes from 0.5mm-2cm, than what is observed in the garnet and amphibole gneiss. A typical example of this texture is shown in figure 5.1.7 D, where the garnets are situated in a quartz vein.

Amphibole enriched zones have been observed in recurring outcrops along the boundaries of the layered eclogite body on Averøya, together with feldspar and a few isolated garnets (see fig 5.1.8 A, B). Exhibiting the same foliated texture as the layered eclogite body and the surrounding garnet and amphibole gneiss, these zones are estimated to have a maximum width of around 30 meters close to Hjertvikbukta and 14 meters at Tøvika. The full extent of this zone at other parts of the boundary of the body is hard to constrain, due to the scarcity of exposures.

Extending out in an SE-NW direction on both sides of the layered eclogite on Averøya, undifferentiated garnet and amphibole gneiss was easily traceable especially along the western and southern coastal exposures on the island. This rock type was only observed on Averøya and have yet to be recognized on the mainland.

Figure 5.1.8: Contacts and their textures at A – Tøvika and B – close to Hjertvikbukta

5.1.4 Eclogite

Undifferentiated eclogite exposures are represented by a dark blue color, as seen on figure 5.1. Layered eclogite bodies exhibits different characteristics from eclogite boudins interlaced within garnet amphibolite and various gneissose hosts and will be described in two separate sections.

5.1.1.1 Layered Eclogite

At least four bodies of layered eclogite with similar characteristics have been mapped both on Averøya and at Lyngstad, close to Visnes quarry. A fifth body was identified on top of Ufsåsen based on the petrographic attributes, because dense vegetation made it hard to observe whether it had the characteristic layered texture in the field. Two of the bodies are located at the Lyngstad intersection and at Hendholmen on the NW Averøya. The Lyngstad body has a width of 17 meters and the Hendholmen body has a width of 32 meters and both are confined within an anticline covered by a mylonitic garnet amphibolite at Lyngstad and a garnet amphibolite at Hendholmen. The E-W to SE-NW extension of these bodies remain unknown. Both of these bodies, shown in fig 5.1.9 A, B, displays a clearly layered texture that changes orientation according to the foliation of the fold, dipping gently towards the NW - WNW in the N and SE-ESE in the S.

The exact width and length of the Averøya-, Visnes- and Ufsåsen layered eclogite bodies remain unknown. Field observations suggest that the Averøya layered eclogite is a continuous body stretching out in a SE-NW direction and covering an area of approximately 1.5x3km. The majority of the foliations recorded in this body is systematically dipping toward the NW - NNW, though some SE dipping layers were observed in the southeastern part of the body, indicating similar geometries as the two bodies on Hendholmen and Lyngstad. One of the best localities to study these characteristics of the layered eclogite on Averøya was a quarry located along the main road on the western side of the island. The furthermost southern extent of the Visnes body remains uncertain, though a minimum area of 1.5x0.5km seems to be covered.

All the layered eclogite bodies exhibit a moderately foliated texture, with small- to medium sized red garnets are set in a green to greyish matrix predominantly of omphacite and amphibole (fig 5.1.10 A – D). A gradational texture is commonly observed in the field with alternating garnet and omphacite-enriched layers, locally disrupted by zones enriched in either amphibole or quartz. Calcite have also been observed in the layered eclogite at the quarry locality on Averøya.

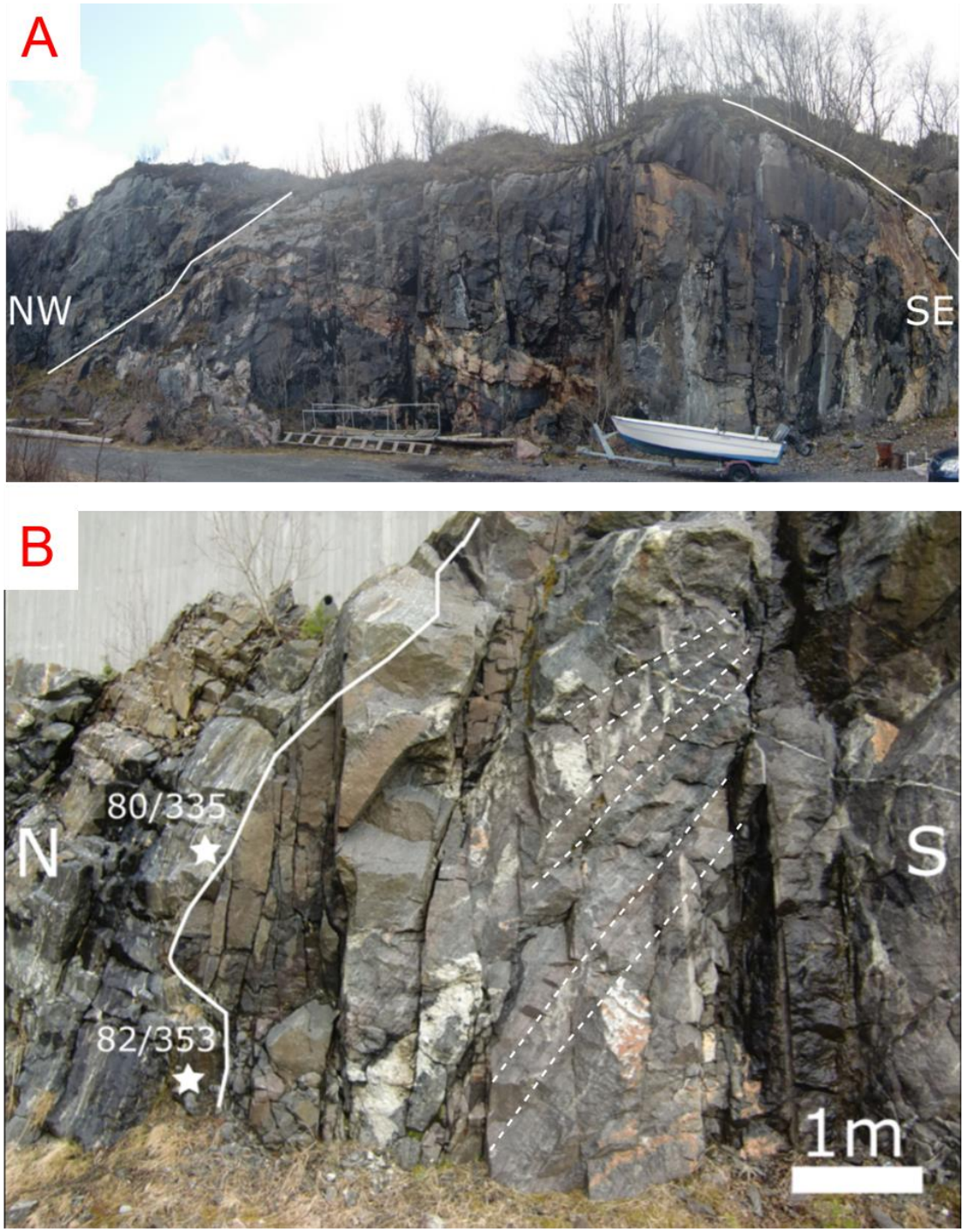

Figure 5.1.9: A) Layered eclogite with the boundaries of the body shown with white lines on Hendholmen, NW Averøya. Notice the large crosscutting pegmatite vein in the middle of the body. B) The northern limb of the fold located on the intersection on Lyngstad, with layered eclogite to the right of the white line and mylonite to the left. Notice the layered texture outlined by dashed lines, which has been cut by veins and irregular melts.

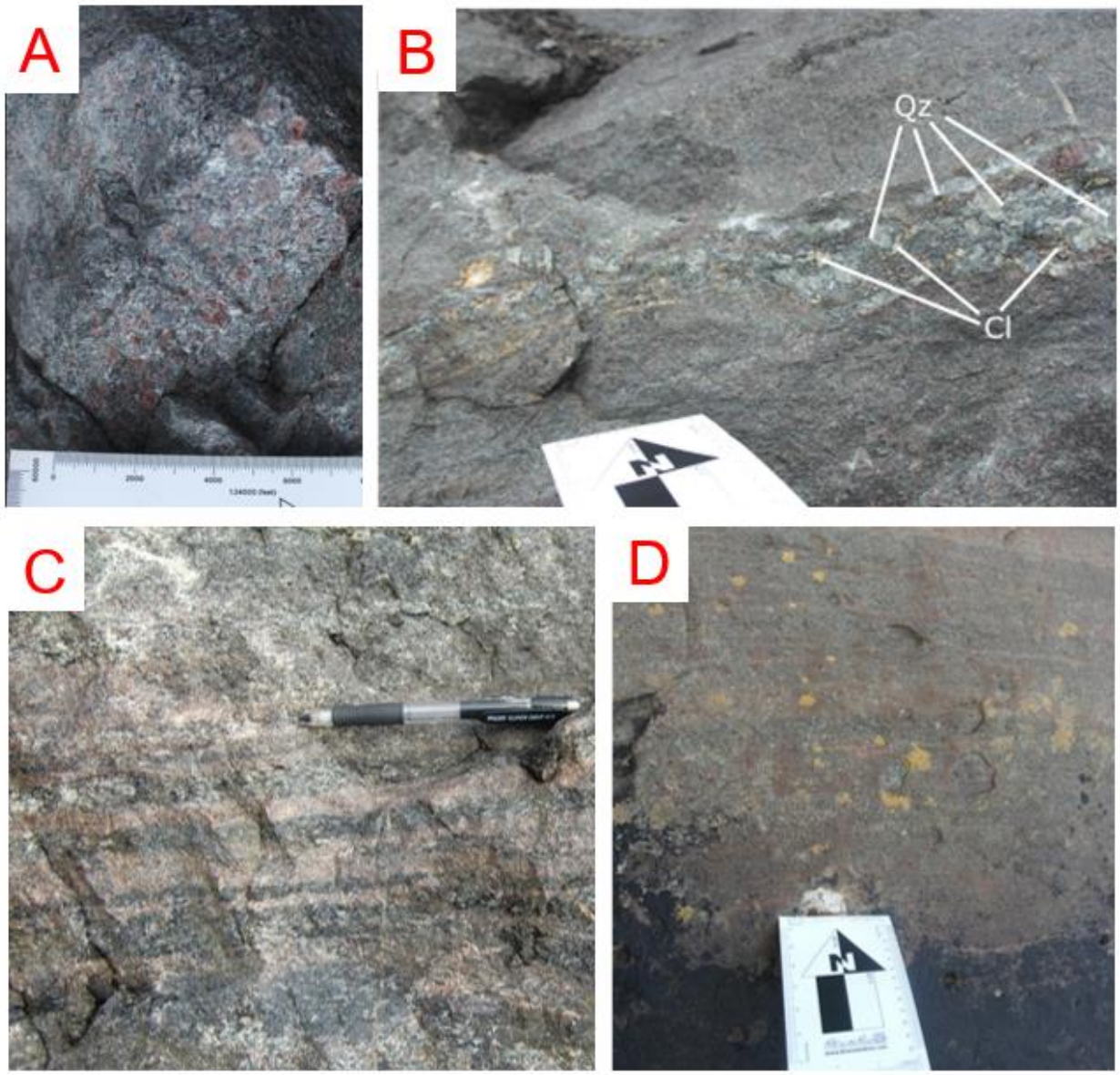

Figure 5.1.10: Photographs showing textural variations in outcrops A,B) Quarry locality on Averøya, C) Lyngstad intersection and D) Coastal extent of the Visnes body. Showing: A) Typical texture of the layered eclogite, minerals include grt + omp + am + pl, B) Layered eclogite with a zone containing porphyroclasts of quartz and interstitial calcite C) Gradational texture, with about 2cm wide zones of amphibole situated within the eclogite D) Layered eclogite observed at the coastal extension of the layered body on Visnes.

5.1.1.2 Boudin eclogite

Numerous boudins in a variety of shapes and sizes, ranging from a few centimeters to several tens of meters across are distributed throughout the garnet and amphibole gneiss, garnet amphibolite and migmatite gneiss. These are commonly symmetrical and exhibit lenticular to elongated rectangular shapes, stretching out in an E-W direction and separated from the host by small scale shear zones. The majority of the eclogite boudins are hosted by the garnet and amphibole gneiss, occurring both as single boudins and swarms of boudins intermixing, shown in figure 5.1.11.

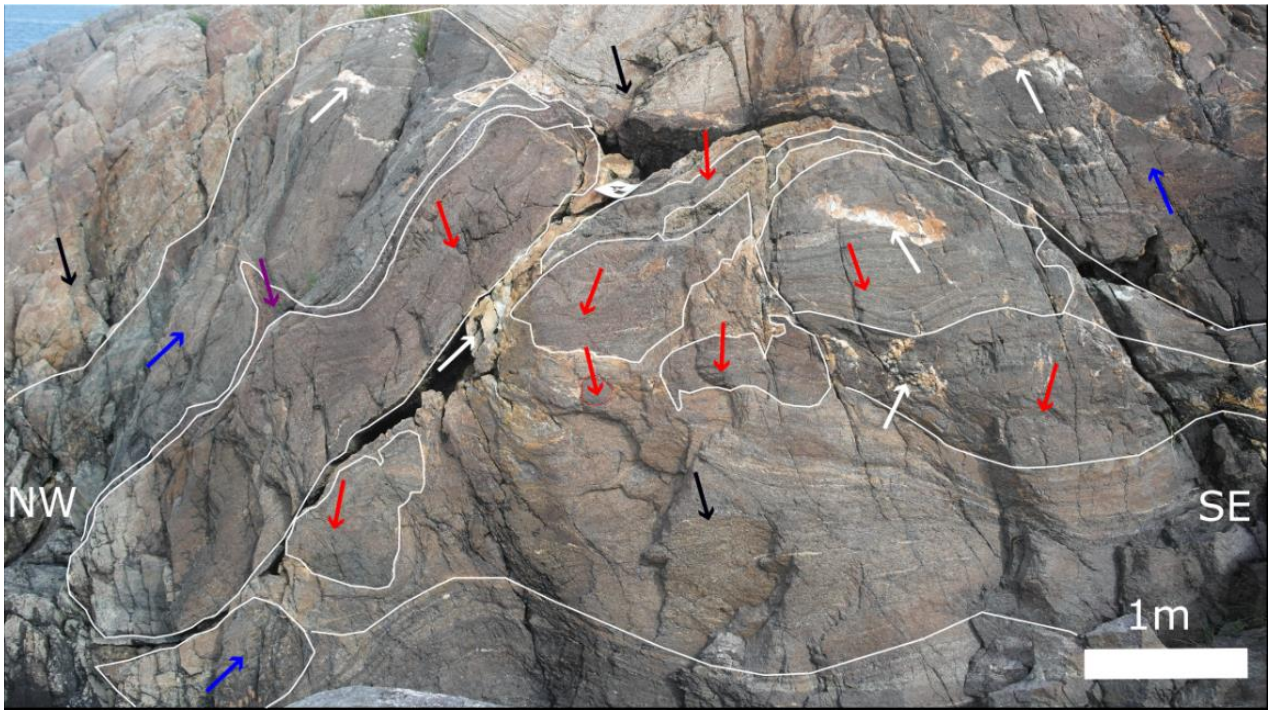

Figure 5.1.11: Outcrop on the west coast on Averøya showing complexly intermixed boudins of amphibole (blue arrows) and eclogite (red arrows) set in a garnet + amphibole gneiss host (black arrow). White arrows indicates pegmatite intrusions and the purple arrow shows a rim of amphibole and coarse-grained garnets enveloping the boudin. There were many similar localities like this especially along the coastal sections on the western and southern parts of Averøya.

The largest boudin eclogite identified in the field has an unknown E – W extension, due to challenging topography making it difficult to trace. Visually it exceeds 15 meters laterally and has a width of 3 meters (see figure 5.1.12 A, B). Crosscutting fractures and shear zones are highly enriched amphibole and produce local small scale boudinage. The mineral assemblage in this body is dominated by fresh green omphacite and coarse garnets, exhibiting a granoblastic texture.

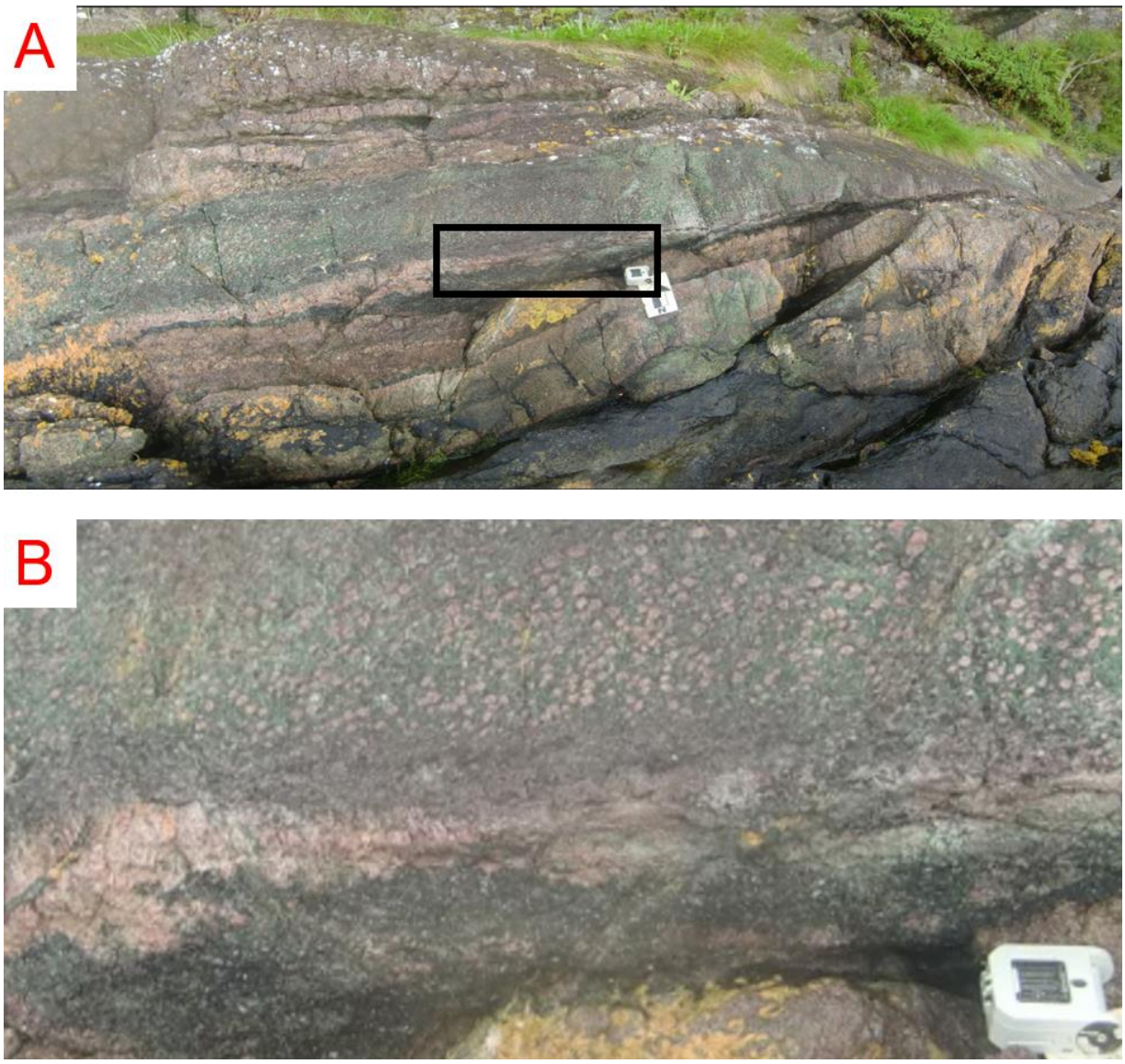

Figure 5.1.12: A) An E-W elongated massive and granoblastic eclogite body located at the southern coast of Averøya. B) A poor resolution photograph showing a bright green omphacite matrix abundant in coarse garnet porphyroclasts. Sample 37559 described in the petrography chapter part 5.4.4.2, was collected from this outcrop.

Compositionally these boudins vary between two extreme endmembers, pure amphibolite and fresh eclogite, where representative examples are shown in figure 5.1.13 A - D. The mineral assemblage is highly variable and consists of garnet + clinopyroxene + amphibole + plagioclase ± biotite ± calcite ± quartz. Typically exhibiting a granofelsic texture, whenever prismatic amphibole and/or biotite present a weak foliation is defined that is co-planar with that of the host

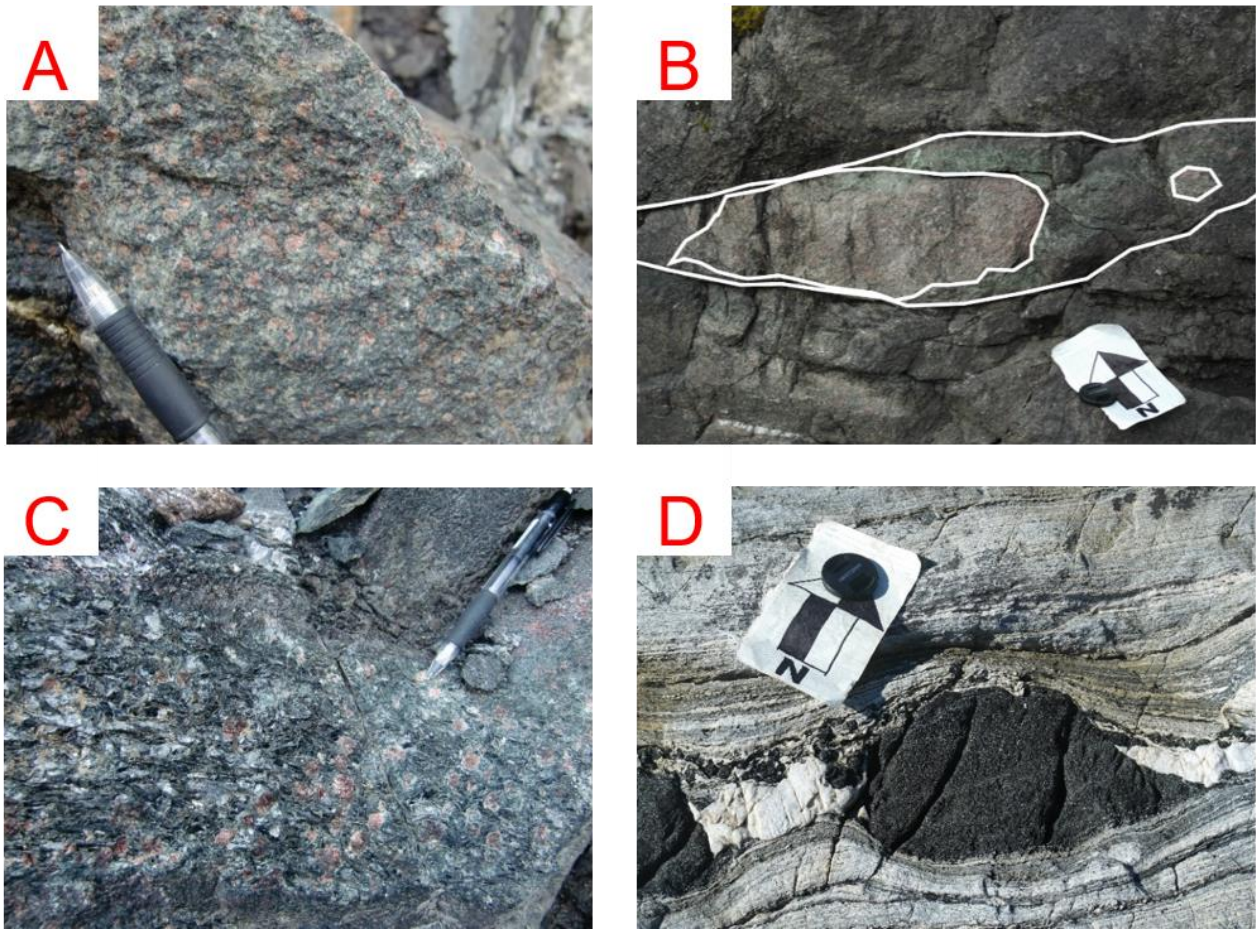

Figure 5.1.13: Photographs of various boudins, showing A) A fresh eclogite boudin in a garnet amphibolite at Hendholmen on the west coast of Averøya, B) An asymmetrical boudin with a fresh eclogitic core enveloped by an omphacite rich zone, hosted in an amphibole rich gneiss on a roadcut close to Tøvika, C) One of the few eclogite boudins observed in the migmatite gneiss on the northwestern part of Averøya, notice the high amount of amphibole and biotite in this sample and D) An asymmetrical boudin located within a layered tonalitic gneiss with pegmatitic pressure shadows, located on the Atlantic ocean road.

rock. The most well preserved eclogite assemblages are found in the cores of the boudins, showing progressively more retrogressed assemblages towards the rims, locally enveloped by a completely amphibolitized zone ranging from 1-20 cm thick. Pegmatite lenses commonly occur in the pressure shadows adjacent to the boudins.

5.1.5 Subordinate lithologies

Subordinate rock types recorded at only one locality each include gabbro, feldspathic quartzite and marble. The gabbro was described as it might reveal important information regarding source rock origins of eclogites in the study area.

The gabbro is located on the coastal part of the western extension at the mainland and has the topographic shape of a dome. Granodioritic to tonalitic migmatite gneiss are found on both sides of this rock type. This rock exhibits an ophitic texture where clinopyroxene laths up to 2cm long are spaced randomly in a plagioclase matrix, shown in figure 5.1.14. Brown weathering covers the surface and have also been observed within fractures in the rock.

Figure 5.1.14: Ophitic texture in the gabbro located on the mainland.

5.2. Structural setting

This chapter is introduced with an overview map in figure 5.2.1 showing strike and dip of foliations with corresponding trend and plunge of lineations distributed throughout the study area. This figure coupled with equal area diagrams S1-S7 and field observations, consistently shows that the structural framework is dominated by a series of ENE-WSW to NE-SW trending folds. A few isolated outcrops on the west coast of Averøya records an additional SE-NW directed folding phase. The migmatite gneiss and garnet amphibolite is dominated by a wide range of ductile structures from small- to larger-scale isoclinal to open folds, boudins and passively folded layers. The layered eclogite and the neighboring gneisses have behaved more brittlely and contain abundant tensile veins, shear zones, conjugate fractures and a few faults.

This chapter will provide a structural overview, followed by a discussion of the distribution and geometry of ductile and brittle structures, finishing with a section on kinematic indicators.

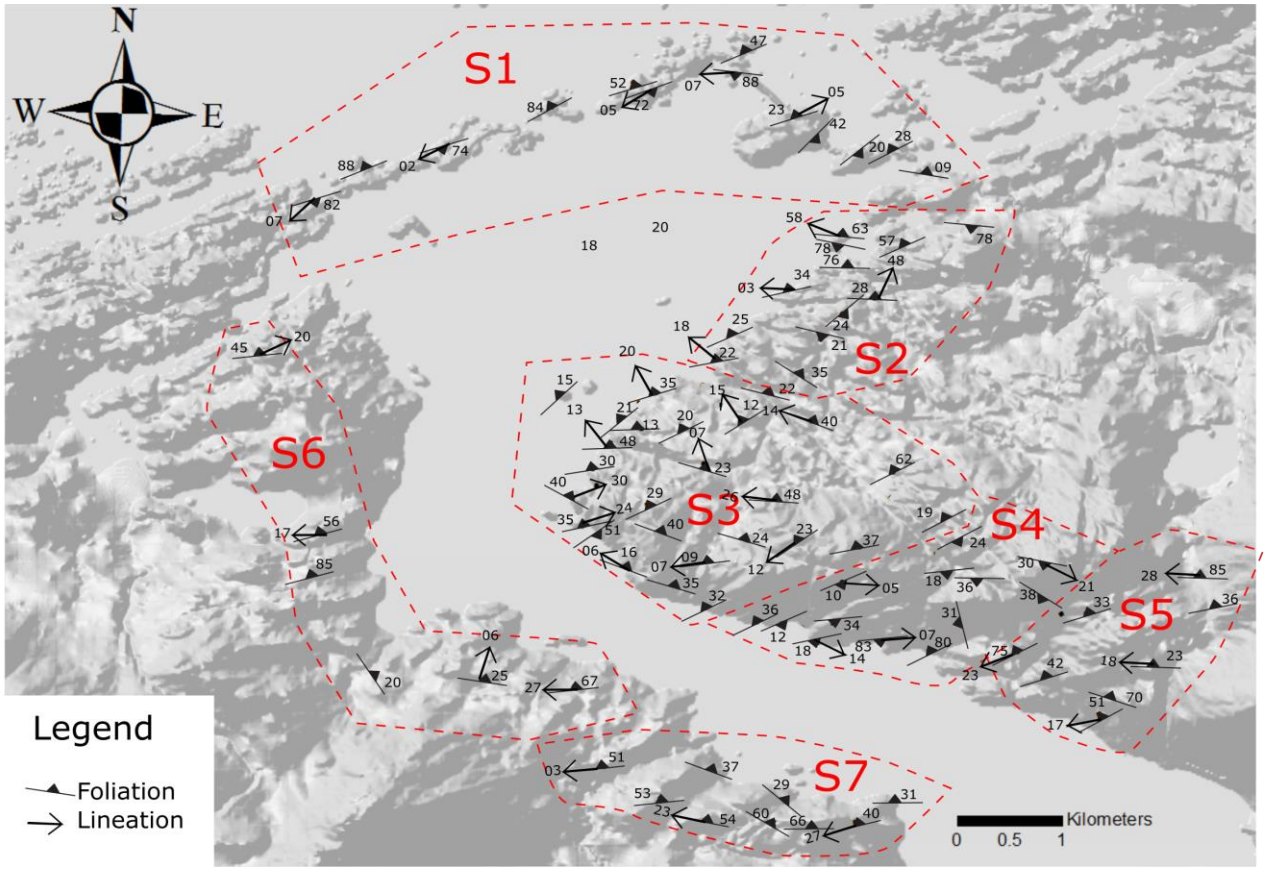

Figure 5.2.1: Strikes and dips of foliation and trend and plunge of lineations in the study area, divided into seven sections.

5.2.1 Structural overview

S1

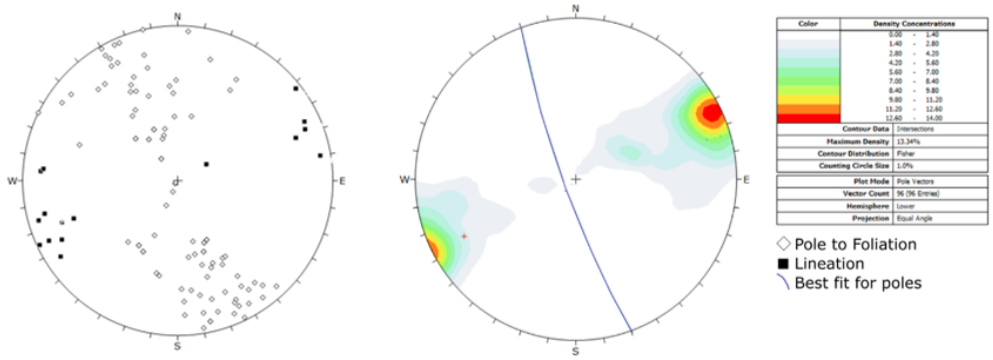

S2

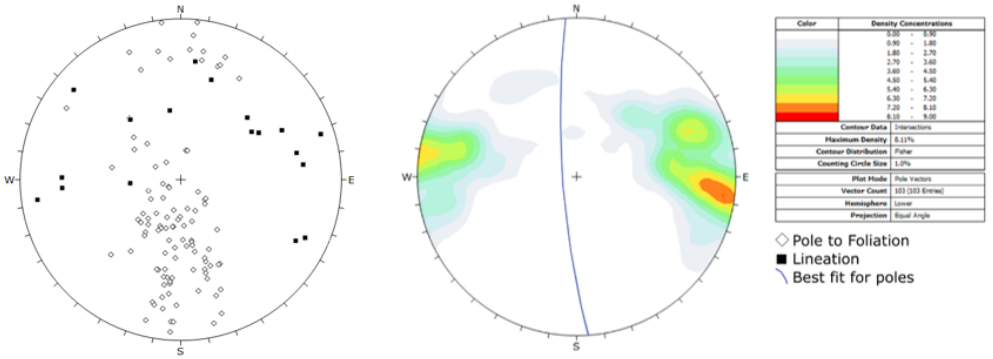

S3

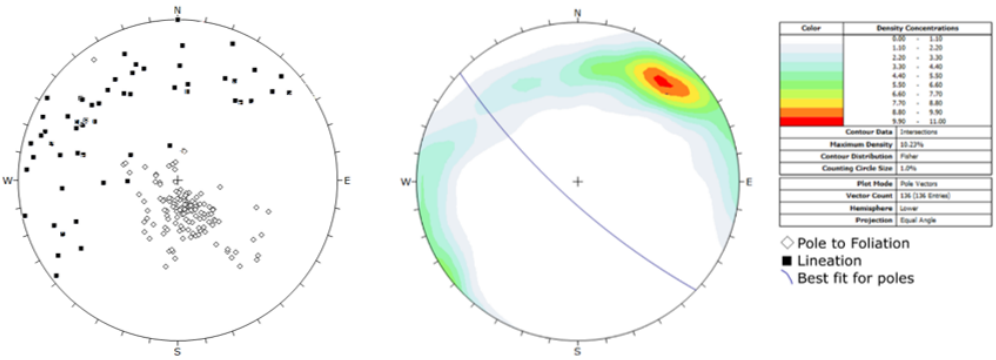

S4

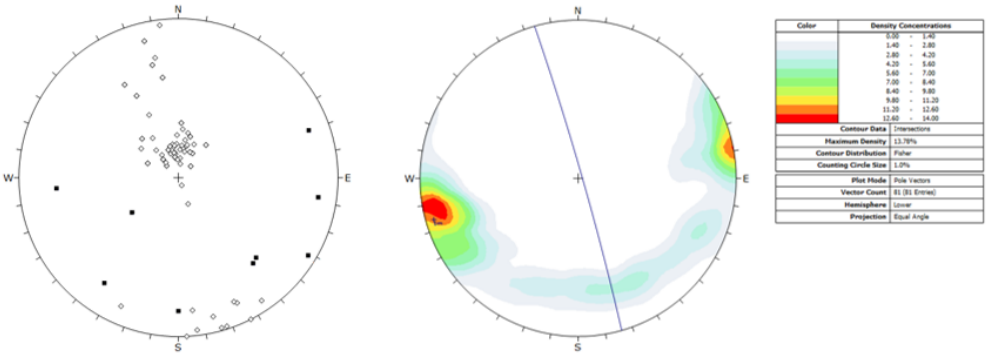

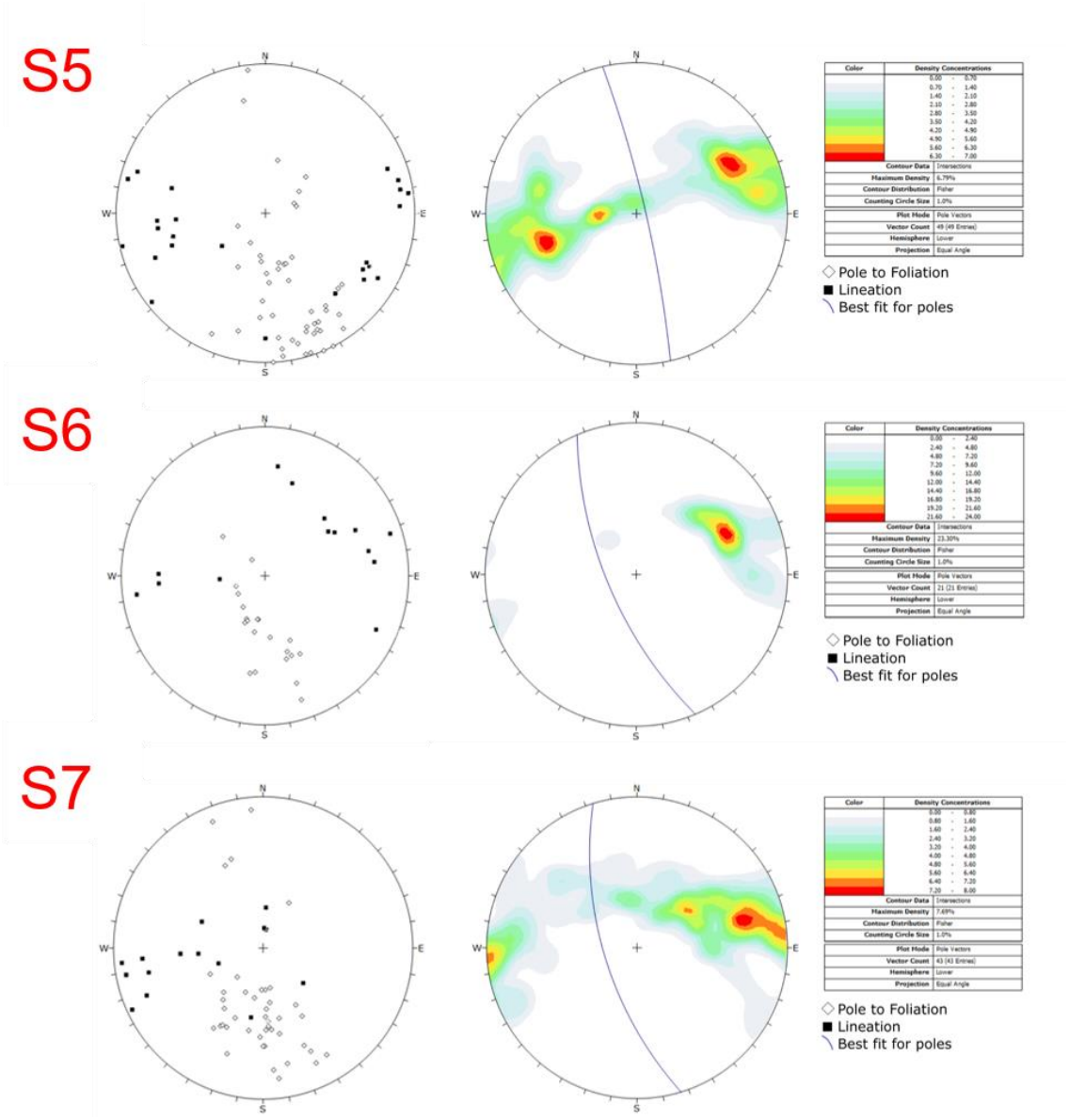

Figure 5.2.2: Summary of equal area lower hemisphere diagrams, where the corresponding distribution of these diagrams are shown in figure 5.2.1 Foliation and lineation measurements are shown in the diagram to the left and best fit for the girdle together with contoured intersections of planes are shown to the right. Showing measurements at: S1: Atlantic Ocean Road, S2: NW Averøya, S3 and S4: Layered eclogite and garnet and amphibole gneiss at Averøya, S5: South Averøya, S6: Roadcuts on the mainland and S7: Lyngstad and Visnes.

The study area was roughly divided into seven sections to improve the understanding of large-scale structural trends. With the exception of S3 and S4, all diagrams systematically show NE-SW to E-W striking foliations and moderate to steep dips. Corresponding lineations plot parallel to the strike and correlate well with the trend of the contoured intersections between planes. All these measurements were derived from migmatite or garnet amphibolite. Diagrams S3 and S4 present measurements in the layered eclogite and neighboring gneiss on Averøya. Both S3 and S4 share similar strikes to the other subareas, but are characterized by more gently dipping foliations to the NW in S3 and to the SE in S4. Lineation measurements in both of these diagrams yield highly scattered distributions, which can be seen by lineation trends on the map (figure 5.2.1). Many of these lineations plunge either to the NW or to the SE, perpendicular to the SE or NW plunging lineations observed elsewhere in the study area.

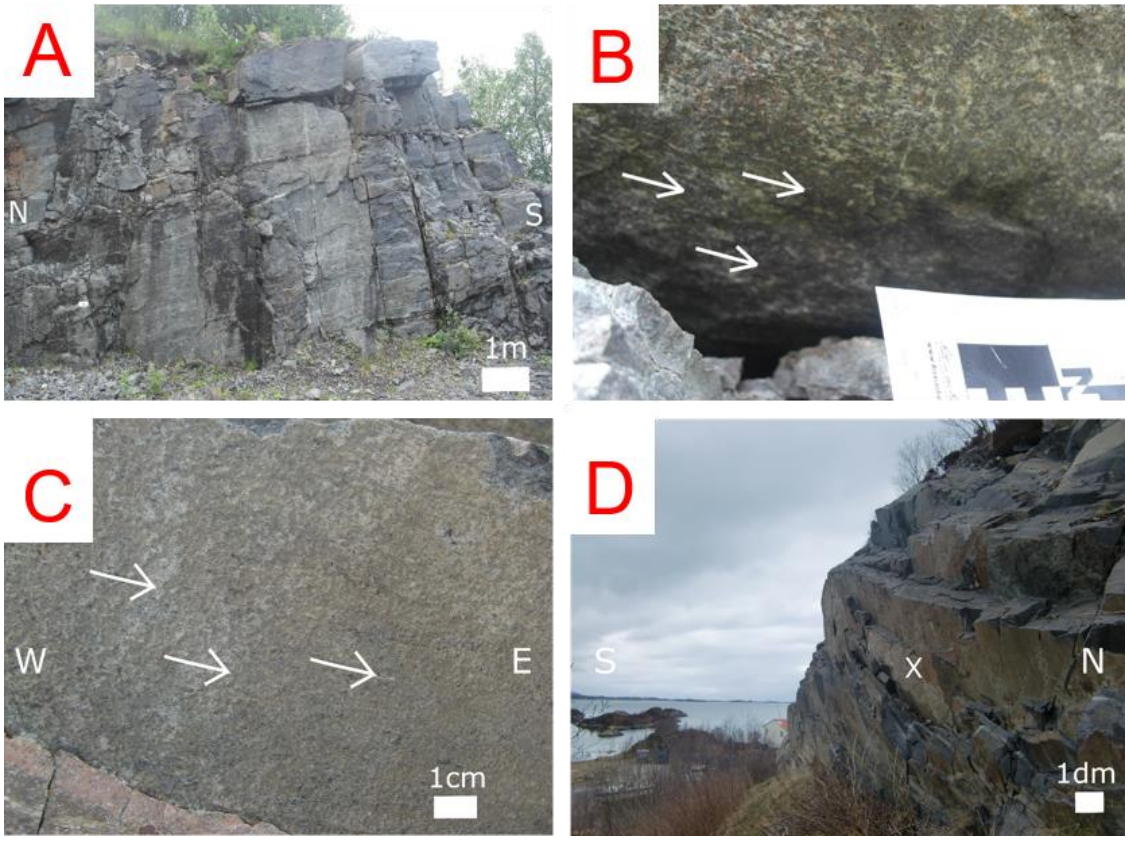

Figure 5.2.3: Selected photographs of foliations and lineations showing A) Gently north dipping foliation at the quarry locality on Averøya, B) North plunging lineation across the road from the quarry, C) Gently east plunging lineation measured in D) Steeply north dipping foliation in migmatite gneiss on the NW coast of Averøya.

5.2.2 Ductile structures

The distribution and estimation of fold axes orientations for three types of folds measured in the field, are displayed in figure 5.2.4. These include tight to open ENE-WSW trending upright folds, isoclinal to open foliation parallel folds and isolated outcrops of recumbent NW- N plunging folds. Foliation parallel folds were especially difficult to measure and because only measured folds were included in figure 5.2.4 many observations of these folds were not incorporated. A selected number of these folds and local equal area diagrams will be described, the remainder can be found in Appendix A1.

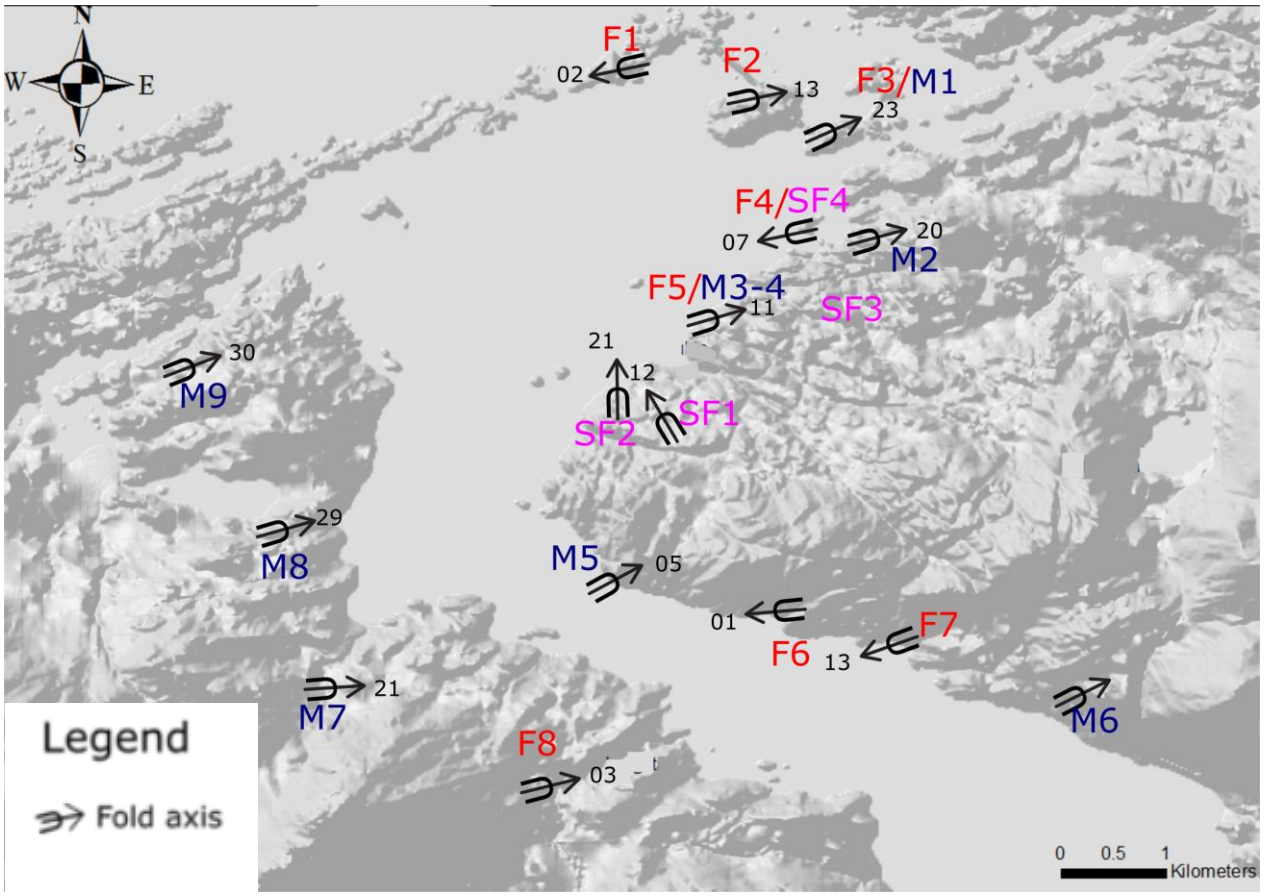

Figure 5.2.4 Estimated fold axis of various measured folds distributed throughout the study area. The different types of folds are represented with red colors for upright tight to open folds, blue for foliation parallel folds and purple for inclined to recumbent folds. When the slash symbol is used it means that foliation parallel folds occur close to upright folds

5.2.2.1 ENE – WSW folds

The ENE – WSW to E – W trending folds plunge less than 15°, characterizing upright and semi-symmetrical folds extending out laterally between a few meters to several tens of meters (Fossen, 2016). According to fold classification, these folds can be described as tight to open folds, with

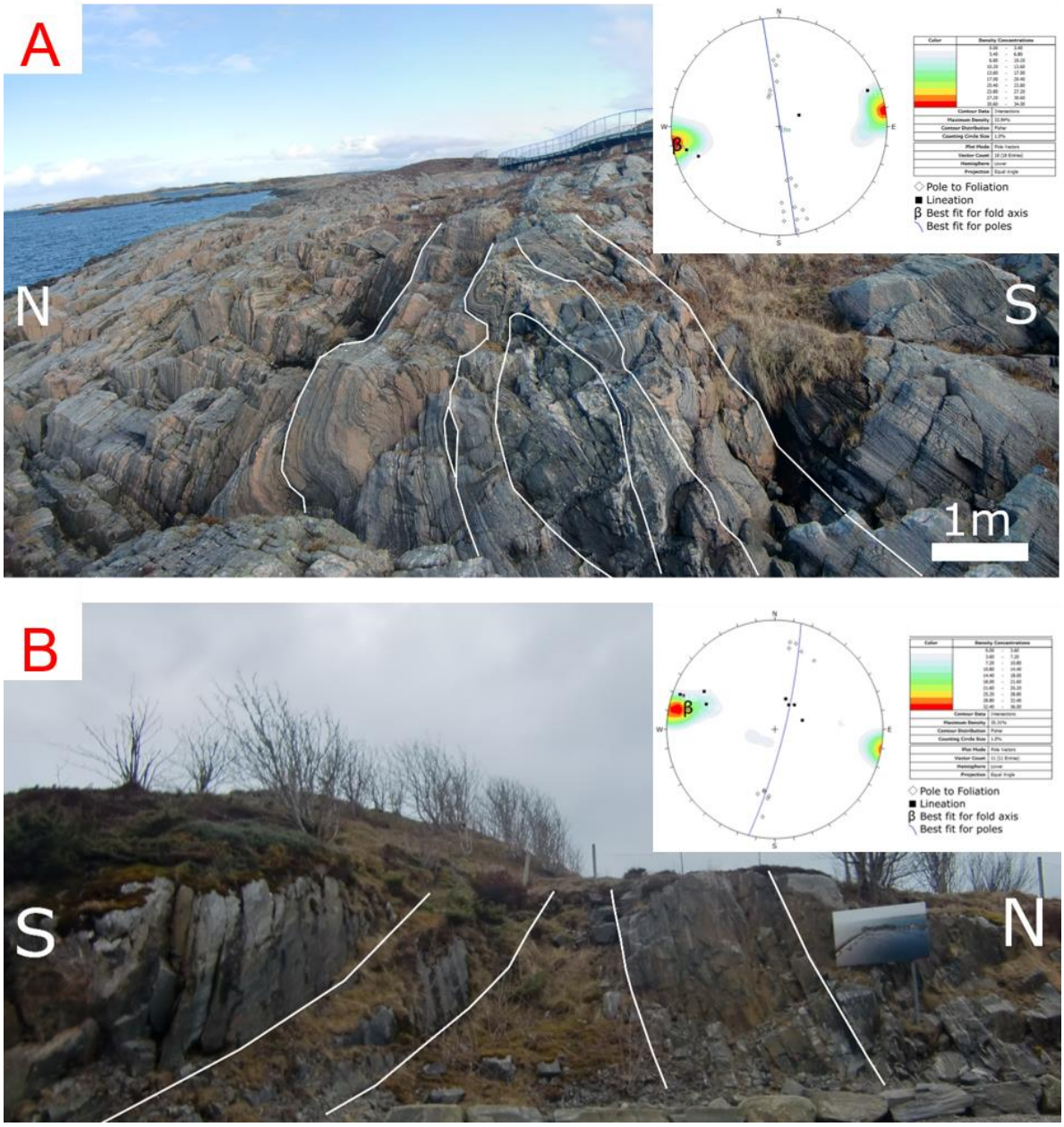

Figure 5.2.5: Photographs of selected folds from A) the Atlantic Ocean Road with belonging equal area diagram SF1 and B) From the NW coast of Averøya with belonging equal area diagram SF4 from NW coast of Averøya.

planar parallel layers. The majority of these folds were examined in the migmatite or the garnet amphibolite and were generally observed with increasing frequency towards the NW and especially on the Atlantic Ocean Road.

Two examples of these folds are depicted in figure 5.2.5 illustrating undulating limbs in fold A and planar parallel layers in B. The former encases a 2m long, lenticular boudin of amphibolite where the edge of the boudin affects the hinge area. The majority of these types of folds were observed containing variously sized boudins, including larger layered eclogite bodies described in 5.1.4.1 at Lyngstad (F8) and Hendholmen (F5). Two of these larger scale folds were discovered on the south coast of Averøya. The geometries of these folds have been inferred based on measurements taken in the immediate surroundings in the field. As seen in figure 5.2.6 A and B the resulting diagrams show ENE – WSW folds, concordant with previous findings.

Numerous of isoclinal to open foliation parallel folds are spaced intermittently within the migmatite gneiss and the garnet amphibolite. With a lateral extension of less than <5m these folds are constrained within the foliations and both estimated fold axes and measured fold axes portray similar orientations as the upright folds, with E – W to ENE – WSW trends. Only a few of these folds were measured and commonly only for three to four planes, which is not representative to conduct proper fold analysis. These equal area diagrams do however give an indication of the general orientation and geometry of these folds. Representative images of these folds throughout the study area are shown in figure 5.2.7, with an equal area diagram M4 corresponding to locality D.

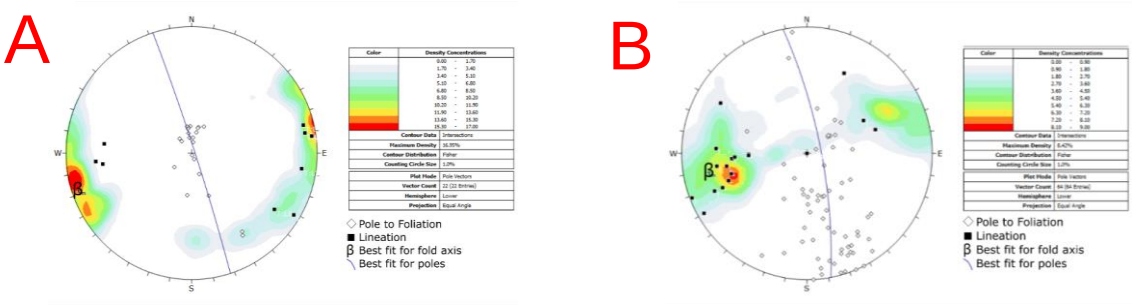

Figure 5.2.6: Lower hemisphere equal area diagrams of poles to foliations and lineations of an anticline A - F6 and a syncline B - F7, located close to Nasvika along the south coast of Averøya.

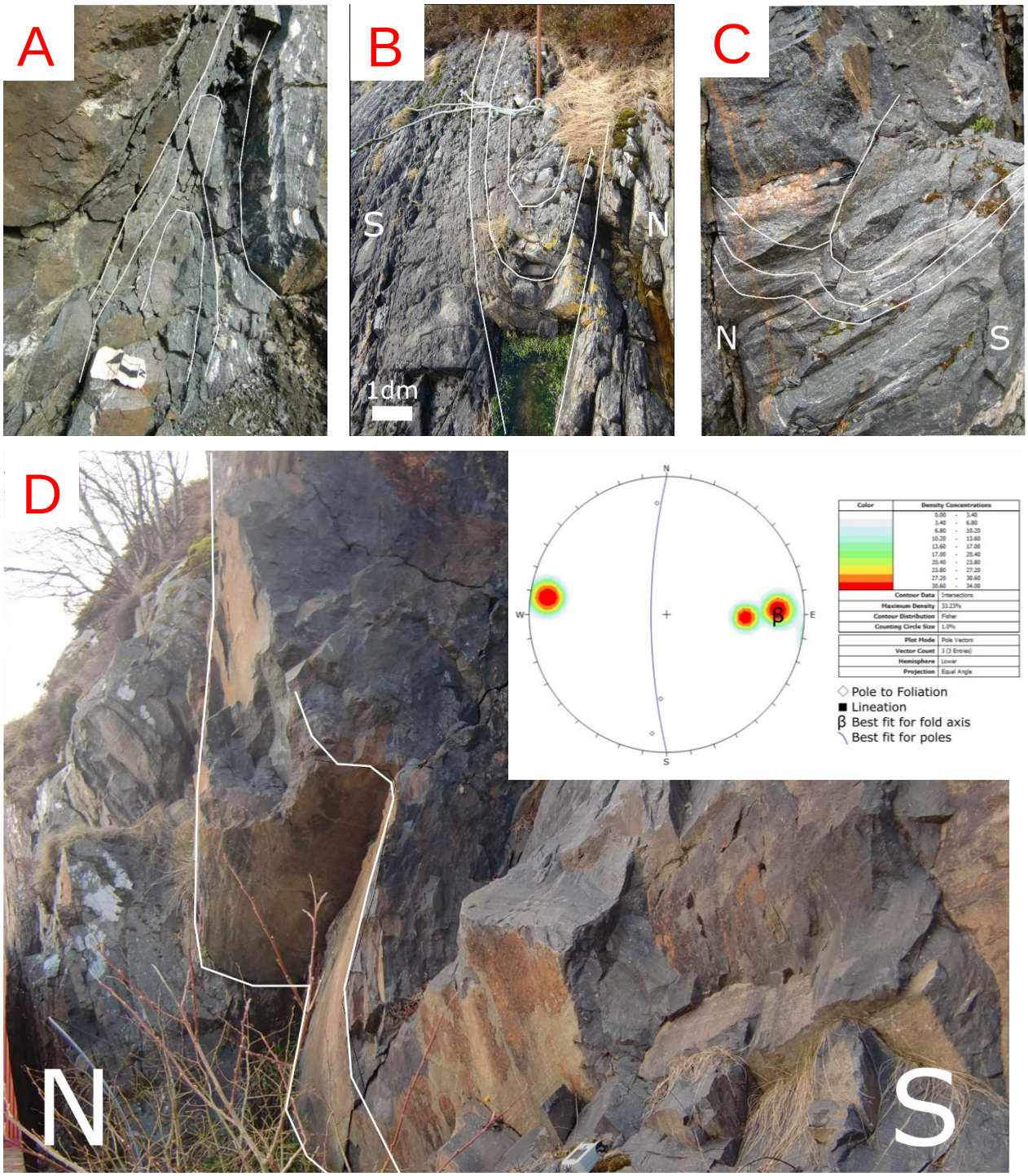

Figure 5.2.7: Photographs of various fold geometries for the foliation parallel folds, A) Upright fold in garnet amphibolite at Lyngstad, B) Upright fold in migmatite gneiss at the Atlantic Ocean road and C, D) Open folds in garnet amphibolite at Hendholmen.

5.2.2.2 NW-N folds

Four inclined to recumbent folds were observed along the western to northwestern coast of Averøya, two in the migmatite gneiss and two in the amphibole and garnet gneiss. The two folds in the garnet and amphibole gneiss were located close to each other on the west coast of Averøya, shown as SF1 and SF2 on figure 5.2.4. Fold SF1 was difficult to visualize in the field, but by measuring multiple foliation planes an inferred geometry was acquired (See figure 5.2.8 A-C). Fold SF2 has a clear isoclinal and inclined geometry, where measurements of the foliation and fold axes were easily obtained (figure 5.2.9 A and SF2). Both of these folds were plunging towards the N-NNW. It was not possible to measure the foliations or fold axes in the two folds in the migmatite (5.2.9 C and SF3), though lineations along an apparent hinge were plunging towards the NE. It remains uncertain whether all these folds formed during the same event

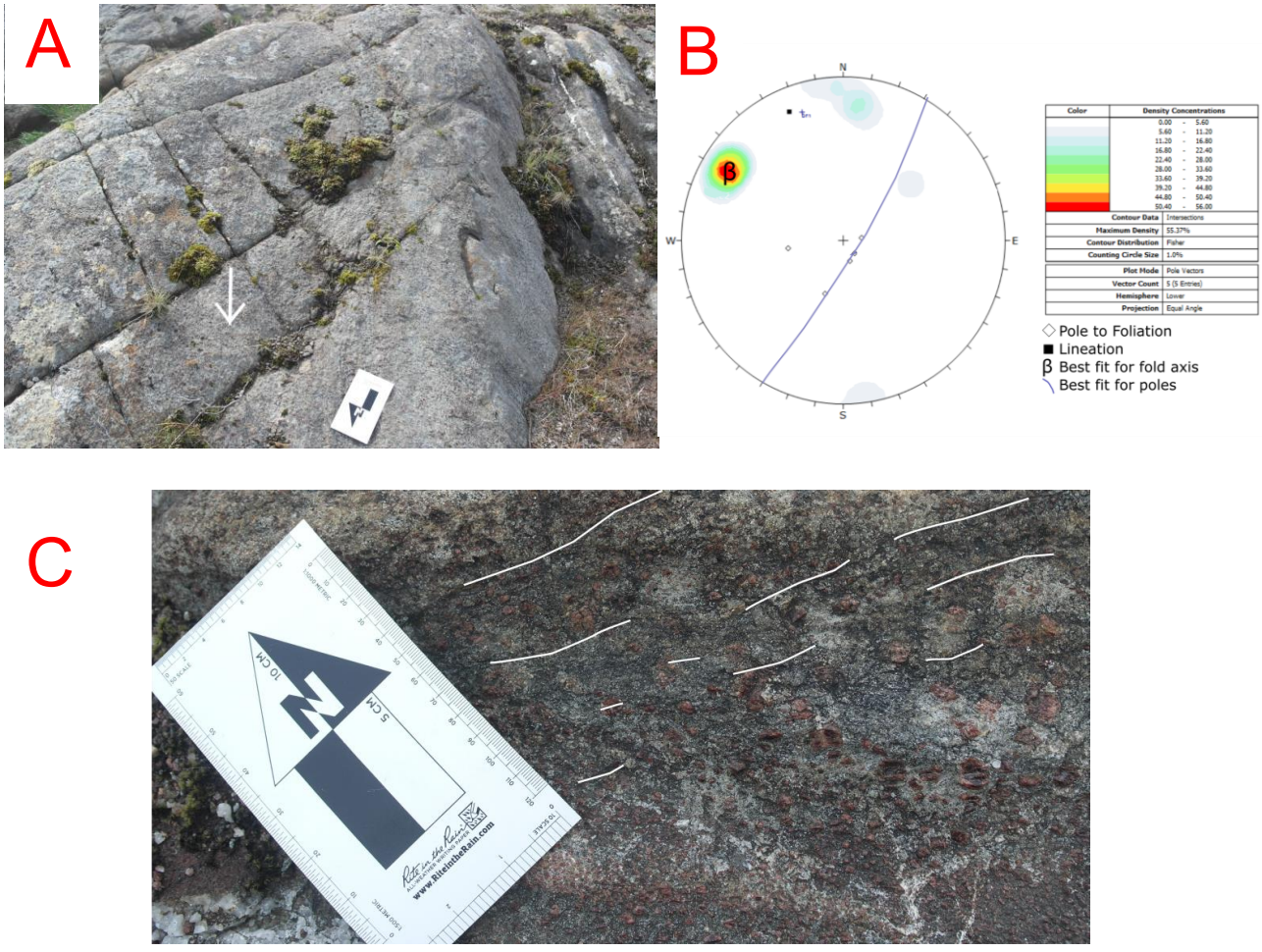

Figure 5.2.8: Fold SF1 **on the west coast of Averøya showing A and B) NNW plunging lineation and C) looking in parallel to the lineation in locality A), showing a NW fabric**

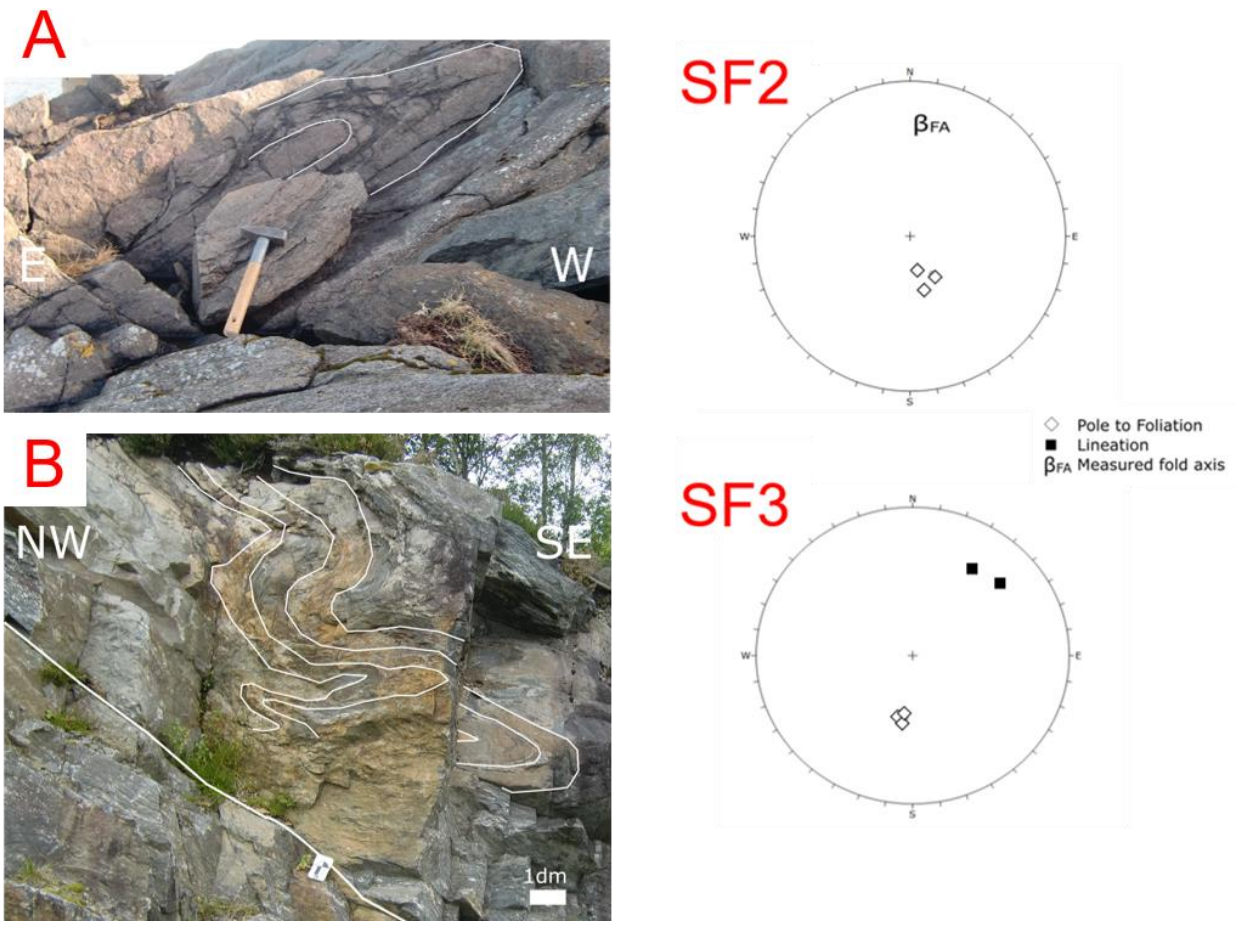

Figure 5.2.9: Photographs of inclined to recumbent folds in the field, where A) Inclined fold (SF2 in figure 5.2.4) in the garnet and amphibole gneiss and B) Corresponds to SF3 in the migmatite gneiss.

5.2.3 Brittle structures

Conjugate fractures and tensile veins are the dominating brittle structures distributed in the layered eclogite and the garnet and amphibole gneiss. Tensile veins truncate the local layering and systematically trend in a N-S to NNW – SSE direction. These veins consist predominantly of quartz, with varying amounts of accessory K-feldspar, plagioclase, biotite, amphibole and garnet. With widths up to 10 cm some of these veins are sheared by crosscutting veins trending in an E – W to NE-SW direction. Conjugate fractures dominates the entire coastal sections on Averøya, with one set of fractures trending SW separated by an angle of approximately 50° to the SE trending set. Representative photographs of these structures area are shown in figure 5.2.9 A-C.

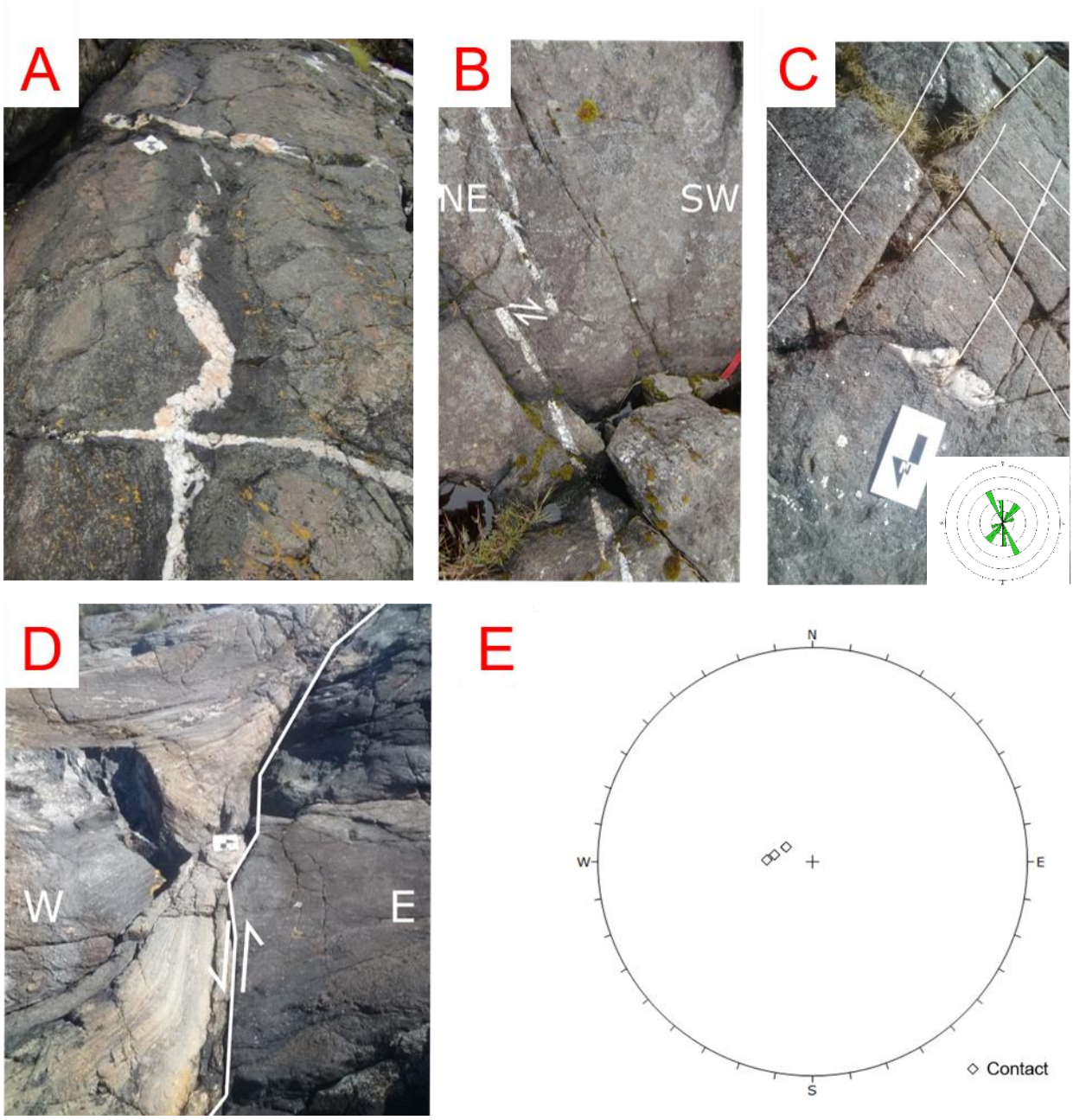

Figure 5.2.10: Photographs of brittle structures, where A) An amphibole rich gneissic host containing an N-S trending quartz vein on the south coast of Averøya, B) A tensile vein that have been crosscut and sheared by a later forming vein. C) Conjugate fractures and their orientation in relation to N in the garnet and amphibole gneiss (small rose diagram). D) Normal fault on the Atlantic Ocean Road and E) Measurements of the contact between migmatite gneiss and garnet and amphibole gneiss on the west coast of Averøya, showing an E-SE plunging contact.

One of the rare brittle structures observed in the migmatite gneiss was a normal fault, observed at the northwestern part of the Atlantic Ocean Road. Striking approximately N-S, slickenlines measured on the surface indicated a movement towards the west. The contact between the migmatite gneiss and the garnet and amphibole gneiss on the west coast of Averøya were measured at two different localities and three measurements of the poles to the foliation are shown in figure 5.2.10 B.

5.2.4 Kinematic indicators

Appendix A2 shows the distribution and the sense of shear for all kinematic indicators recorded in the field area. Structures recording shear sense include asymmetric boudins, shear zones, porphyroclasts and fabrics. Applying the method described by (Fossen, 2016) kinematic indicators were recorded when viewed within planes parallel to the lineation and perpendicular to the foliation. The great majority of these structures were registered in either migmatitic gneiss or amphibolite garnet and demonstrated sinistral sense of shear on steeply dipping structures and top to the SW shear on shallower surfaces.

A small selection of all recorded porphyroclasts are displayed in fig 5.2.9, displaying top to the W-SW sense of shear in all outcrops. Image 5.2.9 A) shows both sigma and delta porphyroclasts in a garnet amphibolite, close to where the oriented thin section was collected. The microphotographs inn 5.2.9B and C come from one oriented sample (sampled from the locality 5.2.9A) that was collected in the garnet amphibolite and yields a seemingly ambiguous sense of shear. Several rotational garnets, pressure shadows around porphyroclasts of garnet and the overall sense of shear for porphyroclasts all consistently indicate a SW sense of shear, whereas localized shear bands may reflect a dextral top to the NE sense of shear. Two additional photographs shows (figure 5.2.9 D) sinistral and top to the SW sense of shear (5.2.9 E).

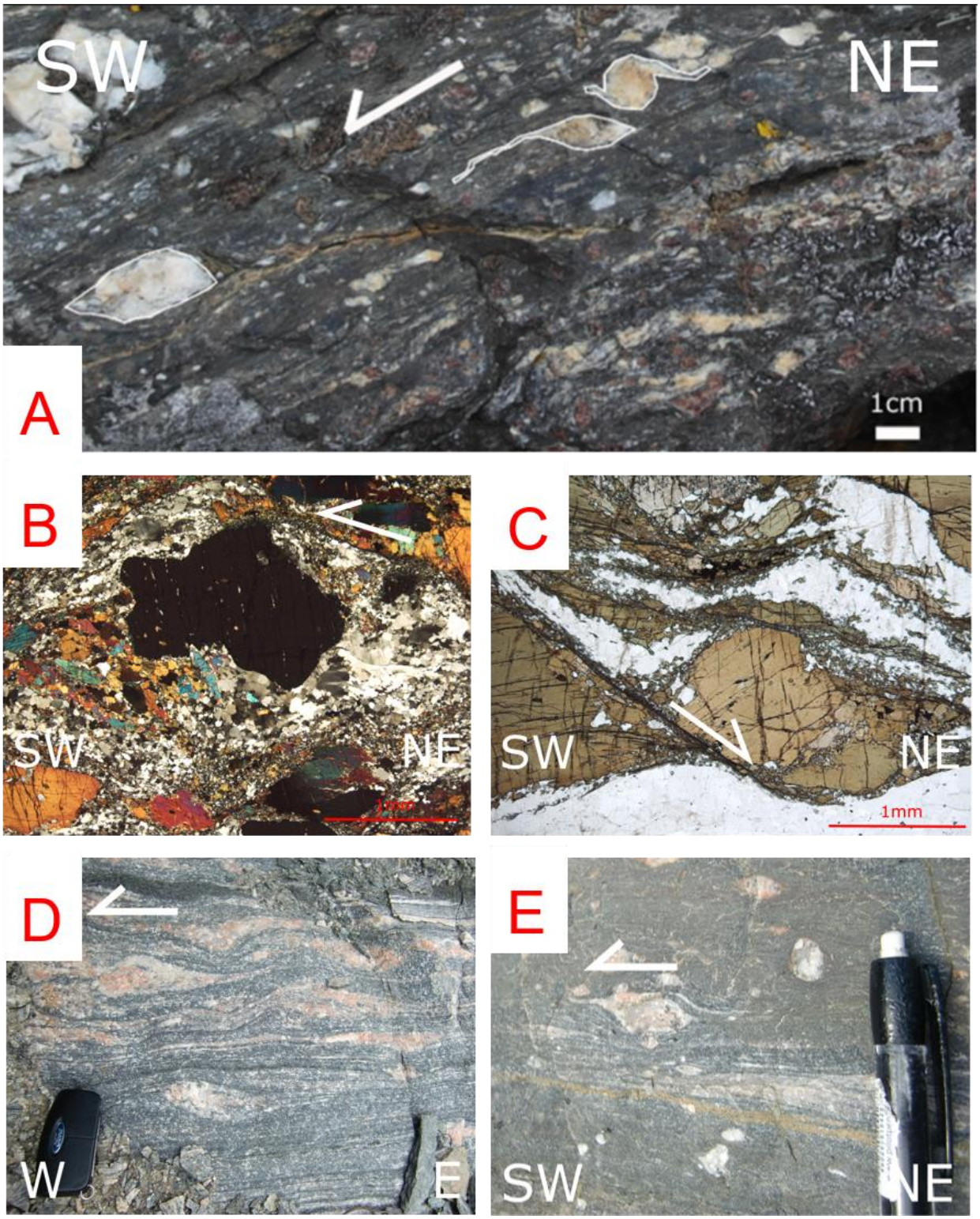

Figure 5.2.11: Outcrop photographs of A) sigma and delta clast in a garnet amphibolite at Nasvika, B and C) Microtextures in the same garnet amphibolite, D) sinistral sense of shear on the NW coast of Averøya and E) top to the SW sense of shear at Lyngstad.

5.3. Mineral chemistry

The chemical compositions of minerals were analyzed in nine thin sections. This included boudin eclogite samples 37559, 37555 and 37600, layered eclogite samples 37560 and 37598, gabbro sample 37554 and various gneiss samples 37601, 37602 and 37698. Garnet, pyroxene, plagioclase and amphibole are the main minerals in the majority of the samples and will be described in detail, with representative analyses shown in table 5.3.1, 5.3.2, 5.3.3 and 5.3.4. NCFMASH projection of the main minerals and analyses from accessory minerals can be found in appendix C, including phengite, biotite, epidote, kyanite, spinel, corundum and rutile.

5.3.1 Garnet

Representative analysis of garnets from all samples are shown in table 5.3.1 and have been plotted in a Mg + Fe + Ca + Mn diagram. All analyses of garnet in eclogite samples correspond to type B eclogite according to the eclogite classification diagram corresponding (Coleman et al., 1965) (figure 5.3.1) with some of the boudin samples bordering onto the type A eclogite field. Garnets in these samples are typically coarse grained, poikioblastic, exhibiting subhedral to anhedral shapes. The majority of the analyses from 37559, 37555 and 37600 yielded high totals in the range of 101-103. A representative core analysis from sample 37559 yields Alm_{27}, Grs_{19}, Py_{53}, Sp_1 with a corresponding rim of Alm_{29}, Grs_{20}, Py_{50}, Sp_1. This trend is also evident in sample 37555, where both samples show an increase in the $Fe^{2+}/(Mg + Fe^{2+})$ ratio from core to rim.

The two samples from the layered eclogite consist of flattened euhedral to subhedral, fine- to medium-grained garnets containing few inclusions. These have lower Mg and slightly higher Ca than the boudin samples. A typical core to rim relationship in this sample is Alm_{34}, Grs_{24}, Prp41 for a selected core and Alm_{35}, Grs_{22}, Prp_{42}, Sp_1 for the corresponding rim. This suggests a slightly decreasing to unaffected $Fe^{2+}/(Mg + Fe^{2+})$ towards the rim.

Sample 37554 contains euhedral garnet growing as a coronitic rim between clinopyroxene and plagioclase. Samples 37601, 37602 and 37698 consist of different gneissic rocks, clearly reflected by different compositions on the diagram. Where 37601 plots well within the type B field with high Mg, 37602 and 37698 remains in field C. All garnets exhibit subhedral to euhedral shapes, varying in sizes from fine-grained specimens in 37602 and 37698 to coarse-grained in 37601. Garnets in samples 37601 and 37698 are fragmented with alteration along

fracture zones and containing several inclusions. Core to rim relationship have not been established, though there is an obviously strong Ca zonation in sample 37601.

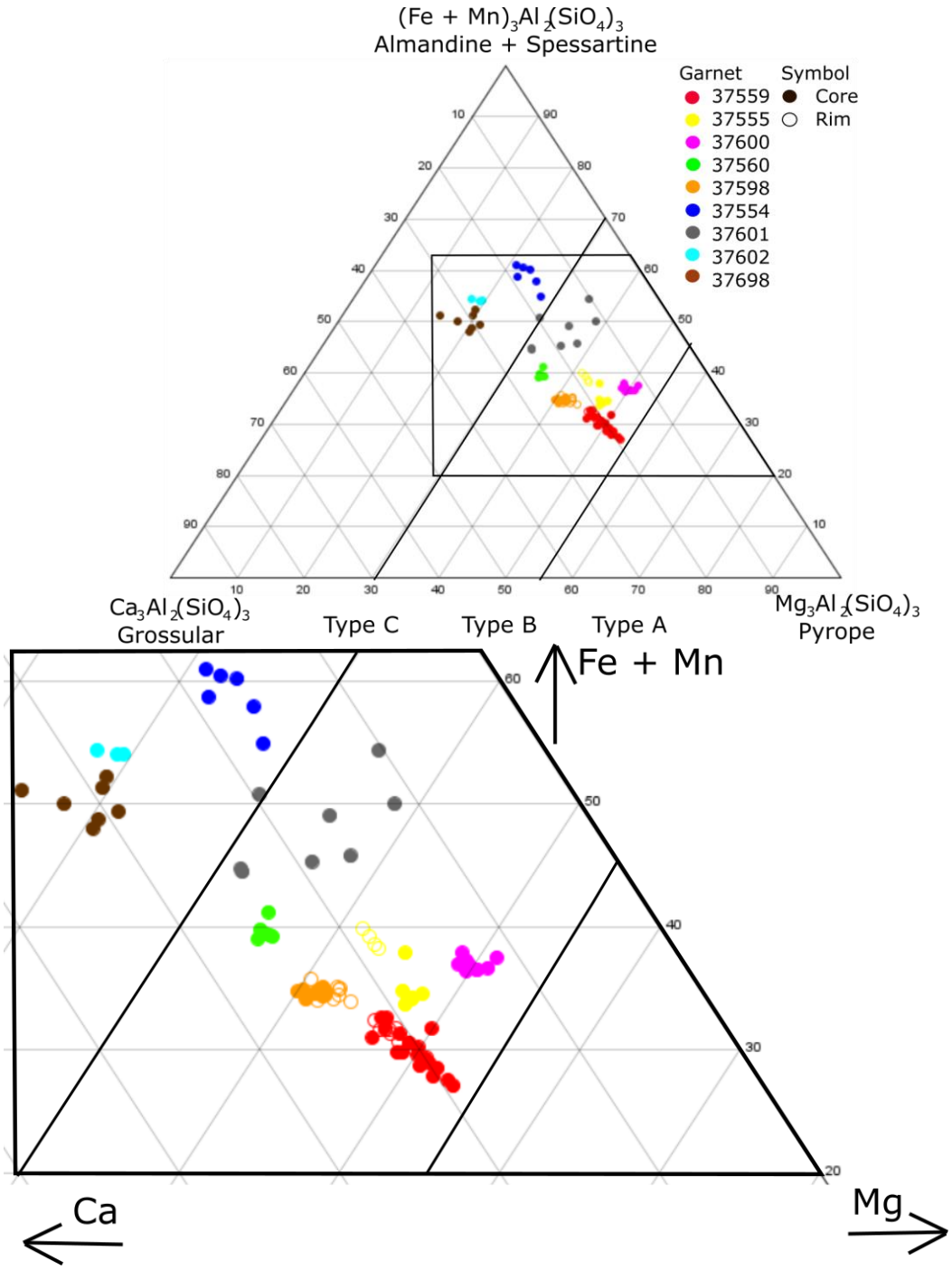

Figure 5.3.1: Garnet formulations normalized to 8 cations and plotted using the classification diagram from (Coleman et al., 1965). Core compositions are shown with filled circles and rim compositions are shown with open circles.

Garnet Analyses

Sample	37559 (6.3) rim	37559 (6.4) core	37555 (4.2) rim	37555 (4.3) core	37598 (4.3) rim	37598 (4.2) core	37554 (5.11) grain	37601 (3.2) grain	37602 (5.1) grain
SiO2	41.132	41.282	40.32	40.885	40.67	40.61	38.28	39.02	39.19
Al2O3	22.97	22.84	22.40	22.89	22.79	22.71	20.90	21.87	21.78
TiO2	0.00	0.02	0.00	0.03	0.02	0.07	0.03	0.00	0.00
Cr2O3	0.19	0.17	0.04	0.06	0.11	0.08	0.06	0.03	0.02
Fe2O3	2.96	2.58	2.64	2.69	0.57	0.00	0.00	22.19	24.80
MgO	14.56	15.29	12.03	13.61	11.64	11.14	5.85	9.63	5.38
FeO Total	15.00	14.15	19.22	17.49	17.02	16.64	27.26	21.85	22.38
FeO	12.34	11.83	16.85	15.07	16.51	16.64	27.26	21.85	22.38
MnO	0.45	0.33	0.46	0.40	0.33	0.32	1.14	0.44	0.62
CaO	7.96	7.79	7.21	6.94	8.60	9.00	6.81	7.16	11.41
Na2O	0.04	0.00	0.04	0.06	0.01	0.05	0.04	0.04	0.03
K2O	0.01	0.00	0.02	0.00	0.00	0.01	0.00	0.01	0.01
Total	102.32	101.87	101.85	102.43	101.24	100.63	100.37	100.05	100.82
Si	2.95	2.96	2.96	2.95	3.00	3.02	2.98	2.96	3.00
Al (IV)	0.01	0.01	0.01	0.01	0.00	0.00	0.01	0.01	0.00
Al (VI)	1.94	1.93	1.95	1.94	1.94	1.96	1.92	1.95	1.97
Ti	0.00	0.00	0.00	0.00	0.01	0.00	0.00	0.00	0.00
Cr	0.01	0.01	0.00	0.00	0.01	0.01	0.00	0.00	0.00
Mg	1.56	1.63	1.32	1.47	1.32	1.23	0.68	1.09	0.61
Fe2+	0.74	0.71	1.03	0.91	1.03	1.03	1.65	1.25	1.40
Mn	0.03	0.02	0.02	0.02	0.03	0.02	0.07	0.03	0.04
Ca	0.61	0.60	0.54	0.76	0.57	0.72	0.57	0.58	0.94
Na	0.01	0.00	0.00	0.01	0.00	0.00	0.01	0.01	0.00
K	0.00	0.00	0.00	0.00	0.00	0.00	0.00	0.00	0.00
Cat Total	8.00	8.00	8.00	8.00	8.00	8.00	8.00	8.00	8.00
Xprp	0.50	0.53	0.42	0.47	0.42	0.41	0.22	0.35	0.20
Xalm	0.29	0.27	0.38	0.34	0.35	0.34	0.57	0.45	0.47
Xgrs	0.20	0.19	0.18	0.17	0.22	0.24	0.18	0.19	0.31
Xspss	0.01	0.01	0.01	0.01	0.01	0.01	0.02	0.01	0.01
FM	0.37	0.34	0.47	0.42	0.45	0.46	0.72	0.56	0.70

Table 5.3.1: Representative analyses of garnet, where endmembers Xprp = pyrope, Xalm = almandine, Xgrs = grossular, Xspss = spessartine and FM = $Fe^{2+}/(Mg + Fe^{2+})$

Pyroxene analysis	37559 3.2 sym	37559 3.7 grain	37555 4.5 sym.	37555 5.1 neck	37555 3.1 grain	37560 5.6 sym	37560 5.2 grain	37554 6.1 Opx lam	37554 6.2 grain	37554 6.4 corona	37601 1.3 grain
SiO2	53.41	53.87	53.35	51.99	52.62	52.13	54.87	52.17	50.99	51.81	49.93
Al2O3	3.90	6.24	2.89	5.73	7.72	5.59	9.38	1.31	3.39	3.37	6.19
TiO2	0.25	0.24	0.04	0.26	0.22	0.34	0.02	0.04	0.19	0.28	0.31
Cr2O3	0.44	0.54	0.02	0.02	0.03	0.17	0.09	0.00	0.01	0.00	0.00
Fe2O3	1.75	2.52	2.29	2.09	2.37	3.46	2.30	4.45	4.29	3.49	3.00
MgO	16.45	14.66	15.80	14.79	13.18	14.09	11.65	22.50	13.92	13.69	11.27
FeTot	3.17	2.71	5.22	5.54	3.90	4.94	2.97	25.08	9.71	11.31	10.08
FeO	1.60	0.45	3.16	3.66	1.77	1.83	0.90	21.07	5.85	8.17	7.38
MnO	0.00	0.02	0.05	0.05	0.02	0.01	0.01	0.31	0.14	0.14	0.25
CaO	22.23	20.22	20.66	20.11	18.88	20.88	15.90	0.59	21.10	19.30	21.17
Na2O	1.02	2.62	1.27	1.40	2.94	1.92	5.09	0.04	0.70	1.03	1.11
K2O	0.00	0.00	0.03	0.03	0.00	0.01	0.00	0.00	0.02	0.01	0.00
Total	101.03	101.37	99.55	100.13	99.74	100.42	100.21	102.48	100.59	100.93	100.60
Si	1.92	1.91	1.95	1.89	1.90	1.89	1.95	1.91	1.89	1.91	1.85
Ti	0.01	0.01	0.00	0.01	0.01	0.01	0.00	0.00	0.01	0.01	0.01
Al IV	0.08	0.09	0.05	0.11	0.10	0.11	0.05	0.06	0.11	0.15	0.15
AlVI	0.08	0.17	0.08	0.14	0.00	0.13	0.34	0.00	0.03	0.12	0.00
Cr	0.01	0.02	0.00	0.00	0.00	0.00	0.00	0.00	0.00	0.00	0.00
Fe2+	0.01	0.02	0.00	0.00	0.00	0.00	0.00	0.00	0.00	0.00	0.00
Fe3+	0.05	0.07	0.06	0.06	0.06	0.09	0.06	0.09	0.12	0.10	0.08
Mn	0.00	0.00	0.00	0.00	0.00	0.00	0.00	0.01	0.00	0.00	0.01
Mg	0.85	0.74	0.86	0.80	0.70	0.76	0.60	0.91	0.77	0.75	0.62
Ca (	0.85	0.77	0.81	0.78	0.73	0.81	0.60	0.02	0.84	0.83	0.84
Na (4)	0.07	0.18	0.09	0.10	0.21	0.13	0.35	0.00	0.05	0.06	0.08
Cat tot	4.00	4.00	4.00	4.00	4.00	4.00	4.00	4.00	4.00	4.00	4.00
Xq	0.93	0.81	0.91	0.90	0.78	0.86	0.64	1.00	0.95	0.92	0.91
Xjd	0.06	0.15	0.06	0.08	0.18	0.10	0.31	0.00	0.03	0.05	0.06
Xae	0.02	0.04	0.03	0.02	0.04	0.04	0.05	0.00	0.02	0.03	0.02
FM	0.05	0.02	0.10	0.12	0.07	0.07	0.04	0.34	0.19	0.25	0.27

Table 5.3.2: Representative analyses of pyroxene, where endmembers Xq = quad (Ca + Mg + Fe), Xjd = jadeite, Xae = aegirine and FM = $Fe^{2+}/(Mg + Fe^{2+})$

Plagioclase analyses

	37559 2.8 inc	37559 3.5 sym	37555 2.2 sym	37555 6.4 moat	37560 6.2 sym	37554 5.10 matrix	37554 6.4 corona	37601 4.4	37698
SiO2	51.68	59.38	56.33	58.99	62.44	52.73	60.52	62.20	64.26
TiO2	0.05	0.00	0.00	0.00	0.00	0.00	0.00	0.00	0
Al2O3	29.50	23.85	20.93	25.14	24.02	27.79	23.71	26.08	18.608
Cr2O3	0.03	0.06	0.00	0.00	0.00	0.00	0.00	0.00	0.025
FeO	0.21	0.15	0.22	0.29	0.20	1.00	0.64	0.19	0.055
MnO	0.00	0.00	0.00	0.03	0.02	0.01	0.06	0.01	0
MgO	0.10	0.30	0.10	0.07	0.03	0.09	0.08	0.01	0
CaO	12.13	6.36	4.69	7.29	5.40	11.62	5.95	5.90	
Na2O	3.87	7.36	8.25	7.44	8.57	4.96	8.15	5.14	1.181
K2O	0.04	0.00	0.02	0.05	0.02	0.07	0.32	0.31	15.283
Total	97.63	97.49	90.56	99.36	100.72	98.36	99.47	99.84	99.41
Si	2.40	2.71	2.77	2.73	2.75	2.79	2.73	2.73	2.98
Ti	0.00	0.00	0.00	0.00	0.00	0.00	0.00	0.00	0.00
Al	1.61	1.28	1.21	1.25	1.25	1.21	1.26	1.35	1.02
Cr	0.00	0.00	0.00	0.00	0.00	0.00	0.00	0.00	0.00
Mg	0.00	0.00	0.00	0.00	0.00	0.00	0.00	0.00	0.00
Fe Total	0.00	0.01	0.00	0.01	0.00	0.00	0.00	0.00	0.00
Mn	0.00	0.00	0.00	0.00	0.00	0.00	0.00	0.00	0.00
Ca	0.60	0.31	0.25	0.28	0.26	0.00	0.29	0.28	0.00
Na	0.35	0.65	0.79	0.71	0.73	0.29	0.71	0.44	0.11
K	0.00	0.00	0.00	0.00	0.00	0.71	0.02	0.02	0.90
tot cat.	4.97	4.98	5.02	5.00	4.99	5.01	5.01	4.82	5.01
Xor	0.00	0.00	0.00	0.00	0.00	0.00	0.02	0.02	0.89
Xan	0.63	0.32	0.24	0.35	0.26	0.56	0.28	0.38	0.00
Xab	0.37	0.68	0.76	0.65	0.74	0.43	0.70	0.60	0.11

Table 5.3.3: Representative analyses of plagioclase, where endmembers Xor = orthoclase, Xan = anorthite and Xab = albite

5.3.2 Pyroxene

All pyroxene analyses were plotted in a Na-Ca classification diagram by the method devised by (Morimoto, 1988). A summary of all pyroxene compositions from all samples have been plotted in figure 5.3.2A, where solid lines separates the different types of pyroxene. Dashed lines outline a triangle that have been enlarged showing the compositions of pyroxene in B) boudin eclogite samples 37559, 37555 and 37600, C) layered eclogite samples 37560 and 37598 and D) gabbro and two gneisses. Representative pyroxene analyses of these rock types are displayed in table 5.3.2, differentiating between grain, lam = lamella, sym = symplectite and neck = necklace compositions. Host to symplectite properties were investigated rather than core to rim properties.

Pyroxenes in the boudin samples are typically coarse-grained and equant, with minor vermicular symplectites forming along the grain boundaries. The majority of the boudin samples systematically show host compositions of Xjd = 20% just within the omphacite field, with symplectites in the range of Xjd = 2-10%.

A similar, though not so consistent trend is shown for the pyroxene grains in layered eclogites. These grains are generally subhedral, quite coarse-grained and variously symplectized, which commonly complicates distinguishing between host and symplectite phases. A typical Xjd = 20 – 35% for host grains and Xjd = 5 – 20% for symplectites.

There are three different types of pyroxenes in sample 37554: coarse-grained clinopyroxene laths, slightly Na enriched corona clinopyroxene and orthopyroxene lamellae. The coarse-grained clinopyroxenes contain abundant orthopyroxene lamellae, which are quite enriched in Mg + Fe plotting in the uppermost corner of figure 5.3.3B. A slight increase in Na seems indicated in the pyroxene coronitic rim along the edge of the clinopyroxene, though there are only two analyses. Both the orthopyroxene lamellae and the Na – clinopyroxene corona have been given open triangles in figure 5.3.3 B).

Pyroxene in the gneiss samples are typically irregular and dusty looking. There are only four analyses of these, plotting in the uppermost Quad field for sample 37602 and with a Xjd = 22% for the only analysis in sample 37698.

A

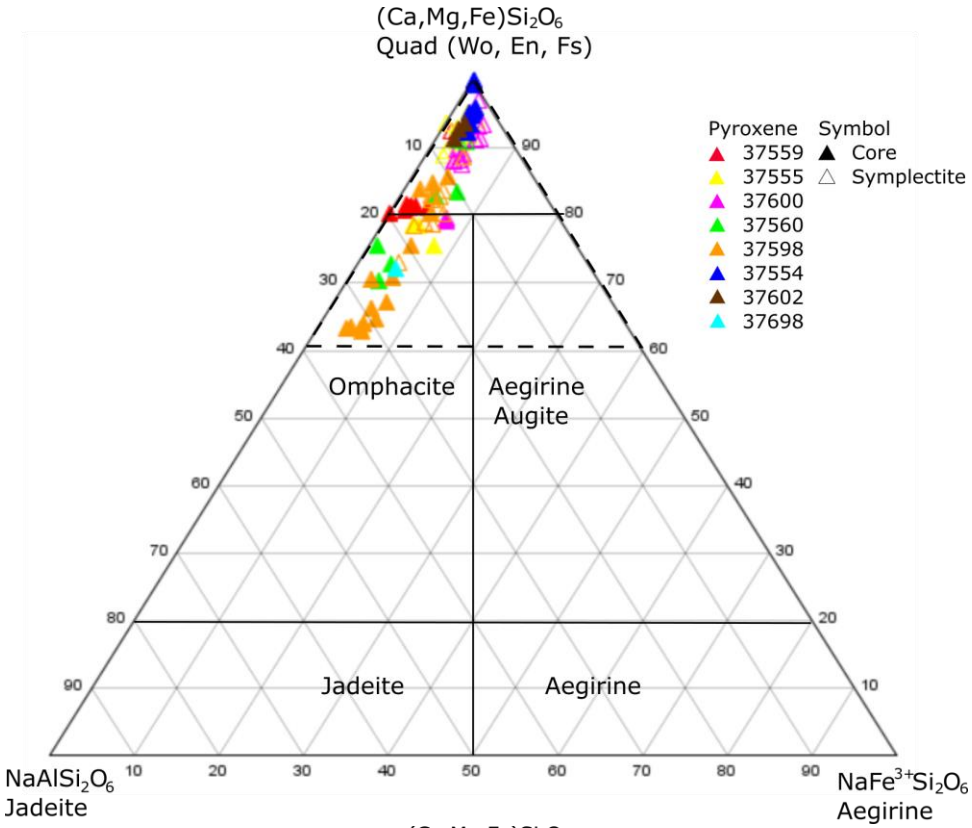

B

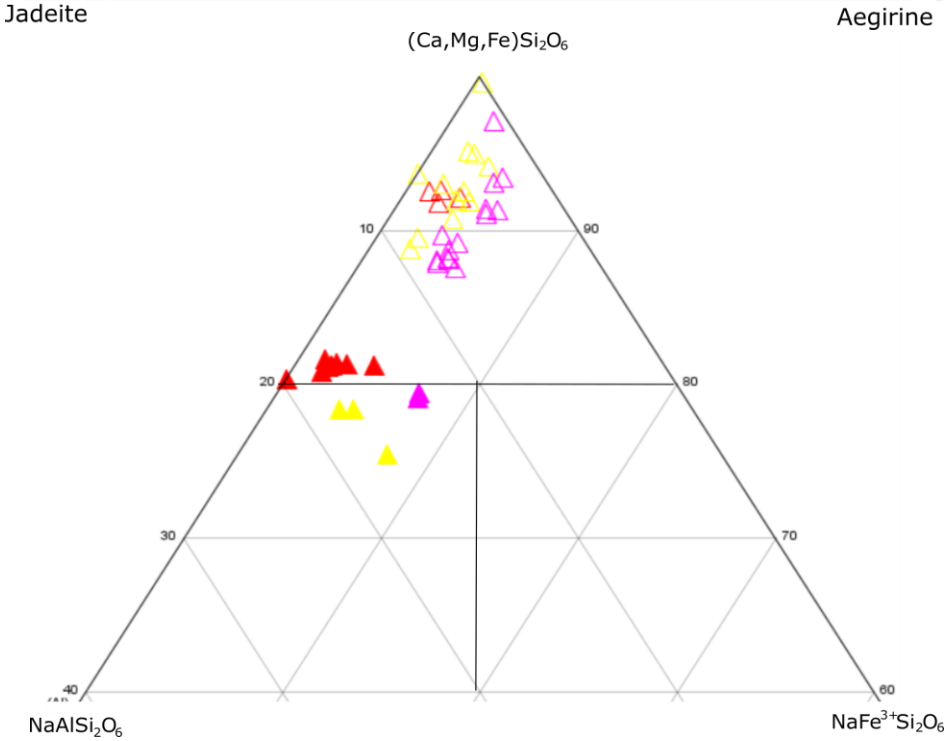

Figure 5.3.2: A) Summary diagram of all pyroxene analyses, where dashed triangle marks the outline of the enlarged diagram with and open tringles show grain compositions and open triangles show symplectite compositions. B) Pyroxene in boudin eclogite samples.

A

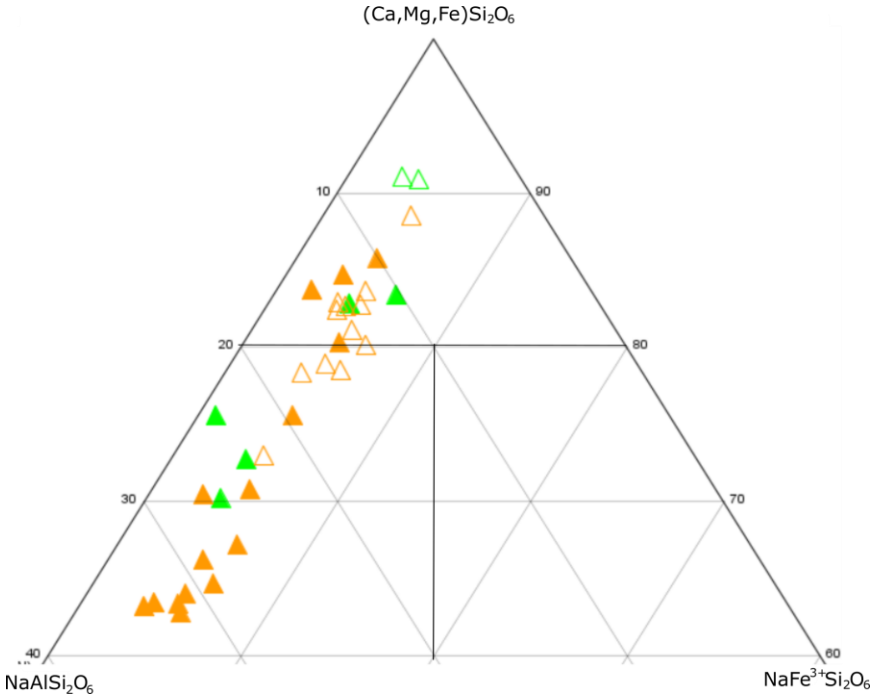

B

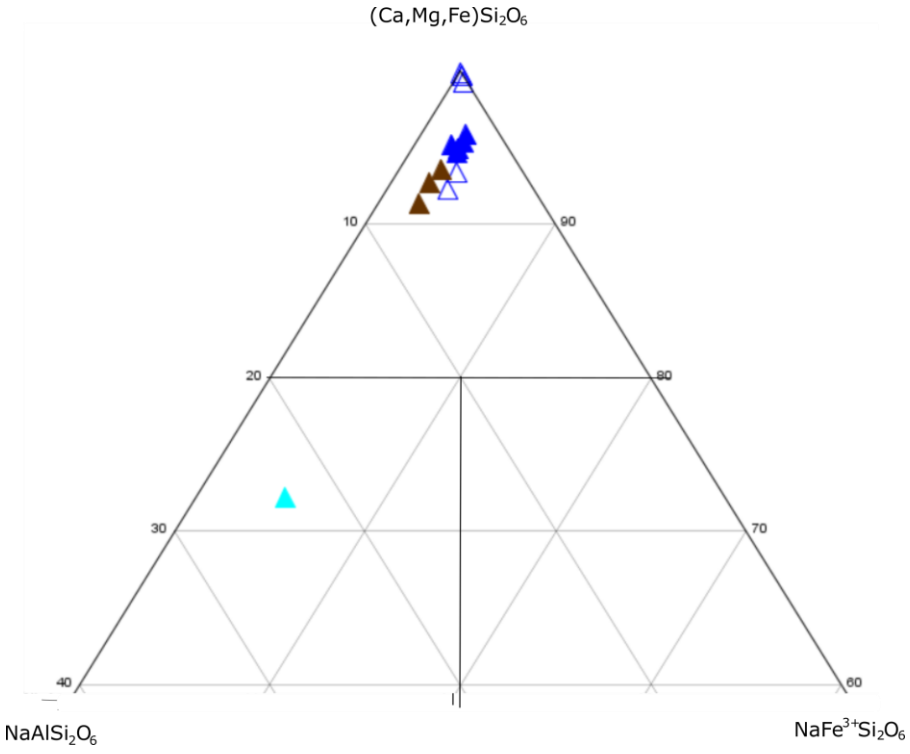

Figure 5.3.3: A) Pyroxene in layered eclogite and B) Pyroxene in gabbro and gneisses.

Amphibole analyses

	inc B1.2.3	sym B1.3.3	sym E4.3.7	sym E11 4.8	sym G1.4.4	inc G1.5.4	grain G6 1.2
SiO2	45.06	49.36	43.47	43.00	52.47	42.89	49.93
TiO2	0.60	1.30	1.77	1.84	0.14	0.31	1.11
Al2O3	15.28	8.56	12.27	14.61	3.21	13.16	6.19
Cr2O3	0.29	0.81	0.08	0.16	0.00	0.01	
FeO	1.86	4.27	11.89	8.80	10.91	11.52	10.08
MnO	0.02	0.04	0.04	0.06	0.03	0.07	0.25
MgO	17.79	18.40	14.72	15.69	17.41	12.16	11.27
CaO	11.17	11.25	10.87	10.86	11.85	10.98	21.17
Na2O	2.43	1.55	2.70	3.13	0.36	1.53	1.11
K2O	0.42	0.04	0.69	0.68	0.12	0.98	0.00
Total	98.84	96.43	98.50	98.84	97.43	97.90	100.45
Si	6.24	6.99	6.33	6.15	7.48	6.30	7.10
Al	1.76	1.01	1.67	1.85	0.52	1.70	0.90
Sum	8.00	8.00	8.00	8.00	8.00	8.00	8.00
Total Al	2.50	1.43	2.10	2.46	0.54	2.28	1.04
Al	0.74	0.42	0.43	0.62	0.02	0.58	0.14
Ti	0.06	0.14	0.19	0.20	0.01	0.03	0.12
Cr	0.03	0.09	0.01	0.02	0.00	0.00	0.00
Fe3+	0.45	0.10	3.19	3.35	0.22	0.53	2.39
Mg	3.67	3.88	1.45	1.05	3.70	2.66	1.20
Fe2+	0.04	0.37	0.00	0.01	1.05	1.20	0.03
Sum	5.00	5.00	5.28	5.24	5.00	5.00	3.88
(MgTotal)	3.67	3.88	3.15	3.30	3.70	2.66	2.38
(Fe Total)	0.67	0.61	1.43	1.04	1.52	1.94	1.19
Fe2+	0.18	0.13	0.08	0.05	0.25	0.22	-0.43
Mn	0.00	0.01	0.00	0.01	0.00	0.01	0.03
Ca	1.66	1.71	1.67	1.64	1.81	1.73	3.21
Na	0.16	0.15	0.24	0.31	-0.07	0.05	-0.81
Sum	2.00	2.00	2.00	2.00	2.00	2.00	2.00
NaTotal	0.65	0.43	0.75	0.85	0.10	0.43	0.30
Na	0.49	0.27	0.51	0.55	0.17	0.39	1.11
K Total	0.07	0.01	0.13	0.12	0.02	0.18	0.00
Sum	0.57	0.28	0.63	0.67	0.19	0.57	1.11
A/TetAl	0.32	0.28	0.36	0.35	0.36	0.34	0.33
Total	15.57	15.28	15.63	15.67	15.19	15.57	15.31
FM	0.06	0.12	0.19	0.10	0.26	0.35	0.27

Table 5.3.4: Representative analyses of amphibole, where inc = inclusion and sym = symplectite. FM = $Fe^{2+}/(Mg + Fe^{2+})$

5.3.3 Amphibole

Representative analyses of amphibole compositions are shown in table 5.3.4. Amphibole occurs predominantly as fine grained symplectites with a weakly yellowish color in both the boudin and layered eclogites. No compositional zonation have been registered, though these grains reflect the chemical composition of individual samples, containing the highest Mg and low FM = 0.06-0.12 in boudin eclogites. Layered eclogites have intermediate Mg and a FM = 0.10-0.19.

In sample 37554, green amphiboles are found interstitially within fractures in clinopyroxene and along grain boundaries in close proximity to the corona texture. A zonation in Mg/Fe is indicated for these grains, showing local variations of FM = 0.26 – 0.35.

Amphibole is a part of the main mineral assemblage in the gneiss samples, excluding sample 37601. These grains are typically subhedral and medium-grained, with a strong green color and pleochroism. Graphic symplectites of plagioclase are locally present in these grains. Amphiboles in the gneiss samples are considerately more enriched in Fe than the eclogite samples, with a typical FM = 0.27.

5.3.4 Plagioclase

With the exception of a few K-feldspar analyses from samples G6 and G7, all analyses of feldspar plot between An_{63} and An_{10} compositions (see figure 5.3.4). Both in boudin eclogite samples and layered eclogites plagioclase commonly occurs as fine- to coarse-grained symplectite in Ca-pyroxene. When plagioclases are present as inclusions in garnet, which have been observed in both B1 and B2, their chemical compositions are considerately more Ca-rich (see table 5.3.3). A typical symplectite composition for plagioclase in either boudin or layered eclogite is An_{20-30} and for inclusions within garnet it is An_{50-60}.

In sample G1 plagioclase occurs both in the fine-grained matrix and as a coronitic rim between garnet and sodic pyroxene. Here the matrix plagioclase is more Ca-rich, whereas the plagioclase corona is more enriched in Na, which is easily observed in table 5.3.3. All analyses of plagioclase in the gneisses were obtained in the matrix and showed only slight variations.

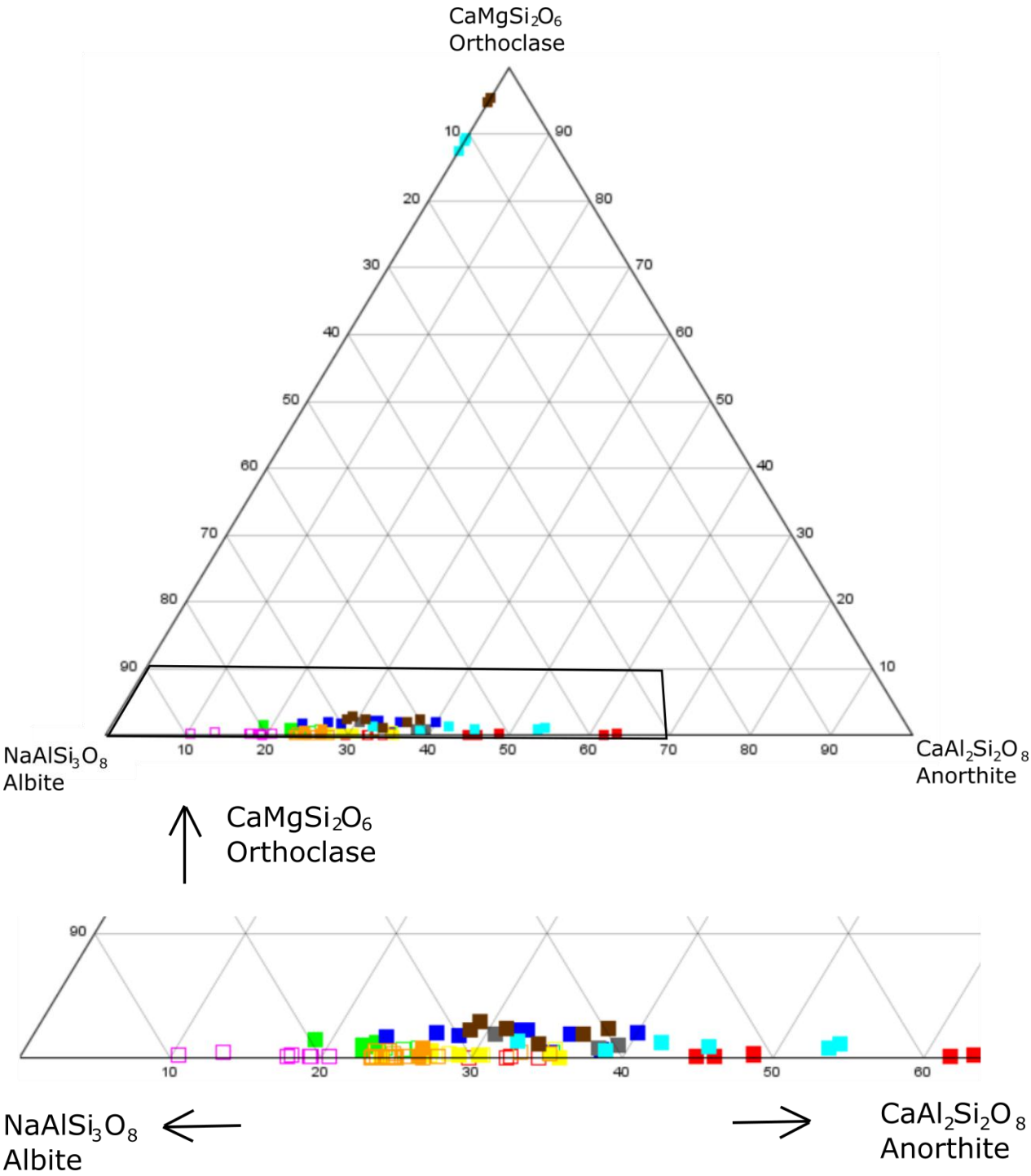

Figure 5.3.4: Plagioclase formulations normalized to 5 cations and plotted using the classification diagram from (Coleman et al., 1965). Core compositions are shown with filled squares and rim compositions are shown with open squares.

5.3.5 Thermobarometry

Phengitic white mica rimmed by biotite was identified in one inclusion in garnet in sample 37598 (figure 5.3.5). Efforts were made by Peter Robinson to calculate the original composition of the phengitic mica, which must have been considerately more enriched in SiO2, but no sound basis could be found to make such a calculation. As a reasonable alternative the chemical compositions of the closest located phengites in the Nordøyane domain at Fjørtoft (Terry, Robinson, & Ravna, 2000) and in Harøy (Butler et al., 2012), together with Ca-garnet and Ca-omphacite analyses from Averøya were used to calculate P-T conditions. Garnet and omphacite analyses from Fjørtoft are more enriched in Ca, whereas the equivalent minerals in the layered eclogite on Averøya are more enriched in Mg. Analyses of garnet, omphacite and phengite from Fjørtoft and Averøya are shown in table 5.3.5

Help was provided by Jared Butler and Mike Terry who applied the Ca-garnet – phengite – omphacite barometer coupled with the garnet – omphacite thermometer to obtain P-T estimates for the Averøya layered eclogite (Krogh Ravna & Terry, 2004).

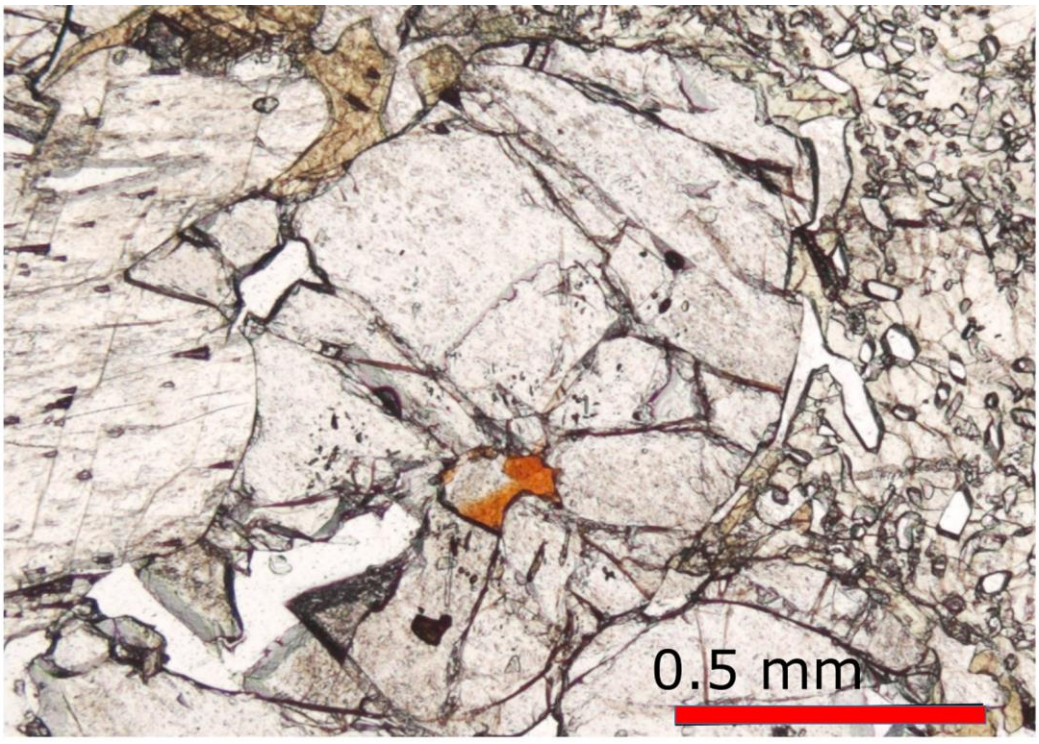

Figure 5.3.5: Phengitic mica as an inclusion in a garnet porphyroclast.

Peak conditions of P = 3GPa and T = 800 °C, with an uncertainty of ± 0.7GPa and 100 °C.

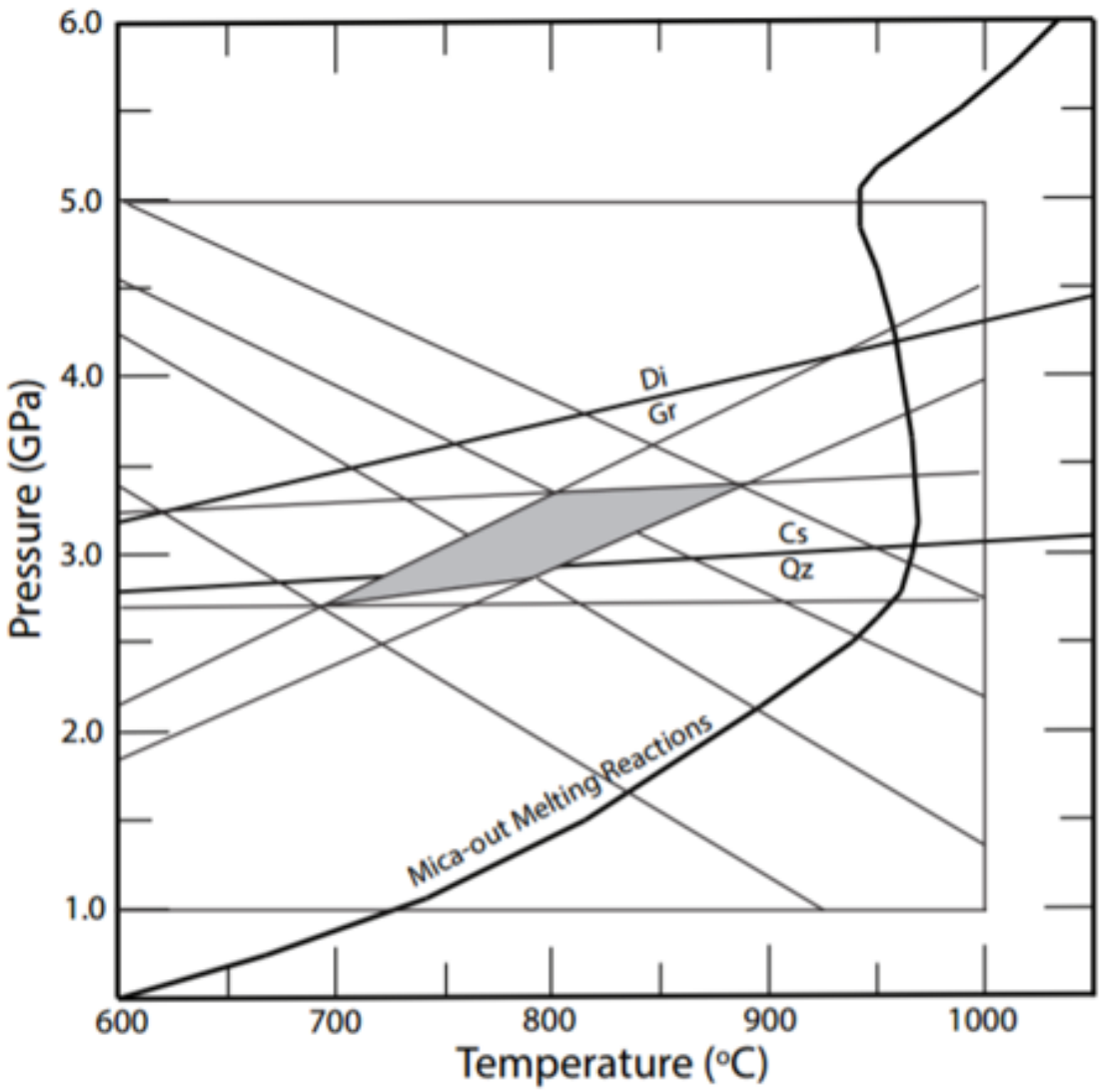

Figure 5.3.6: P-T diagram constructed by M.P Terry (June 12.2017) and revised with text by P. Robinson (June 14.2017), with text. This diagram is based on co-existing garnet and omphacite compositions identical to analyzed phengite (Si = 3.49) from the Fjørtoft eclogite 1066b. Mica-out melting reactions summarized from (Auzanneau, Schmidt, Vielzeuf, & Connolly, 2010) mark the likely low T limit of fluid-absent melting of granitoids rocks.

Omphacite Analyses	1066b	37598 5.2
SiO2	54.100	54.871
Al2O3	6.610	9.375
TiO2	0.100	0.019
Cr2O3	0.130	0.093
MgO	14.080	11.654
FeO Total	1.660	2.971
MnO	0.070	0.009
CaO	21.020	15.900
Na2O	2.370	5.085
K2O	0.000	0.000
Total	100.150	100.013
Si	1.940	1.946
Al (iv)	0.060	0.054
Al (vi)	0.220	0.338
Ti	0.003	0.001
Cr	0.004	0.003
Mg	0.752	0.616
Fe2+	0.050	0.027
Mn	0.002	0.000
Ca	0.807	0.604
Na	0.165	0.350
K	0.000	0.000
Cat Total	4.000	4.000

Phengite analyses	1066b	37598 11.5
SiO2	53.260	47.457
Al2O3	27.290	29.426
TiO2	0.270	2.565
Cr2O3	0.000	0.184
MgO	3.360	2.078
FeO	1.050	0.814
MnO	0.000	0.007
CaO	0.010	0.000
Na2O	0.600	0.133
K2O	9.510	10.342
Total	95.350	93.239
Si	3.493	3.230
Al	0.507	0.770
Sum	4.000	4.000
Total Al	2.110	2.360
Al	1.603	1.590
Ti	0.013	0.131
Cr	0.000	0.010
V	0.000	0.005
Mg	0.328	0.211
Fe Total	0.058	0.046
Mn	0.000	0.000
Sum	2.002	1.994
Ca	0.001	0.000
Na	0.076	0.018
K	0.796	0.898
Sum	0.873	0.915
Cat Total	6.875	6.909

Garnet Analyses	1066b	E11.3.1
SiO2	39.540	40.027
Al2O3	23.150	22.195
TiO2	0.060	0.036
Cr2O3	0.060	0.089
MgO	13.710	11.460
FeO Total	10.040	17.035
MnO	0.290	0.329
CaO	12.310	9.751
Na2O	0.030	0.063
K2O		0.000
Total	99.160	101.108
Si	2.921	2.973
Al	2.015	1.943
Ti	0.003	0.002
Cr	0.004	0.005
Mg	1.509	1.269
Fe2+	0.620	1.058
Mn	0.018	0.021
Ca	0.974	0.776
Na	0.004	0.009
K		
Cat Total	8.069	8.056

Table 5.3.5: Chemical compositions of garnet, omphacite and phengite from Averøya compared to analyses from Fjørtoft.

5.4. Petrography

Sample	Main minerals	Accessory minerals	Characteristics
5.3.1 Granodioritic to tonalitic migmatite gneiss			
37553/M1	qz, k-fsp, pl	grt, bt, ep, mag, hem, ilm	SF, R, RG, P
5.3.2 Garnet Amphibolite			
37591/G2	Grt, am, qz, pl, cpx	rt, hem, ilm and mag	SF, CT, RG, PG, S, M
37699/G8	Grt, am, cpx, pl,	qz, ap, ti, rt, cal, bt, mag and py	SF, S, DO, PG, M
37700/G9	Grt, am, cpx, pl, qz	Ti, rt, ap, chl, zr, mag and ilm	SF, S, DO, PG, M, RG
5.3.3 Garnet and amphibole gneiss			
37558/E3	grt, pl, qz, am, cpx	rt mag. ilm	GF, R, S3, AR, DO, PG
37591/G4	pl, qz, k-fsp, am	ti, ep, bt, cpx, hem, ilm, mag	GF, R, S3, P, S
37592/G3	am, qz, bt, qz, pl	grt, rt, ep, k-fsp, mag, sul, chl	GF, S3, DO, P, R, S, C
37594/B3	grt, qz, bt, pl	rt, chl, fsp, hem, ilm	GF, PG, C, S
37597/E10	grt, bt, am, pl,	fsp, rt, cpx, qz, mag	SF, CV, SG, DO
37601/G5	grt, bt, pl, qz	phn, ti, sul, mag	GF, PG, R
37602/G6	grt, am, qz, cpx, fsp, bt	scp, ti, rt, hem, ilm, mag	GF, S3, M, PG, P
37698/G7	am, pl, cpx , bt, k-fsp,	grt, cal, ep, hem, ilm, mag	GF, S4, P, DO, S
5.3.4 Layered eclogite			
37556/E1	grt, pl, am, cpx	bt and qz, py, hem, ilm	GF, CV, S4, DO, PG, CT
37557/E2	grt, am, omp/cpx, pl,	bt, cal, mag, rt	GF, PG, CV, S4, DO
37560/E4	grt, omp/cpx, pl	rt, qz, mag, ilm, am	SF, 32, M, MN
37562/E5	grt, omp/cpx, am	cal, qz, pl, rt, hem, ilm, mag	GF, S4, DO, PG, R
37563/E6	am, grt, omp/cpx, pl	rt, qz, opx, hem, ilm, mag	GT, S2, S4, CV, AR, R, CT
37564/E7	grt, omp/cpx, pl	am, bt, rt, ilm, mag, sul, qz	GT, TJ, CV, EL, S3, S4, CT, AR, MN
37565/E8	grt, pl, omp/cpx, am, bt	rt, qz, fsp, cal, hem, ilm, mag	GF, PG, DO, S4, MN, R
37566/E9	grt, omp/cpx	rt, pl, ep, am, mag, ilm	GF, M, S3 – S4, DO
37598/E11	grt, omp/cpx, am	cal, rt, qz, sp, crn, ap, ky, phn	GF, PG, S3 (crn + pl). S3, TJ.
37697/E12	cpx, grt, pl, am	bt, cal, fsp, ep, sul, rt	GF, P, S4, DO, S, PG
5.3.5 Boudin eclogite			
37555/B2	grt, omp/cpx, am	qz, rt, ap, pl, mag, py	GT, MN, EL, S3, AR, DO
37559/B1	grt, omp	am, rt, pl, ky, zr, ep, mag, qz	GT, S1, TJ, EL, PG
37595/B4	grt, omp/cpx. pl	qz, rt, am, bt, ilm, hem, mag	GT, PG, AR, EL, S4, M, R
37596/B5	grt, am, omp/cpx, pl	qz, ap, rt, ilm, hem, mag	GF, M, PG, S4, DO, R
37599/B6	am, grt, bt, qz, pl	cpx, rt, ap, ilm, hem, mag	GF, AR, S4, DO, PG
37600/B7	omp/cpx, grt, am	rt, qz, ap, cal, mag	GT, PG, DO, S1, TJ, AG, CV
5.3.6 Gabbro			
37554/G1	gabbro: Cpx, pl	am, bt, opx, mag, ilm, grt	GT, R, CT, EL, DO

Table 5.4.1: Mineral abbreviations: Am – amphibole, ap – apatite, bt – biotite, cal – calcite, chl – chlorite, cpx

– clinopyroxene, ep – epidote, fsp – feldspar, grt – garnet, hem – hematite, ilm – ilmenite, ky – kyanite, mag – magnetite, omp – omphacite, phn – phengite, pl – plagioclase, py – pyrite, qz – quartz, rt – rutile, scp – scapolite, sul – sulfide, ti – titanite, zr - zircon. Textural abbreviations: AG – atoll garnet, AR – cpx grain altered into amphibole along rim, C – chloritization, CT – corona texture, CV – crosscutting vein, DO – dusty overprint on cpx, EL – exsolution lamellae in cpx, GF – gneissose foliation, GT – granofelsic texture, M – moat of plagioclase around garnet, MN – moat of plagioclase and necklace of pyroxene, P – perthite, PG – poikioblastic garnet, R – recrystallization, RG – ribbon grains, S – sericitization, Symplectites of predominantly cpx + pl ± am, where: S1 – medium/coarse symplectites along grain boundaries, S2 – thin secondary formation of symplectites, S3 – coarse graphical to skeletal symplectites, S4 – dendritic symplectites and TJ – triple junction.

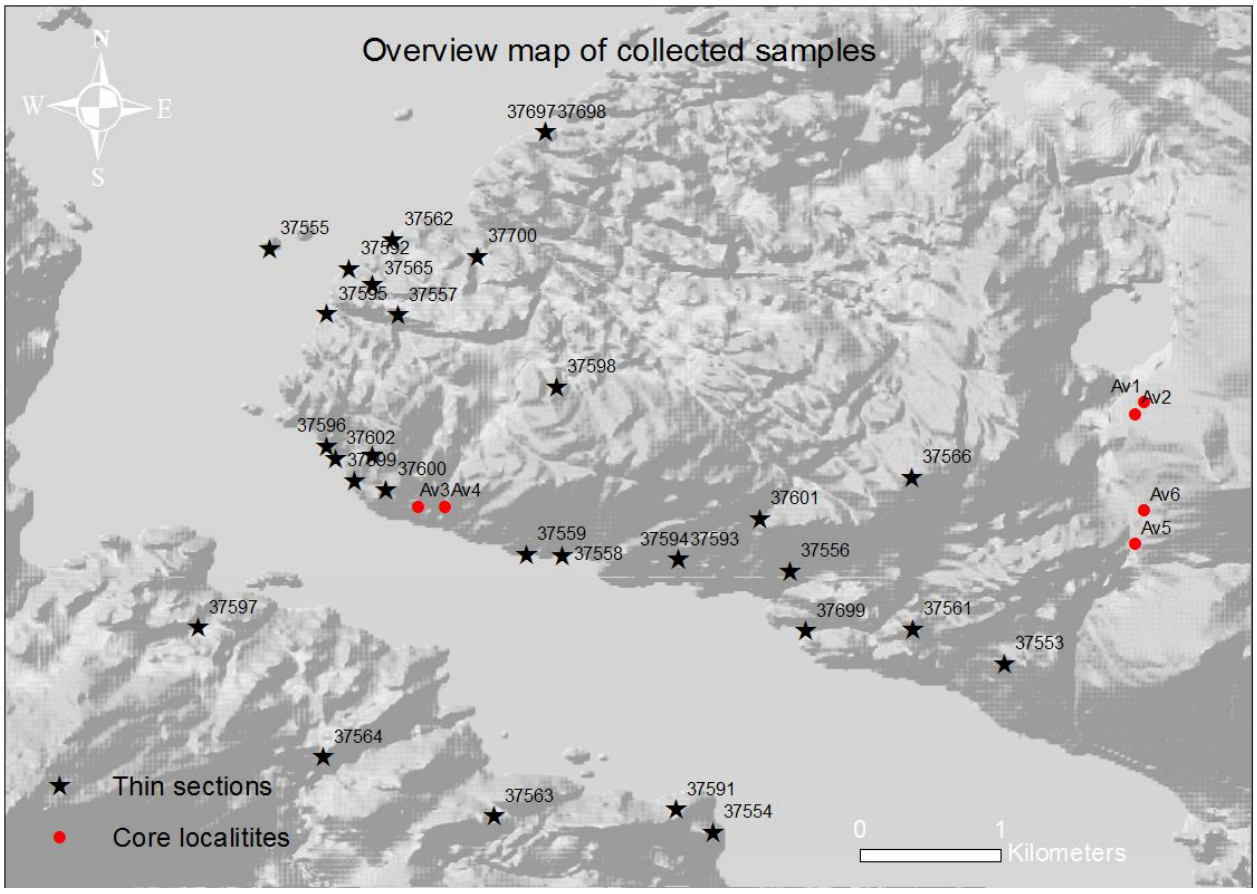

Figure 5.4.1: Sampling localities for oriented cores marked with red dots and thin section stars. A full summary of all mineral assemblages and textures within individual thin sections can be seen table 5.4.1.

A full compilation of all textures, assemblages and localities for the samples are shown in figure 5.4.1 and table 5.4.1. The same subdivision of rock types that was used in the field chapter will be applied to describe these samples.

5.4.1 Granodioritic to tonalitic migmatite gneiss

One sample from this rock type is characterized by small-scale, semi-continuous layers of biotite alternating with recrystallized fine-grained layers of quartz and feldspar, defining a strong foliation. Small- to medium-sized porphyroclasts of garnet predate the dominant foliation that wrap around these grains. A relict foliation of oriented biotites has been preserved as a snowball texture within garnets, attesting to a rotation of the garnets during growth (see figure 5.4.2). There are two anomalously large grains of around 2mm in diameter, situated in the otherwise fine-grained sample, one is an euhedral epidote and the other is a perthitic feldspar.

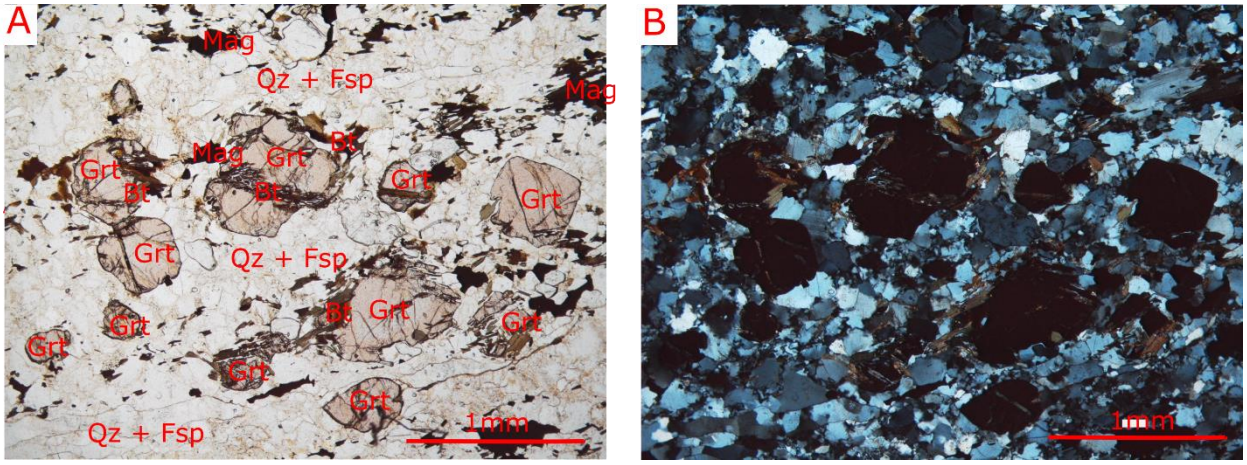

Figure 5.4.2: PP and XP images of a predominantly quartzofeldspathic matrix with porphyroclasts of garnet.

5.4.2 Garnet amphibolite

Three samples were collected from this rock type, where all samples consist of porphyroclasts of garnet ranging from 1 - 20mm set in a dark greenish and strongly anastomosing matrix of amphibole and minor clinopyroxene. Light layers of quartz and feldspar are variously present in the samples, culminating in a 0.5 cm wide continuous layer in sample 37591 (see figure 5.4.3). These layers are usually associated with garnet porphyroclasts, typically enveloping the entire garnet with enhanced recrystallization in the pressure shadows.

The matrix is a mixture of fine grained, irregular and inequigranular strongly oriented amphibole and clinopyroxene interchanging with interstitial recrystallized quartz and feldspar. Coarser sigmoidal amphiboles and dusty symplectized clinopyroxene commonly occur in sample 37700 and locally in sample 37591. The presence of quartz ribbon grains, shear bands and a

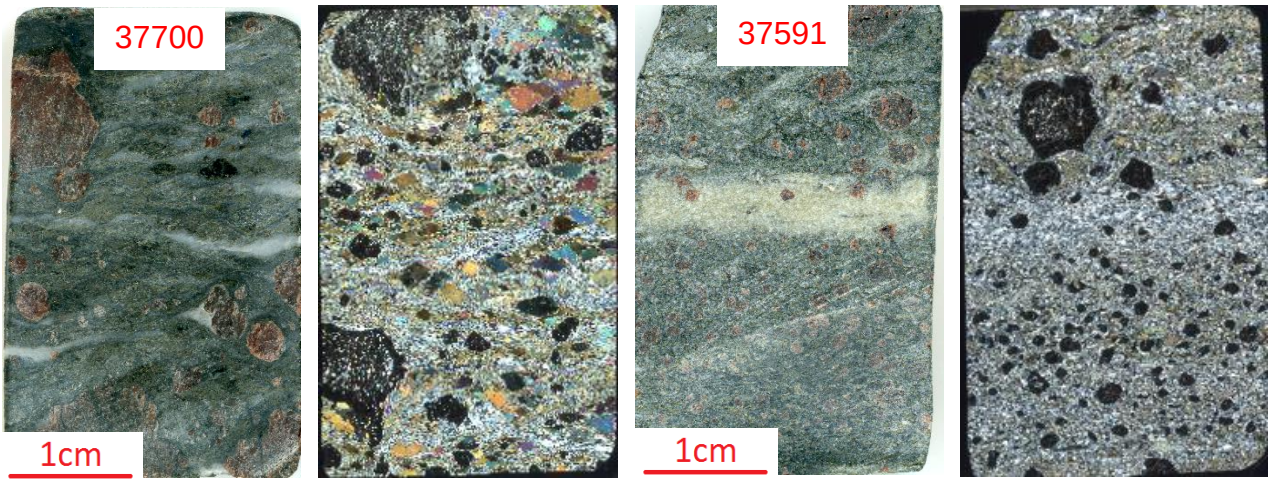

Figure 5.4.3 Hand sample images and scanned XP images of two samples from garnet amphibolite

polygonised, irregular and extremely fine-grained predominantly, quartzofeldspathic matrix indicates high amounts of strain and shear. Many additional microstructures have been described from sample 37700 in chapter 5.3.4.

Porphyroclasts of garnet typically exhibit embayed shapes (fig 5.4.4 A,B) and contain a variety of inclusions like titanite, plagioclase, amphibole, chlorite, apatite and minor rutile. In some of these grains the inclusions are restricted to the core of the grain and a later growth zone envelops this core (5.4.4 C). Sericitization occurs both within localized zones in the matrix and in inclusions of plagioclase within garnets, as a response to the infiltration of fluids along fractures in the host. All of these samples contain abundant oxides like hematite, ilmenite and magnetite with minor rutile locally (5.4.4 D). These rutiles commonly have large overgrowths of ilmenite.

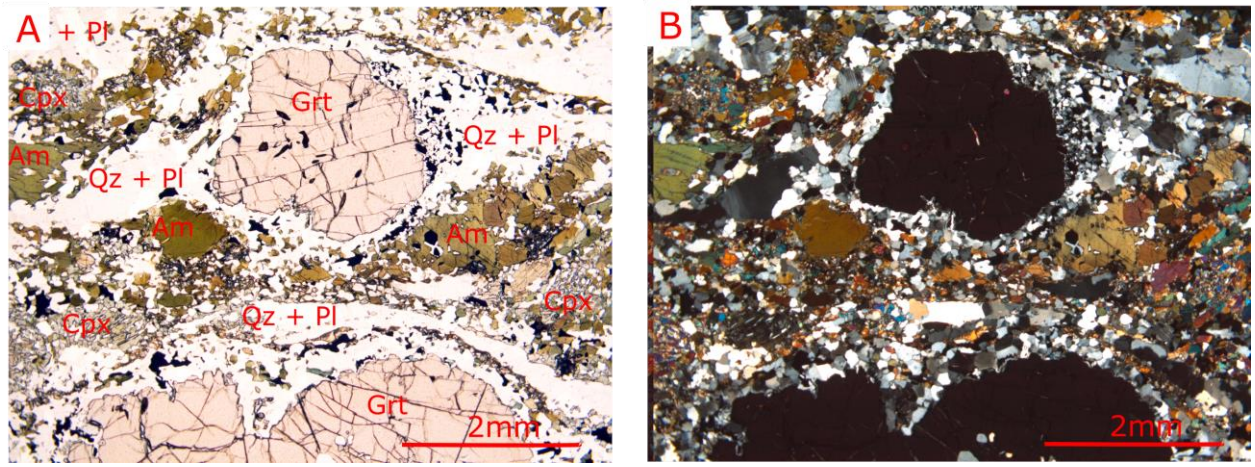

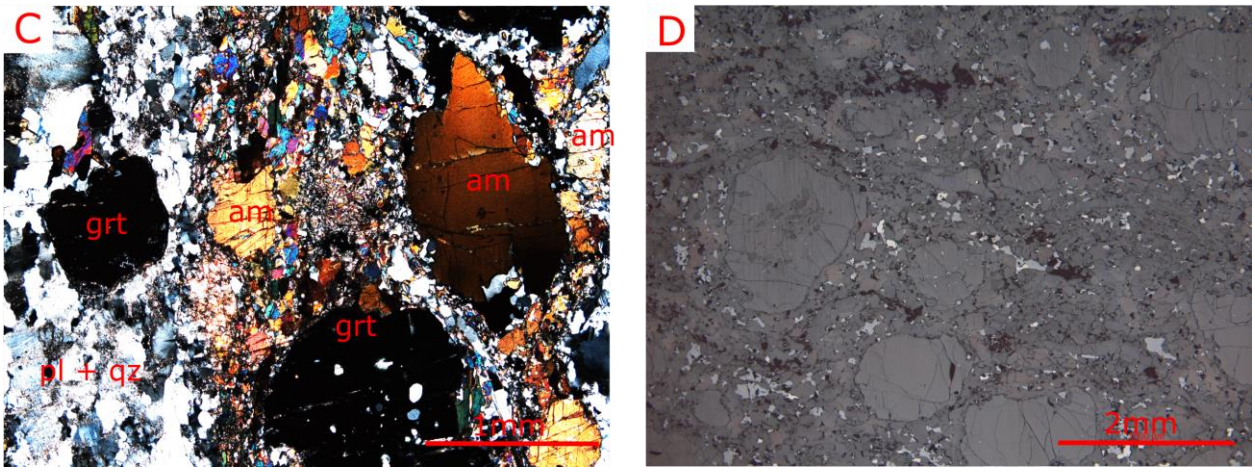

Figure 5.4.4: Photomicrographs pf representative textures in the garnet amphibolite, where A,B) PP and XP images of porphyroclasts of embayed garnet in sample 37591, C) Fine-grained recrystallized matrix with local porphyroclasts of garnet and amphibole in sample 37700 and D) Abundant magnetite and ilmenite with hematite lamellae in sample 37591.

5.4.3 Garnet and amphibole gneiss

This rock type can be subdivided into three subtypes: 1) Garnet + biotite gneiss, 2) Garnet + amphibole gneiss and 3) Amphibole + biotite gneiss that is depleted in garnet. The overall main mineral assemblage includes garnet ± amphibole + quartz + plagioclase ± K-feldspar + biotite ± clinopyroxene. An undulating gneissose foliation is defined by the preferential alignment of prismatic amphibole and biotite, coupled with recrystallized layers of quartz and feldspar. Two samples from the boundary of the layered eclogite exhibit similar attributes as the amphibole + biotite gneiss and have therefore been included in this section. Two hand samples are shown in figure 5.4.5, from an amphibole + biotite gneiss (37698) and garnet + amphibole gneiss (37602) respectively.

The majority of these samples are dominated by inequigranular layers of biotite and amphibole interchanging with recrystallized fine-grained layers of plagioclase and quartz (see figure 5.4.6 A, B). Irregular and dusty-looking clinopyroxene contains small rod shaped symplectites of plagioclase commonly propagating into an enveloping rim of amphibole. Porphyroclasts of garnet are flattened and typically have prismatic amphibole and biotite wrapping around them. Other locally occurring textures associated with garnets are snowball texture, rotated grains and

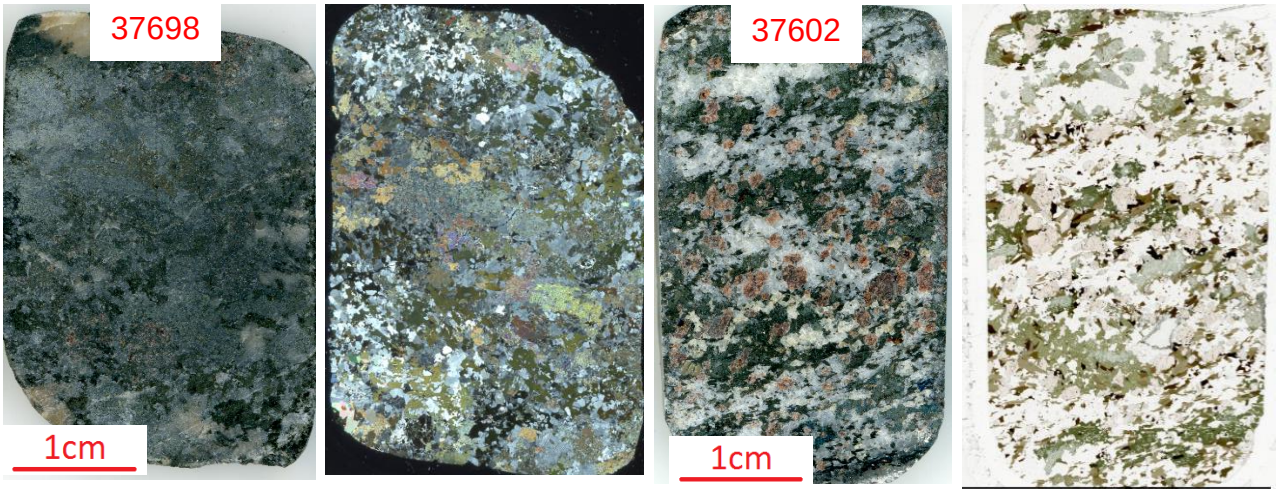

Figure 5.4.5: Textural variations within hand samples from an amphibole dominated gneiss (37698) close to the boundary of the layered eclogite and a garnet + amphibole gneiss (37602). Notice the predominantly symplectized matrix of K-fsp + pl + am + bt + cpx.

extensive fragmentation of grains with associated formation of alteration products along fractures. Garnets contain a variety of inclusions like rutile, phengite, biotite and plagioclase.

Epidotes are spaced interstitially throughout the matrix, consisting of relict euhedral and elongated grains that are pervasively fractured. These grains were replaced in a varying degree by magnetite + Ca plagioclase + calcite symplectites. Other accessory minerals include titanite, apatite, phengite, calcite, scapolite, epidote, rutile, magnetite, hematite and ilmenite. Scapolite and phengite were only found in one sample each.

The two amphibole-enriched samples are characterized by extremely coarse amphibole + plagioclase + clinopyroxene ± biotite symplectites completely dominating the matrix (see figure 5.4.6 C, D). Some wider sections of predominantly K-feldspar and plagioclase are easily distinguishable in the sample due to tartan twinning and Albite twins respectively. Perthite texture also occur locally and many of the feldspar grains have experienced varying degrees of sericitization along fractures and deformation bands. These samples contain abundant magnetite and ilmenite with hematite lamellae, whereas rutile is commonly found in the garnet enriched samples (see figure 5.4.6 E, F).

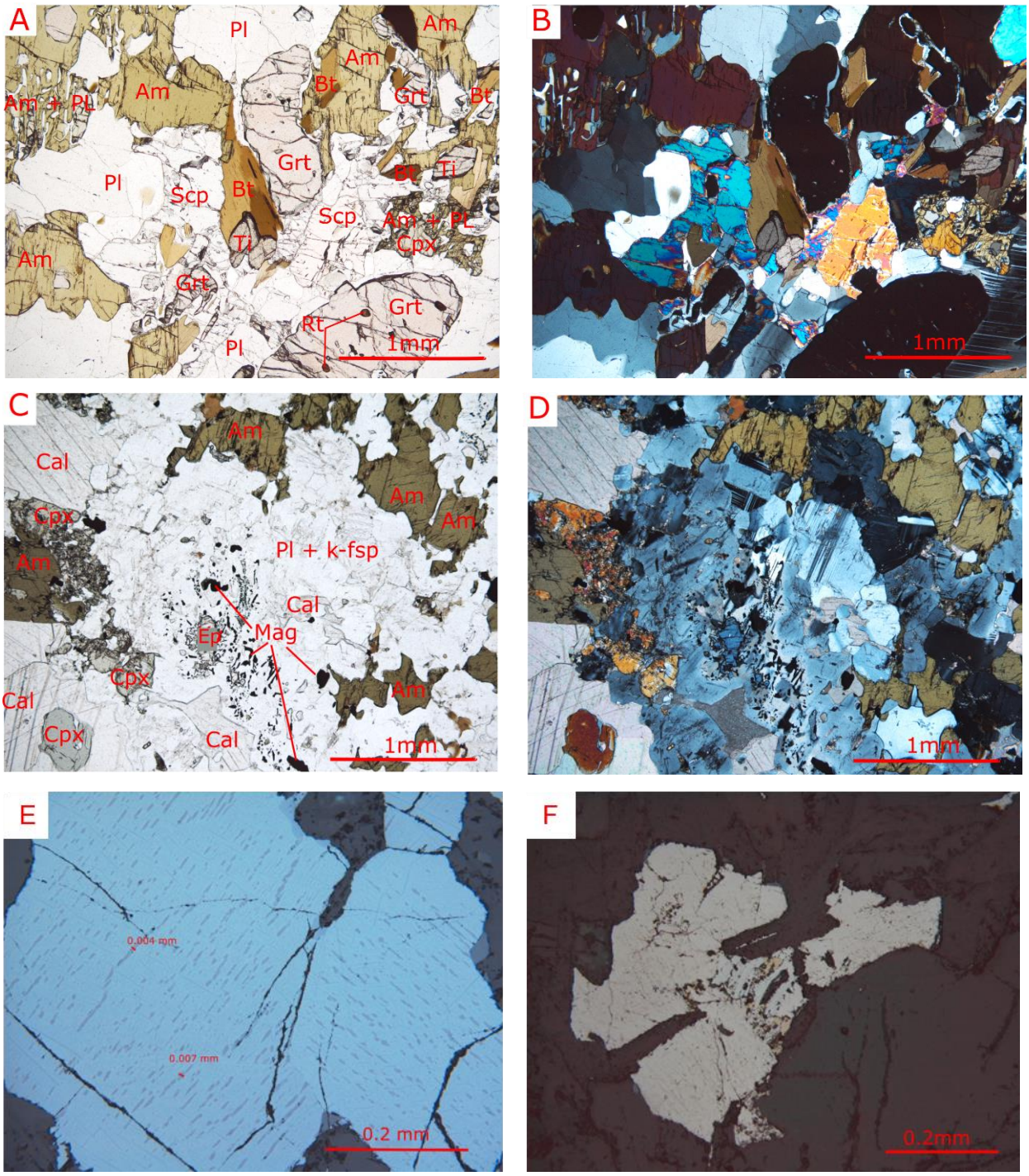

Figure 5.4.6: Photomicrographs with PP images to the left and XP images to the right. A,B) Textures in a garnet + amphibole gneiss (37602) and C,D) textures in an amphibole gneiss (37698). Common oxides occurring in these rocks are E) ilmenite with hematite lamellas from thin section 37591 in and F) magnetite in 37601.

5.4.4.1 Layered Eclogite

Six samples were collected from various parts of the main body on Averøya providing a good representation of the mineralogical and textural variations within the main body. An additional four thin sections come from layered bodies at Visnes, Lyngstad, Ufsåsen and Hendholmen. Although all samples consist primarily of fine to coarse-grained porphyroclasts of garnet set in a green to greyish matrix of relict omphacite ± amphibole ± plagioclase, the relative abundance of main and accessory minerals is highly variable.

A representative selection of hand samples with corresponding scanned thin section images to the right hand side are shown in figure 5.4.7. Color variations within individual samples provide a good indication of the mineral assemblage and the main textures. Darker mineral assemblages as seen in samples 37563 indicates a high amount of amphibole in the matrix. Amphibole is otherwise more of an accessory mineral, occurring most frequently associated with veins or forming coronas around garnets as seen in sample 37556. The majority of the samples show a greasy green color in the matrix. Coupled with scanned photos typically this color indicates the presence of symplectite produced by the breakdown of omphacite to Ca pyroxene + plagioclase. Other accessory minerals visible in the hand samples include quartz, calcite and plagioclase.

Petrographic studies resulted in a tentative subdivision of the samples into two different groups based on similar attributes and stage of retrogression. Samples 37560, 37564, 37566 and 37598 displays a strongly foliated texture and comprises of a homogenous mineral assemblage dominated by omphacite and garnet (see figure 5.4.8 A, B). This layered texture is not as dominating in samples 37556, 37557, 37562, 37563, 37565 and 37697, consisting of a considerately more heterogeneous mineral assemblage than the former.

Homogenous layered samples

These samples contain equigranular garnet and omphacite exhibiting subhedral to euhedral, elongated shapes that are only slightly irregular along the boundaries due to symplectite growth. Well preserved triple junctions occur intermittently, indicating a relict granoblastic texture. Small-scale, rod shaped symplectites of plagioclase occur variably within omphacite grains, locally restricted to narrow zones within the grain to widespread symplectitzation throughout.

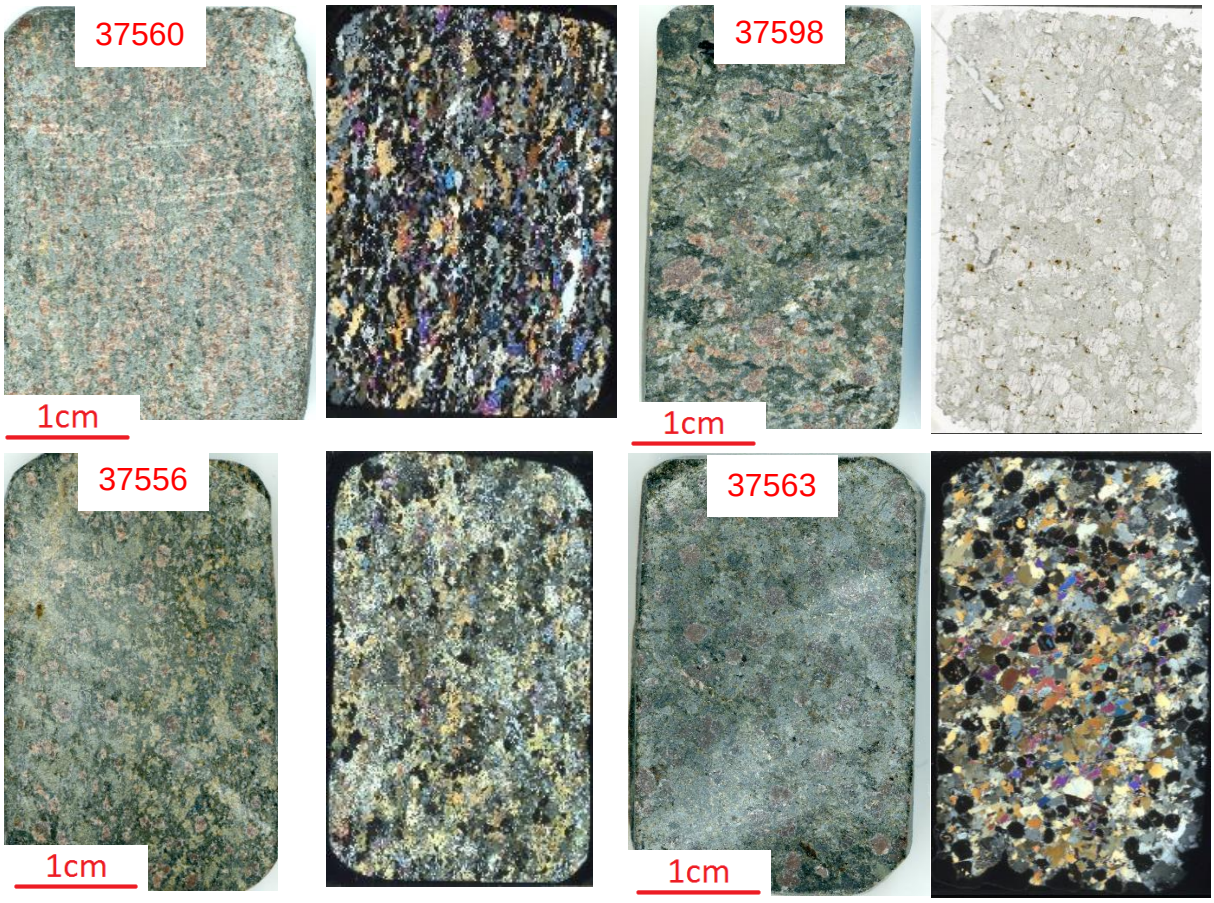

Figure 5.4.7: Selected images of layered eclogite hand samples and corresponding scanned XP or PP images of increasing amounts of symplectite and amphibole from 37560 to 37563.

All samples typically have moats of plagioclase enveloping garnets, shown in figure 5.4.8 C, D. Samples 37560 and 37564 contain a localized zone of recrystallized quartz, which has resulted in the formation of semi-continuous necklaces of clinopyroxene ± orthopyroxene ±amphibole on the outside the moat. Accessory minerals include apatite, rutile, quartz, calcite, kyanite, corundum and epidote. Rutile forms medium-sized aggregates both in the matrix and as inclusions within garnets, commonly rimmed by brown amphibole and containing ilmenite intergrowths.

A single kyanite grain was discovered using EMPA in sample 37598 coming from the middle part of the layered eclogite body on Averøya. This grain is enclosed within an extremely fine-grained corundum + sapphirine + plagioclase symplectite. Arrows on figure 5.4.8E) show the direction of movement of the symplectite as kyanite gradually decomposed. Between the garnet and the kyanite there is a development of fine-grained symplectites of spinel + plagioclase.

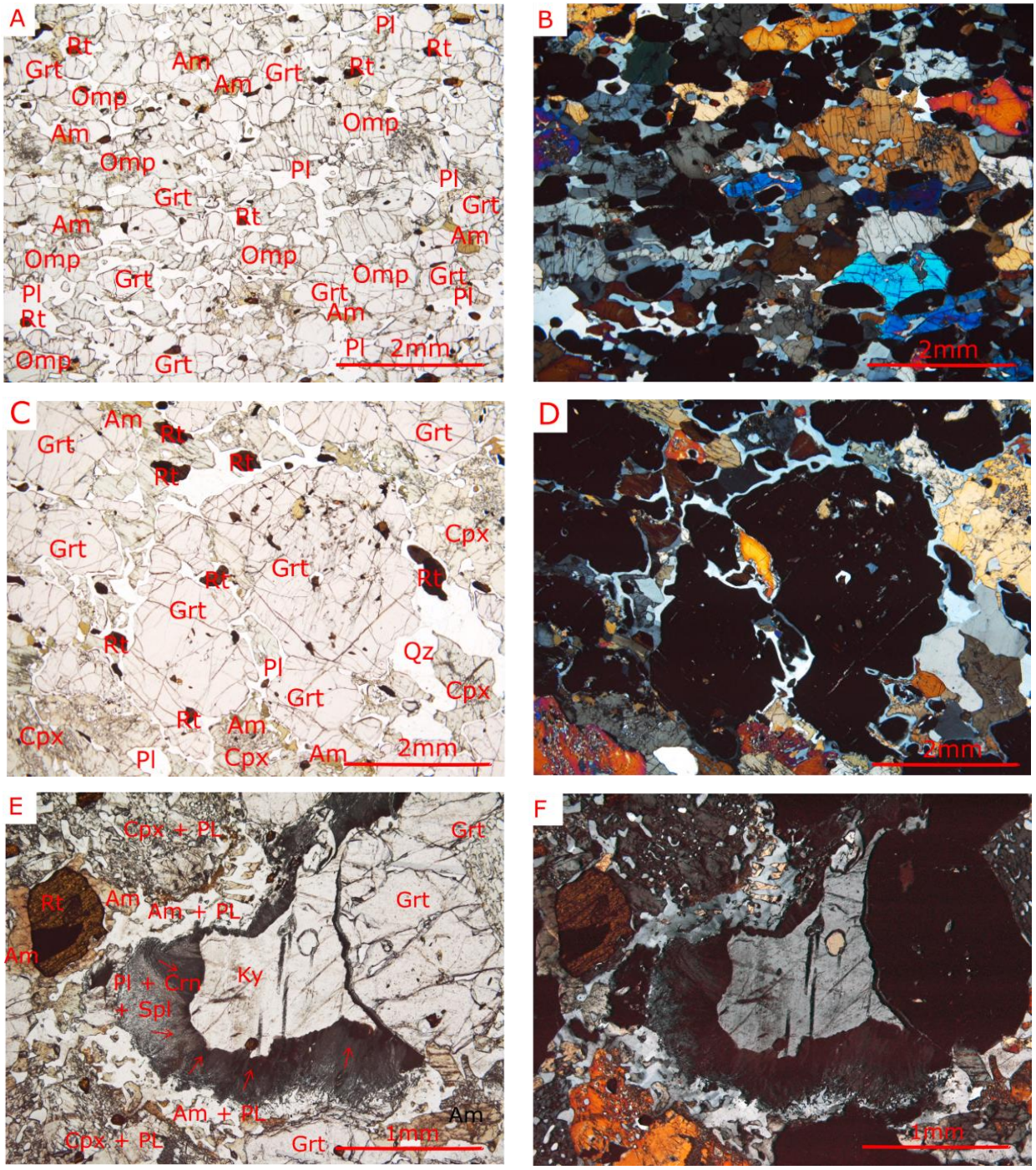

Figure 5.4.8: Photomicrographs of PP and XP images from A,B) Strongly foliated eclogite from sample 37560, C, D) Garnet enveloped by a moat of plagioclase and local formation of a clinopyroxene necklace in sample 37564 and E,F) The decomposition of kyanite into fine-grained corundum + sapphirine + spinel + plagioclase in 37598. Notice the secondary rim off amphibole + plagioclase enveloping the fine-grained symplectite.

Heterogeneous layered samples

These samples consist primarily of a mixture of small- to medium-sized, inequigranular and irregular grains of garnet, amphibole, clinopyroxene and plagioclase. Relict omphacite has been replaced by medium to coarse-grained graphic symplectites of plagioclase + clinopyroxene ± amphibole± biotite (see figure 5.4.9A, B). A dusty overprint is typically observed in clinopyroxene, becoming more pervasive if crosscut by a vein.

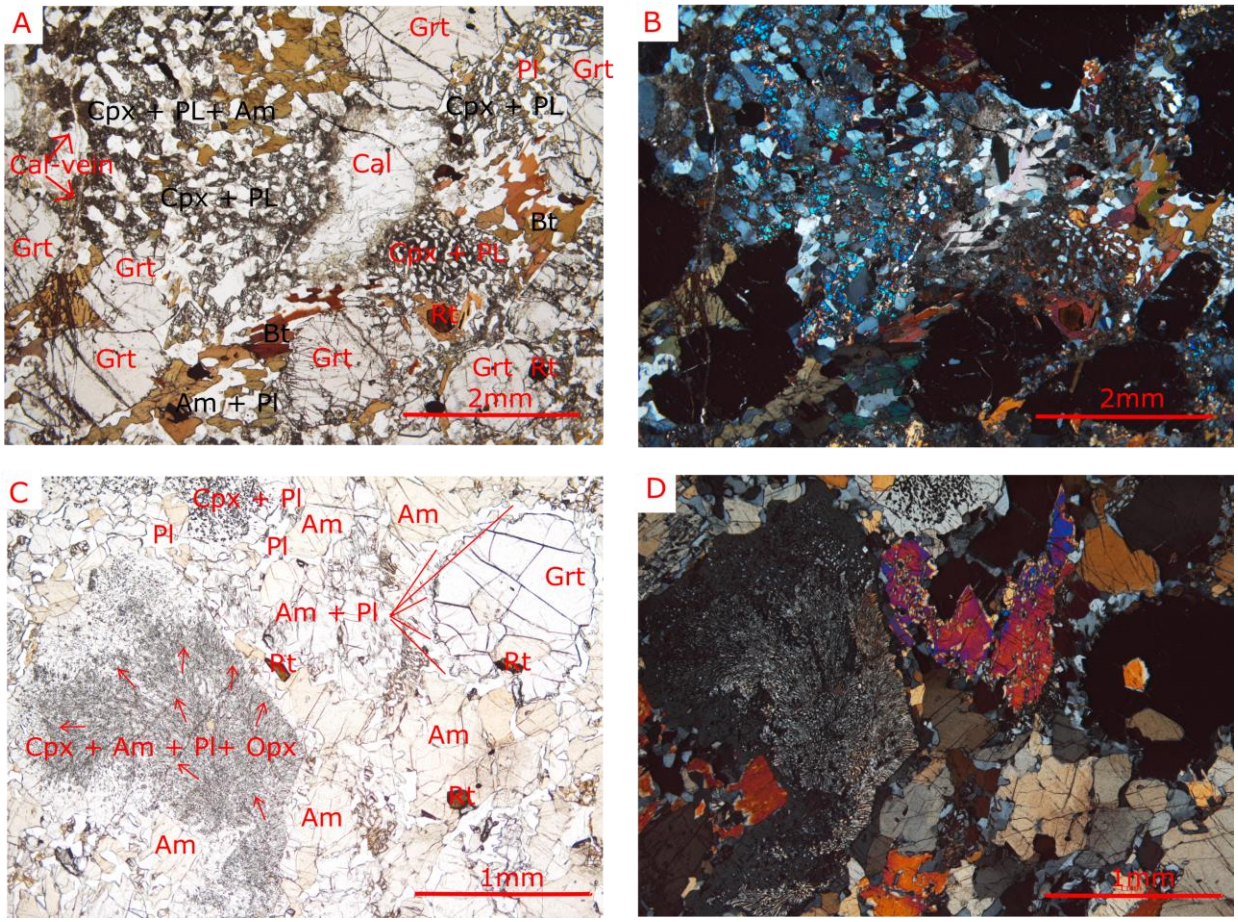

Figure 5.4.9: PP and XP photomicrographs of A, B) Matrix dominated by pervasive amphibole + clinopyroxene + plagioclase ± biotite symplectites. Interstitial garnet + rutile + calcite. E,F) Two stage formation of clinopyroxene + amphibole + plagioclase + orthopyroxene phases with preserved omphacite at the rims. Notice the gradual thinning of lamellas towards the rim, where arrows shows the direction of movement. There is also a development of amphibole and plagioclase symplectite enveloping a garnet.

All samples contain abundant medium to coarse, subhedral garnets containing rutile, calcite, hemo-ilmenite, plagioclase and amphibole. These are extensively fractured with a fine-grained alteration product of magnetite, plagioclase and chlorite forming along fracture planes. Calcite is a common constituent in most samples, occurring both as medium-sized grains in the matrix and within crosscutting veins. Other accessory minerals include rutile, biotite, calcite, quartz and apatite. Both rutile and magnetite are abundant in the matrix, rutile inclusions in garnets are generally more preserved than rutile in the matrix that are strongly overprinted by ilmenite.

Sample 37563 displays different attributes from the heterogeneous eclogite samples as it comes from an amphibole rich zone within the layered body at Visnes. Here the matrix consists predominantly of equigranular, subhedral to euhedral amphibole and garnet separated by small zones of fine grained recrystallized plagioclase. Rutile, plagioclase, quartz and clinopyroxene are accessory minerals dispersed throughout the matrix. There are three different types of symplectite formation in this sample, 1. plagioclase + amphibole forming coronas around garnets, 2. Extremely fine grained dendritic intergrowths of plagioclase + amphibole + clinopyroxene + orthopyroxene leaving only a small rim of the original omphacite (see figure 5.4.9 C, D) and 3. Small rod-shaped intergrowths of plagioclase in the core of the relict omphacite.

5.4.4.2 Boudin Eclogite

Six samples were collected from various smaller boudins from different localities in the neighboring gneiss. Hand samples in figure 5.4.10 clearly illustrate the composite and textural variations of two of the boudins in question. Sample 37554 consists of coarse grained omphacite and garnet, demonstrating a clear granofelsic texture. In sample 37596 garnets are just distinguishable from an otherwise diffuse greenish grey matrix, which is dominated by pervasive symplectite. All of the remaining samples comprises of similar mineral assemblages, demonstrating the same medium- to coarse-grained granofelsic texture and representing intermediate phases between these two endmembers.

Samples 37554 and 37600 both comprises of coarse-grained, equigranular omphacite and garnet exhibiting well developed triple junctions along grain boundaries defining a granoblastic texture.

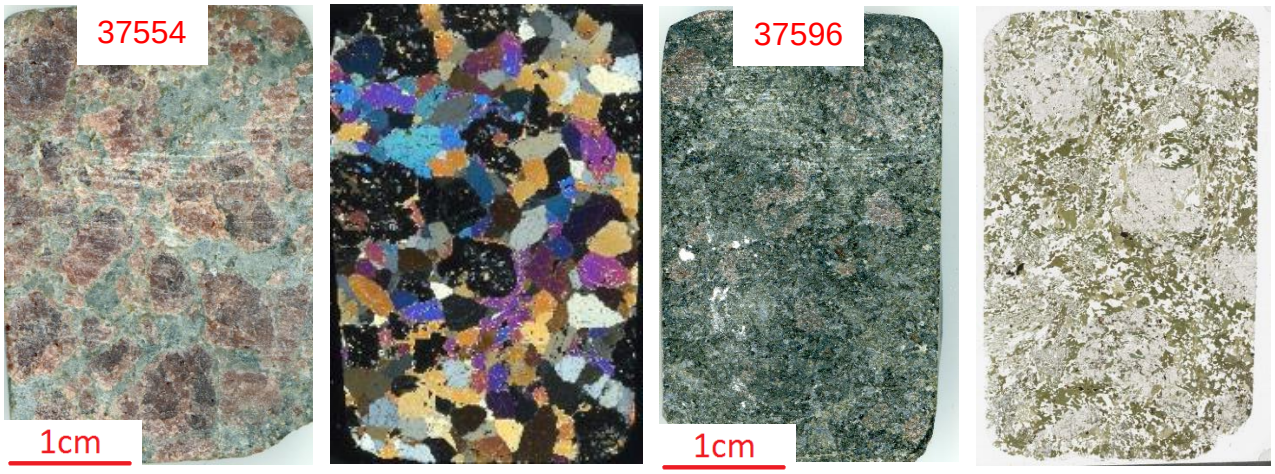

Figure 5.4.10: Photographs of hand samples from and corresponding scanned images of thin sections of boudin eclogite. Notice the coarse grained and massive assemblage in sample 37554 and the diffuse mix in sample 37596.

Small-scale lamellar symplectites of plagioclase ± amphibole locally form along grain boundaries (see figure 5.4.11 A, B), some omphacite grains occasionally contain cleavage parallel lamellae of an unknown mineral. Subhedral to anhedral garnets are situated interstitially and contain inclusions like amphibole, plagioclase, epidote, kyanite, quartz (coesite?), rutile and omphacite. These inclusions are typically confined to the core of the garnets, enveloped by an inclusion free zone on the rim. Sample 37600 differs slightly from 37554 because it was collected along the rim of a boudin, comprising therefore of an amphibole enriched zone.

Samples 37555 and 37595 demonstrated many of the same properties as the homogenous layered eclogite, though retaining an equigranular and coarse-grained granofelsic texture. Sample 37595 differs from other eclogite samples as zones of quartz are situated interstitially to the main assemblage of symplectized omphacite and coarse-grained, subhedral garnet. These zones have reacted with the garnets, forming moats of plagioclase and necklaces of clinopyroxene ± amphibole ± orthopyroxene that permeate the sample (shown in figure 5.4.11 C, D).

The last two samples are characterized by minerals that are seemingly fused together with very few clear grain boundaries. Relict coarse-grained garnets are situated in a matrix of inequigranular, symplectized amphibole + clinopyroxene + plagioclase. The garnets are typically enveloped by moats of plagioclase along the rim, but these rims also occur within the grains dividing the host garnet and inclusions. Containing a variety of inclusions like rutile, quartz,

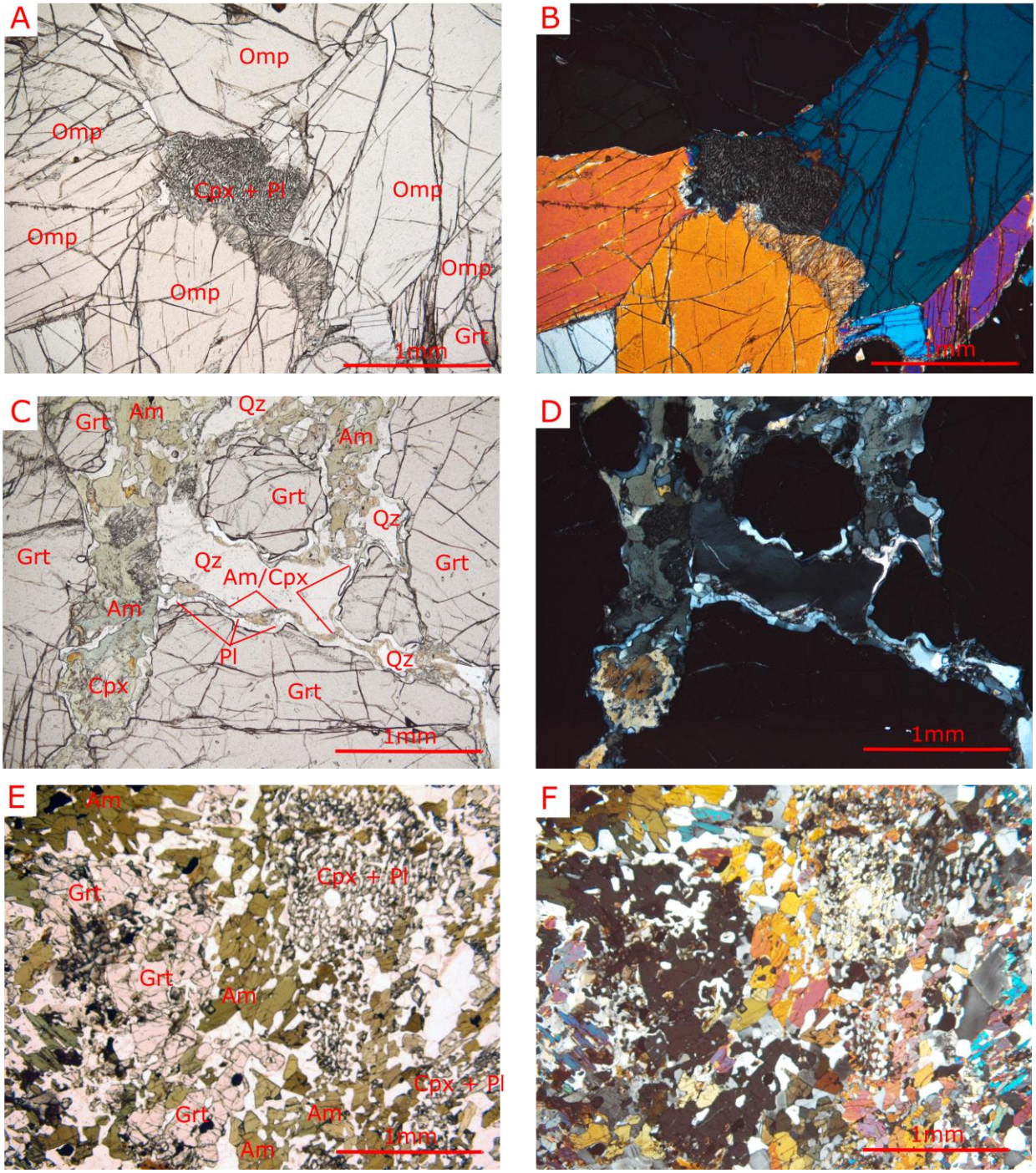

Figure 5.4.11: PP and XP photomicrographs showing textural and compositional variations within boudins, where A, B) Comes from sample 37554, showing fine-grained symplectites along the grain boundaries of omphacite, C, D) Moat of plagioclase and necklace of clinopyroxene + amphibole ± orthopyroxene between garnet and quartz in sample 37555 and E, F) Pervasive amphibole + plagioclase + clinopyroxene symplectite

amphibole and apatite, the garnets are also heavily fractured and pervasively altered within these zones, clearly shown in figure 5.4.11 E, F.

5.4.5 Gabbro

The gabbro consists of a matrix of extremely fine-grained, subhedral and recrystallized plagioclase (see figure 5.4.12). Porphyroclasts of clinopyroxene ranging in size from 1.5-2 cm are dispersed throughout the matrix. These grains generally exhibit a dusty appearance and contains lamellas of orthopyroxene and plagioclase. Granulated aggregates of both clinopyroxene and plagioclase locally exhibit coarser pseudomorph textures. Ilmenite, amphibole and biotite are amongst the fine grained alteration products within crosscutting veins.

A multiple coronitic texture has formed at the contact between the plagioclase matrix and the clinopyroxene, forming consecutive concentric rims of garnet + plagioclase + secondary clinopyroxene, from the plagioclase matrix to the boundary of the clinopyroxene grain. The garnet corona contains some needle shaped and fine grained granulated inclusions that were undeterminable. Randomly oriented prismatic biotite and amphibole grains are spaced intermittently along some of these rims. The oxide mineralogy comprises of sulfides, ilmenite and a high amount of magnetite in the matrix.

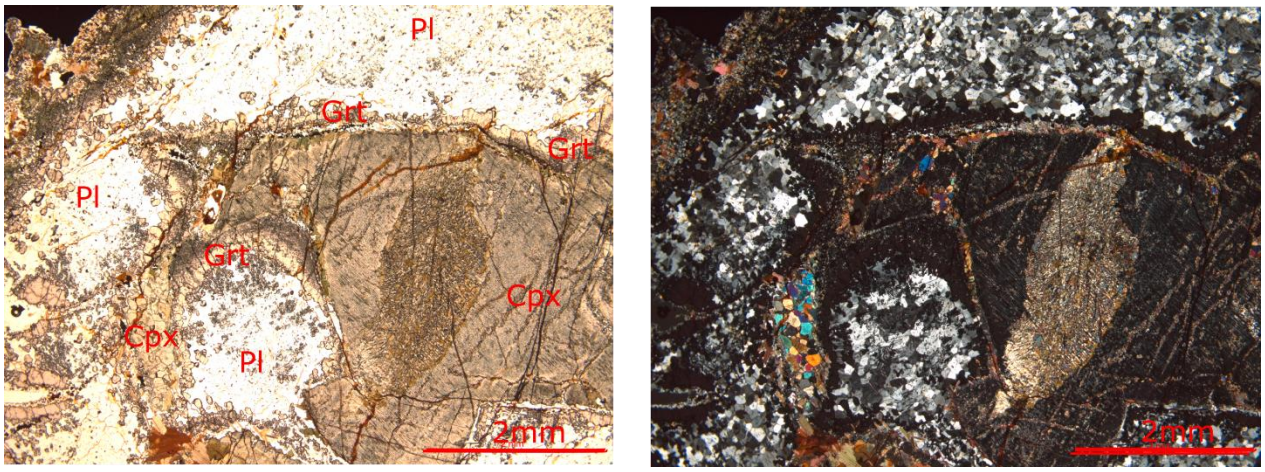

Figure 5.4.12: PP and XP microphotographs of the fine-grained recrystallized plagioclase matrix with interstitial coarse porphyroclasts of clinopyroxene.

5.5. Magnetic properties

Sample	Mass - g	Density - g/cm^3	Volume – cm^3	Bulk susc	Susc. Vol corr	Rock type
37553/M1	17.431	2.716	6.417894	0.3293	0.05131	Migmatite Gneiss
37591/G2	12.5807	3.015	4.172703	0.3807	0.09124	Garnet Amphibolite
37699/G8	8.5222	3.173	2.685849	0.0201	0.00748	Garnet Amphibolite
37700/G9	6.3016	3.172	1.986633	0.01526	0.00768	Garnet Amphibolite
37558/E3	12.9909	2.851	4.556612	0.002188	0.00048	Garnet + Amphibole Gneiss
37593/G4	18.8732	2.956	6.384709	0.1153	0.01806	Amphibole Gneiss
37592/G3	16.0452	2.779	5.773732	0.00288	0.00050	Garnet + Amphibole Gneiss
37594/B3	18.9475	3.154	6.007451	0.01356	0.00226	Garnet Gneiss
37597/E10	13.9222	3.227	4.314286	0.009189	0.00213	Garnet Gneiss
37601/G5	12.998	2.801	4.640486	0.003154	0.00068	Garnet + Biotite Gneiss
37602/G6	11.1515	2.952	3.777608	0.0155	0.00410	Garnet + Amphibole Gneiss
37698/G7	7.3524	2.926	2.512782	0.1196	0.04759	Amphibole Gneiss
37556/E1	14.7362	3.016	4.886008	0.006946	0.00142	Layered Eclogite
37557/E2	19.0713	3.194	5.970977	0.01949	0.00326	Layered Eclogite
37560/E4	12.7145	3.328	3.820463	0.003157	0.00083	Layered Eclogite
37562/E5	16.4643	3.126	5.266891	0.003672	0.00069	Layered Eclogite
37563/E6	18.5913	3.168	5.868466	0.003901	0.00067	Layered Eclogite
37564/E7	23.7884	3.392	7.01309	0.06926	0.00988	Layered Eclogite
37565/E8	17.3958	2.973	5.851261	0.1318	0.02253	Layered Eclogite
37566/E9	14.8096	3.363	4.403687	0.003895	0.00088	Layered Eclogite
37598/E11	22.0373	3.296	6.686074	0.004657	0.00070	Layered Eclogite
37697/E12	10.2262	2.982	3.429309	0.001696	0.00049	Layered Eclogite
37559/B1	22.4618	3.507	6.404847	0.006596	0.00103	Boudin Eclogite
37555/B2	15.6953	3.363	4.667053	0.003941	0.00084	Boudin Eclogite
37595/B4	14.9206	3.142	4.748759	0.01245	0.00262	Boudin Eclogite
37596/B5	14.1733	2.915	4.862196	0.01239	0.00255	Boudin Eclogite
37599/B6	16.3064	3.052	5.342857	0.01239	0.00232	Boudin Eclogite
37600/B7	6.565	3.121	2.103492	0.001013	0.00048	Boudin Eclogite
37554/G1	46.84	3.063	15.2922	1.846	0.12072	Gabbro

Table 5.5.1 – Full summary of thin section chip properties.

5.5.1 Density, remanence and susceptibility

A summary of densities and volume corrected susceptibilities of the 29 unoriented thin section chips are shown in table 5.5.1. Remanence was also measured for these samples, but have not been added to table 5.5.1 due to difficulties with correcting for the background field. Table 5.5.2 summarizes the density, susceptibility and remanence measured in the six oriented cores taken in the study area (see figure 5.4.1 for localities).

For the migmatite gneiss there is only one thin section chip recording susceptibility and density, showing a susceptibility of 0.051 (SI) and density of 2.7 g/cm^3. Field measurements of this rock type suggests a highly variable distribution of susceptibilities ranging from 0.00062 – 0.14030 (SI).

Garnet amphibolite samples are represented both as core samples and thin section chips. Susceptibilities in this rock type generally range from 0.00784 – 0.022 (SI), with an abnormally high susceptibility = 0.091(SI) recorded in sample 37591. Densities both in core samples and thin section chips are similar and falls within the range of 2.9 -3.1 g/cm^3.

The garnet + amphibole gneiss samples show susceptibilities ranging from 0.00012 – 0.01482. Amphibole enriched gneisses differs from the former by showing elevated susceptibility measurements ranging from 0.02475 – 0.12760 (SI). The highest susceptibilities were only measured locally in the field. The highest densities in this group are 3.1-3.2 g/cm^3 found in samples 37594 and 37597, which are derived from two garnet enriched gneisses. The remainder amphibole + garnet gneisses and amphibole gneisses all have densities ranging between 2.7-2.9 g/cm^3.

By comparing the susceptibilities of the thin section chips and field measurements in table 5.5.3 all susceptibility measurements consistently falls within the same range of 0.00050 – 0.02253 (SI) both for layered eclogite and boudin eclogite. The densities in these samples however varies from 3.5 g/cm^3 in the most pristine boudin eclogite sample 37559 to around 3.3 g/cm^3 in the homogenous layered eclogite samples to 3.1 g/cm^3 in the heterogeneous layered eclogite samples. Sample 37554 coming from the gabbro close to Visnes has a susceptibility of 0.120 (SI) and density of 3.06 g/cm^3.

	Rock type	Mass - g	Density - g/cm^3	Volume -cm^3	Bulk susc	NRM [A/m]	Dec	Inc	Sus. volcorr (SI)	NRM volcorr - A/m	Ji	Q
AV1	Garnet Amphibolite	29.908	2.857	10.468	0.229	0.459	281.900	33.500	0.022	0.489	0.895	0.546
AV2	Amphibole gneiss	29.785	2.985	9.978	1.099	1.180	107.000	13.900	0.110	1.319	4.510	0.292
AV3	Eclogite	32.369	3.283	9.859	0.041	0.055	26.800	24.100	0.004	0.062	0.170	0.362
AV4	Eclogite	33.899	3.248	10.437	0.169	0.119	4.900	14.000	0.016	0.127	0.664	0.191
AV5	Garnet amphibolite	31.728	3.182	9.971	0.033	0.047	201.800	47.200	0.003	0.052	0.135	0.389
AV6	Garnet amphibolite	32.187	3.028	10.630	0.077	0.141	92.400	45.300	0.007	0.147	0.297	0.497

Table 5.5.2: Selected measurements of the properties of oriented cores.

1.	2.	3.	4.	5.	6.	7.	8.	9.	10.
0.01707	0.00314	0.00583	0.00771	0.01472	0.00135	0.00012	0.04822	0.01517	0.00062
0.04454	0.00195	0.00050	0.00179	0.01347	0.00251	0.01363	0.11400	0.01496	0.00068
0.00974	0.00184	0.00482	0.00244	0.00251	0.00077	0.00011	0.11250	0.00187	0.01432
0.00940	0.00068	0.01613	0.00142	0.00076	0.00954	0.00180	0.12760	0.01387	0.00614
0.00640	0.00146	0.00079	0.00098	0.00954	0.00441	0.00132	0.11710	0.00784	0.00020
0.00271	0.00600	0.00097	0.00593	0.00441	0.00070	0.00102	0.12310		0.00189
0.00892	0.00826	0.00919	0.00498	0.00070	0.00059	0.00103	0.04258		0.00192
0.00080	0.00105	0.00070	0.00872	0.00059		0.01482	0.02724		0.00099
0.00408	0.00049	0.01606	0.01228	0.00220		0.00437	0.02475		0.14030
0.00218	0.00526	0.01205	0.00180	0.00647		0.00600	0.14030		0.01845
0.00350	0.00049	0.00512	0.00356	0.00890		0.00620	0.03939		0.00640

Table 5.5.3: These susceptibilities were measured by a handheld susceptibility meter and their unit is in (SI). Selected susceptibility measurements in the various parts of the study area for eclogite in row 1- 7, located 1) Visnes eclogite, 2) West coast Averøya, 3) Tøvika, 4) Mid island, 5) SE Averøya and the remaining rows show susceptibilities in 7) Garnet and amphibole gneiss, 8) Amphibole gneiss, 9) Garnet amphibolite and 10) Migmatite gneiss.

5.5.2 Modelling

Modelling was conducted on the profile marked with a red line on figure 5.5.1 A, with the profile modelled shown in 5.5.1B.

All susceptibility measurements used in the profile have been derived from either field measurements or from core- or thin section chip measurements. Because these values are generally well known in the study area, when adjustments were made to the the model, it was primarily the Q-value that was changed. Table 5.5.2 shows that most of the Q-values in the cores range from 0-1, indicating that induced magnetization dominates over remanence. Although only core av3 and av4 directly occur along the profile, it was attempted to keep q-values below 1 in the profile. When Q = 1 remanence and induced magnetization are equal.

This profile reflects the magnetic characteristics of the lithologies in the area and polygons marks areas of similar attributes and not necessarily individual lithologies. All bodies with orange color are predominantly garnet to amphibole gneisses, though variously retrograded eclogite boudins are spaced intermittently. The brown bodies are amphibolite gneiss and purple bodies are garnet amphibolite.

At the western end of the profile, amphibole gneiss is known to occur at Tøvika ferry wharf and typically show elevated susceptibilities taken in the field (0.03 – 0.1 SI). Although this body is generally outside of the profile it has been placed at the edge to account for the following low as a result of susceptibility contrast between body 1 and body 2. The anomaly that occurs between body 3 and 4 is concordant with the trace of an outward bound anticline marked on figure 5.2.4 as F6. A Q-value of 3 had to be used in this body to account for the high anomaly. At the eastern edge of the profile three anomalies seem to imply crossing lithological boundaries followed by the trace of a syncline.

The modeled profile seem to represent the subsurface geology in a valid way. Both the anticline and the syncline along this transect shows up on the anomaly map. Lithological boundaries seem to be concordant and either negative or positive anomalies shown in figure 5.5.1A. Of especial interest is that the traced outline of the layered eclogite body on Averøya shown on this figure is seemingly enclosed within positive magnetic anomalies that could be from the amphibole gneiss.

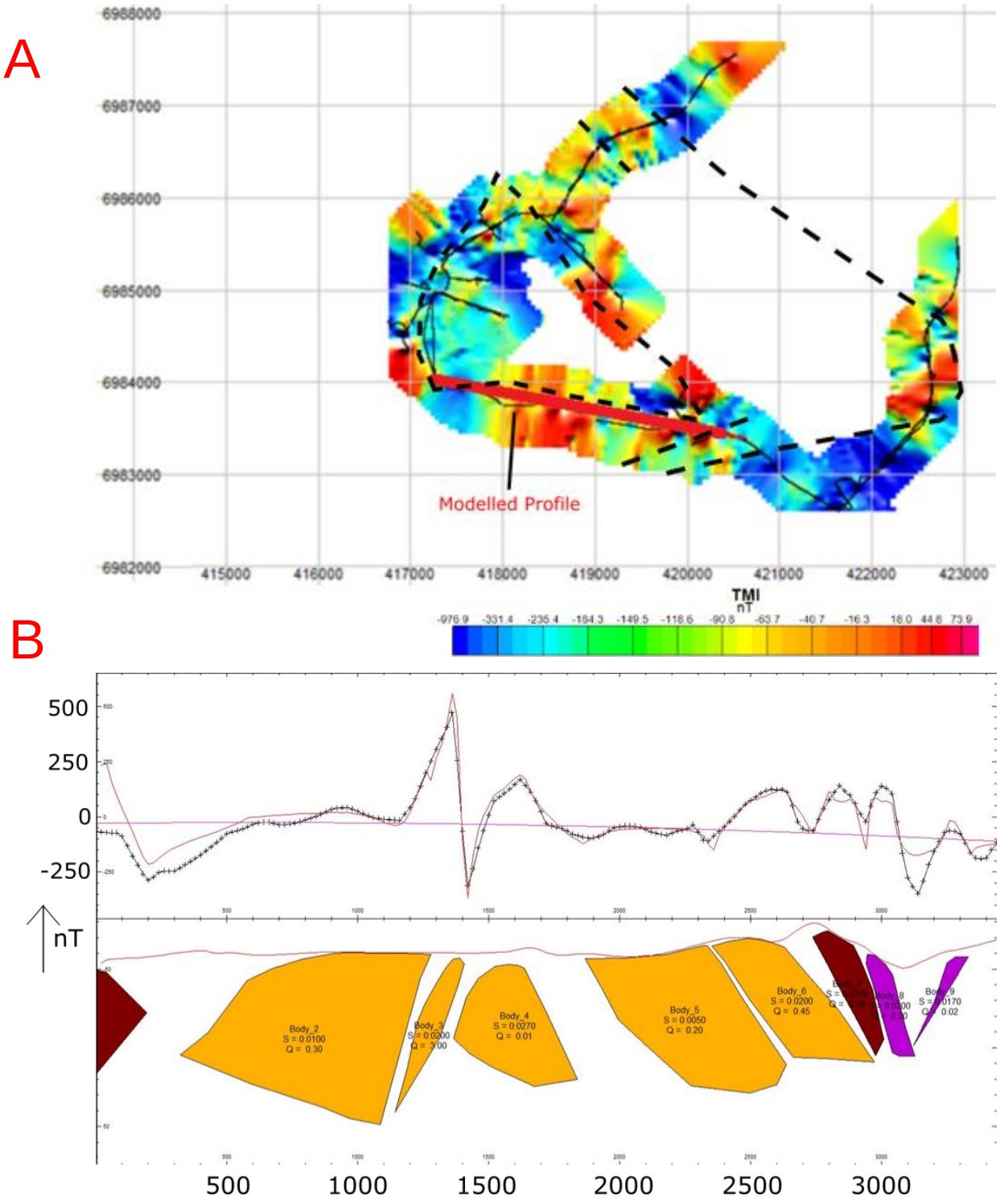

Figure 5.5.1: A) Showing the gridded magnetic anomaly map derived from the ground magnetic survey, with dashed outline of anomalies concordant with lithological boundaries. B) Modeled bodies with properties S = susceptibility and Q = Q-value. Y-axis shows nT and X- axis shows distance in meters. Where the background is given by S = 0.0001 and Q = 0.

Chapter 6 – Discussion

6.1. The Structural framework

The final geological map was constructed on the basis of field work. This was aided by the study of magnetic anomalies on the gridded magnetic map, to improve the accuracy of the inferred and approximate unit boundaries. The boundaries between the basement migmatite gneiss and the garnet amphibolite is highly uncertain both on the southeastern part on Averøya and close to Visnes and Lyngstad on the mainland. Mapped boundaries on a previous map by NGU was used locally to infer these boundaries on the final map.

6.1.1 Local tectonostratigraphy

The resulting map is shown in figure 6.6.2, it illustrates the geometry and relationship between the basement rock and the nappe unit. In the results chapter section 5.1 the four main rock types in the study area are described and presented according to the local tectonostratigraphic order. The Baltic basement unit consists of the tonalitic to granodioritic migmatite gneiss with local metamorphosed mafic dykes, pegmatites and rare eclogite boudins ((P. Robinson, 1995; Terry & Robinson, 2003; Tucker et al., 2004).

The structurally overlying Blåhø nappe of the Middle allochthon consists of garnet amphibolite and garnet and amphibole quartzo-feldspathic gneiss. Both of these rock types wrap around the various layered eclogite bodies, including the Averøya eclogite and abundant small-scale granoblastic eclogite boudins. Differentiating between Baltic basement rocks and overlying nappe units is commonly difficult (per com., P. Robinson) in the WGR, however at Averøya both the garnet amphibolite and garnet and amphibole gneisses are characteristic rock types assigned to the Blåhø unit (P. Robinson, 1995; P. Robinson et al., 2003). On the west coast of Averøya there is a well-established SE-dipping contact between the Baltic basement unit and the overlying nappe unit that could be a thrust, an extensional fault or a thrust reactivated as an extensional fault.

The contact between the garnet amphibolite and the garnet and amphibole gneiss in the nappe unit remains uncertain and could be either transitional or tectonic. It was decided to include the

amphibole gneiss shown in the outcrop figure 5.5.1, with the garnet and amphibole gneiss unit in the finalized map, because of its relatively scattered and random distribution. Along the northern margin of the layered eclogite body the amphibole gneiss occurs as a semi-continuous zone that could be relict eclogite subjected to pervasive amphibolitization through the influx of fluids or shear deformation imposed by the surrounding gneiss (D. Carswell et al., 2003; Cuthbert et al., 2000; Hollocher, 2014).

Most of the confusion regarding the affinity of the layered eclogite on Averøya, seems to be related to the apparent contact of the layered eclogite and the Baltic basement unit at Tøvika ferry wharf. In this thesis it is suggested that the layered eclogite resides within the Blåhø nappe unit, more specifically within the garnet and amphibole gneiss, where it is sandwiched up very close to the contact with Baltic basement unit at the ferry wharf. A small stretch of amphibole and garnet gneiss was observed between the basement and the layered eclogite. In further support of this statement is that all the other layered eclogite bodies at Visnes, Lyngstad, Hendholmen and Ufsåsen reside in either garnet and amphibole gneiss or the garnet amphibolite in the Blåhø nappe (see figure 5.5.1 for localities). The Lyngstad and Visnes bodies are located close to the marble quarry, which is an additional rock type commonly associated with the Blåhø unit (Cuthbert et al., 2000).

The exaggerated ovoid shaped symbols on the geological map indicate zones particularly enriched in eclogite boudins in the field. The spacial relationship between these granoblastic eclogite boudins and the layered eclogite remains poorly understood. Considering the close proximity to the layered eclogite and that the majority of the eclogite facies boudins reside within the nappe unit, a similar origin of these and the layered eclogite seems likely (per com., P. Robinson). The granoblastic texture in these boudins may however indicate that the boudins are derived from a slightly different protolith from the layered volcanics, interpreted to be the source of the layered eclogite body (Hollocher et al., 2007).

Both layered eclogite and boudin eclogite must have formed as a response to either shear-induced recrystallization or widespread diffusional processes caused by fluid infiltration during peak metamorphism (Mørk, 1985). Tectonic separation of individual smaller boudins and layered eclogite from the larger body appears to have occurred, demonstrated in the geology of Flem (Mørk, 1985; Terry & Robinson, 2004). These smaller boudins in local shear zones, had higher

chances of preserving original eclogite facies granoblastic textures from the amphibolite stage reworking that took place in surrounding more sheared rocks (Cuthbert et al., 2000; Krabbendam & Dewey, 1998).

Similar tectonostratigraphic sequences have been described in the central and southern belts of Nordøyane (Terry & Robinson, 2004), the Moldefjorden belt (P. Robinson, 1995) and in the Norbotten and Jamtland domains corresponding to the Seve nappe in Sweden (equivalent to Blåhø)(Gordon, Whitney, Teyssier, Fossen, & Kylander-Clark, 2016). Geochronological data have yet to be obtained from the Nordøyane and the Moldefjorden belt, but ages of the Seve nappe in Sweden have been estimated in several places. Three separate localities yield pre-Scandian ages of 450 – 505 Ma (Brueckner, Van Roermund, & Pearson, 2004; Essex, Gromet, ANDRÉASSON, & Albrecht, 1997; Hacker & Gans, 2005; Mørk, Kullerud, & Stabel, 1988). Even though both eclogite crystallization age of 415 Ma and an overprinting garnet and amphibole age of 410 Ma have been obtained for the Averøya layered eclogite (T. E. Krogh et al., 2011), this part of the Blåhø nappe can theoretically have experienced a similar pre-Scandian deformational history as the recorded Seve Nappe in Sweden.

Why do some nappe units contain eclogite facies mineral assemblages and others lack them remains a problem. According to (P. Robinson et al., 2014) out of sequence thrusting and subsequent recumbent folding of previously subducted basement and eclogite must be involved to the solution of this problem.

6.1.2 The structure and geometry of the layered eclogite

Any pre-Scandian fabrics or structures are seemingly completely overprinted by fabrics formed during the Scandian orogeny in the study area. Early eclogite facies NW-N plunging lineations and NW-N plunging folds are preserved locally in the garnet and amphibole gneiss and the layered eclogite bodies, showing almost a 90° angle to the late lineation. This has been decided mostly on previously collected information in other localities in the WGR like the Haram gabbro (Terry & Robinson, 2004), Vårdalsnes eclogite (Engvik & Andersen, 2000) and Salt Mylonite Zone (Renedo et al., 2015) where the overprinting have been established in the field.

The pervasive amphibolite stage overprinting fabric, observed through much of the WGR, also dominates in the study area. Most foliations in the study area are consistent with the regional NW

or SE dipping foliations and corresponding gently NE-SW plunging lineation (Terry & Robinson, 2003). Chapter 5.2 describes the majority of the structures associated with this stage, including ENE – WSW upright and foliation parallel folds, pervasive passive folding and local melting in the basement rocks and gneisses (described in chapter 5.1.1). (Andersen et al., 1994; Osmundsen et al., 2006; Terry & Robinson, 2003). Sinsitral and top to the SW senses of shear are also connected to this stage and have been recorded in various porphyroclasts and asymmetric boudins throughout the study area. The more competent garnet and amphibole gneiss and layered eclogite contain brittle features like tensile veins and conjugate fractures consistent with regional N-S shortening and E-W stretching.

The shape of the layered eclogite body and the encasing garnet and amphibole gneiss are indicated in illustration (figure 6.1.1) and by dashed lines in the final map (figure 6.1.2) (per

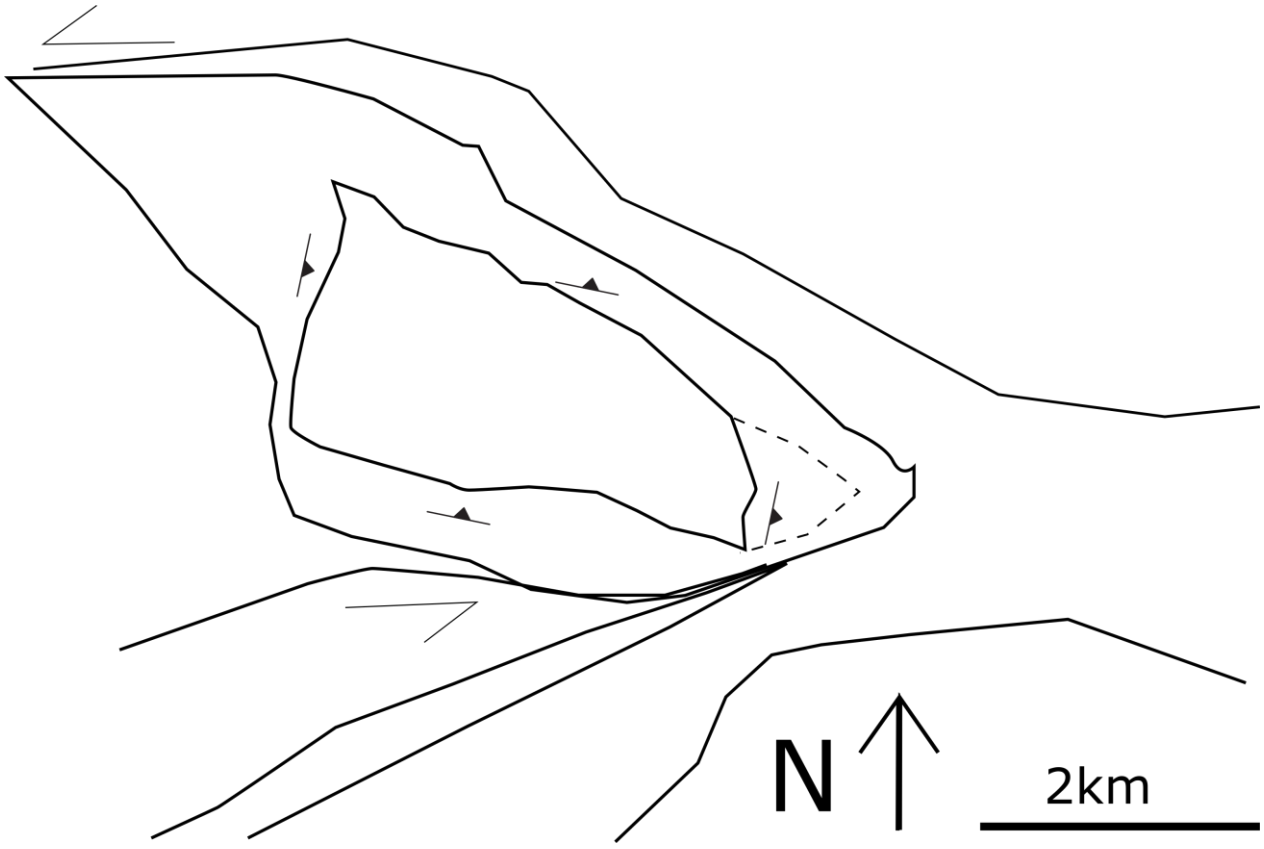

Figure 6.1.1: An illustration of the inferred outline of the layered eclogite and the surrounding garnet and amphibole gneiss. Both of these rock types have asymmetric and ovoid shapes.

com., P. Robinson). The coastal sections on the eastern part of the mainland were not covered during the field studies, but on the previous map by NGU this area is marked as a part of the basement migmatite gneiss. This means that both the layered eclogite and the garnet and amphibole gneiss must be pinching out somewhere between Averøya and the mainland. Both the garnet and amphibole gneiss and the layered eclogite have been given slightly asymmetric and ovoid shapes and have presumably been shaped by sinistral shear zones along these boundaries. The dashed outline in figure 6.1.1 marks a possible extension of the layered eclogite body to include the outcrop on Ufsåsen on Averøya.

The outline of the garnet amphibolite is also shown on the final map in figure 6.1.2. This rock type also seems to pinch out with the garnet and amphibole gneiss to the west and wraps around both the garnet and amphibole gneiss and the layered eclogite along the northern margin. It does not pinch out to the east, but forms a semi-continuous layer from the southeastern part of Averøya across the ocean towards Visnes on the mainland. On the previous map from NGU the boundary of the garnet amphibolite has been inferred to go along the layered eclogite body on the southern coast and extend further north on the mainland than what is shown on figure 6.1.2. The boundaries between the garnet amphibolite and the migmatite gneiss should be covered more thoroughly in the future.

Foliation measurements in the area were not easily matched with the resulting overall structure. Local perturbations were caused by NW dipping foliations, with rare SE dipping foliations, consistent with regional amphibole stage late folding. Foliations along the length of the main body were commonly relatively parallel to the unit boundaries, the problem was to sort out the contacts along the ends of the body. Figure 6.1.1 shows how the foliations and boundaries were interpreted to be, based on the orientation of the majority of the foliations locally in the areas.

Two cross sections were constructed on the basis of figure 6.1.1 and 6.1.2. Both were projected parallel to each other and perpendicularly to the late NE-SW folding trend in the study area. These resulting profiles are shown in figure 6.1.3, starting on the top from profile 1 to profile 2 on the bottom, projected along the NW - SE. The horizontal and vertical axes for all profiles have been scaled up times x2 to the original line drawn in figure 6.1.2.

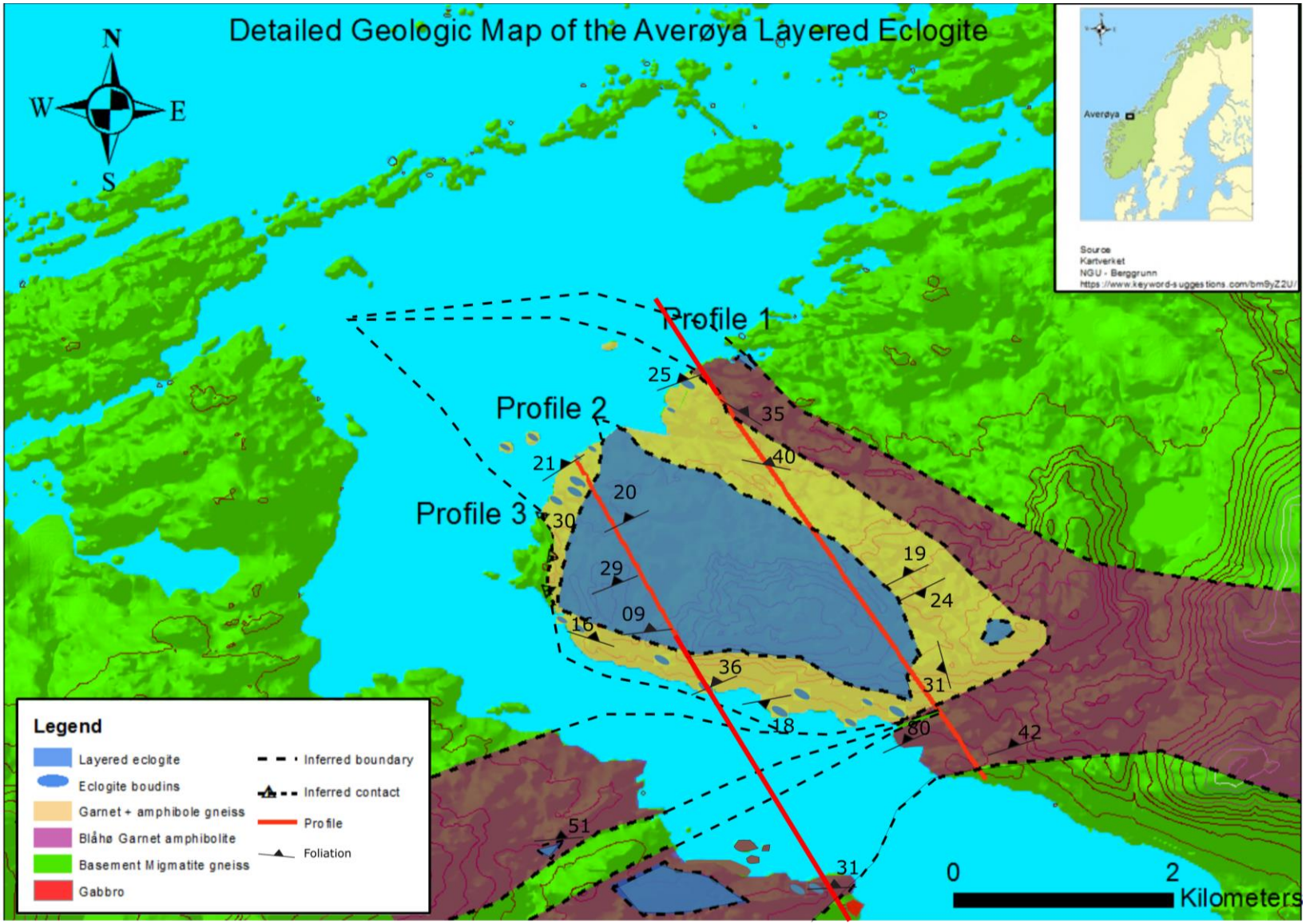

Figure 6.1.2: Detailed geological map over Averøya.

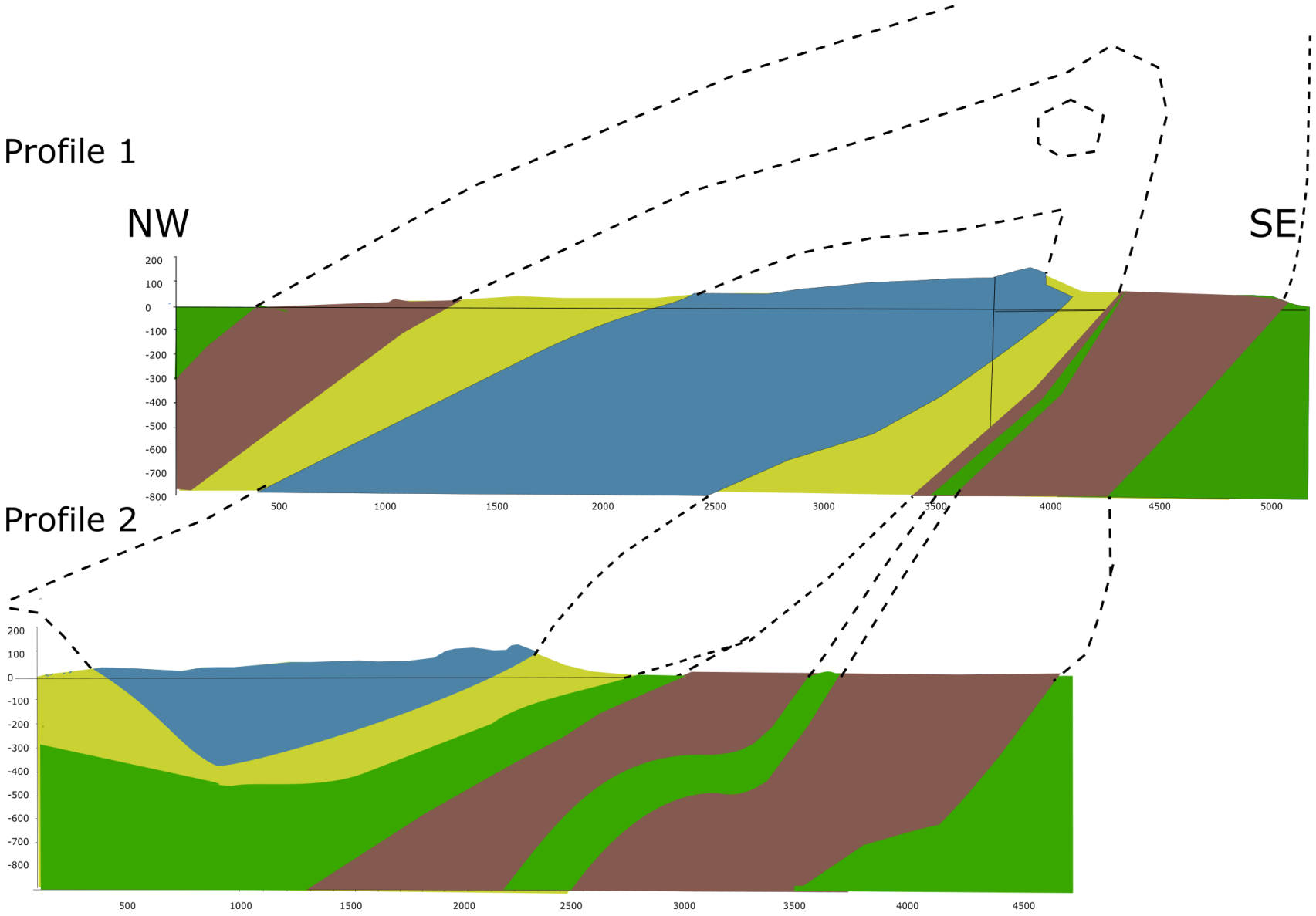

Figure 6.1.3: The two profiles from figure 6.1.2, showing possible geometry of the layered eclogite body

6.2. Metamorphic evolution

Several separate metamorphic stages can be defined for the study area by establishing coexisting mineral assemblages, zoning patterns within coarser minerals and the distribution of inclusions chiefly within garnets. Although the distribution of these samples do not define a concrete regional metamorphic pattern, the textural and compositional variations record a continuously evolving metamorphic history from early subduction to late exhumation processes. Hints of the igneous and/or metamorphic history of some of the rocks before the Scandian metamorphism is rare, but was discovered in one of the samples. The most important textures, mineral compositional characteristics and reactions of these stages will be discussed.

6.2.1 Pre-Scandian petrology

A good candidate for a protolith for the basement eclogites in the study area is sample 37554 derived from a gabbro lense within the basement migmatite gneiss. The relict igneous to metamorphic assemblage in this sample consists of plagioclase + clinopyroxene + orthopyroxene + ilmenite + magnetite. The overprinting metamorphic texture and mineral assemblage makes it hard to derive the pre-Scandian history of this rock type.

6.2.2 Pre-eclogite stage

Sample 37554 shows both compositional and textural evidence of partial eclogitization of the pre-Scandian igneous to metamorphic assemblage described in 6.2.1. This metamorphic assemblage consists of garnet + amphibole + Na – plagioclase + Na clinopyroxene + biotite ± spinel. Similar rock types in the WGR have been described by (Mørk, 1985) in the olivine + plagioclase + pyroxene Flem Gabbro, in the predominantly pyroxene and plagioclase rich Haram Gabbro (Terry et al., 2000), in gabbros in the Moldefjorden area by (Hernes, 1954) and in a coronitic eclogite (Engvik, Austrheim, & Erambert, 2001). All these studies have been concerned predominantly with gabbroic rocks with slightly varying mineral assemblages.

The multiple coronitic reaction textures between plagioclase and pyroxene and plagioclase and olivine in these rock types do not vary much. In sample G1 this texture can be expressed accordingly from plagioclase matrix towards the edge of the clinopyroxene grain: Ca Garnet +

Na plagioclase + Na pyroxene, the reaction forming these phases should look something like equation 6.2-1.

Equation 6.2-1: $\boldsymbol{Opx + Ca\ pyroxene + Ca - plagioclase \rightarrow Ca\ Garnet + Na\ plagioclase + Na\ pyroxene}$

All observations regarding mineral chemistry in the gabbro have been made on a limited sample pool, though consistently indicating that primary magmatic plagioclase and pyroxene are enriched in Ca. Subsequent metamorphic pyroxene and plagioclase forming as a part of the corona texture shows higher Na in both phases because Ca goes into the grossular component of garnet. This is similar to other findings in (Hernes, 1954), (Terry et al., 2000) and (Mørk, 1985). The random orientation of biotite and amphibole along grain boundaries and fractures within grains suggests an introduction of fluids during decompression under the amphibolite-stage metamorphism. There is a consensus that these rock types were prevented from becoming eclogites due to a lack of sufficient hydration or deformation during peak metamorphism (Bucher & Grapes, 2009; Engvik et al., 2001; Lutro et al., 1997; Mørk, 1986). Such preservation of metastable states seems to be very common in the WGR (P. Robinson, 1991).

6.2.3 Prograde eclogite stage

The main mineral assemblage during prograde to peak eclogite metamorphism in the eclogites has been interpreted to consist of omphacite + rutile + garnet. Accessory minerals include kyanite + epidote + phengite + quartz/coesite, which are present as inclusions in garnets locally in the study area. These assemblages are with the exception of coesite pseudomorphs or proven coesite, similar to assemblages found in UHP eclogite boudins at Fjørtoft, Flemsøy (Terry et al., 2000) and Harøy (Butler et al., 2012). There are inclusions of SiO_2 in garnets both in sample 37559 and 37600, though the characteristic PCQ texture and appropriate shape characterizing coesite pseudomorphs have yet to be observed.

The chemical attributes for the boudin eclogite samples (37559, 37555 and 37600) are characterized by high Mg garnet (Xprp53), low Jd omphacite (Xjd15) coupled with a low $Fe^{2+}/(Mg + Fe^{2+})$ ratio for omphacite, consistent with attributes of the boudin eclogite sample from Fjørtoft. The preferential partitioning of Mg/Fe^{2+} between garnet and clinopyroxene is a known geothermometer, suggesting the highest preserved temperature conditions are in sample

37559 where Xprp = 53 and $Fe^{2+}/(Mg + Fe^{2+}) = 0.02 – 0.05$ for pyroxene grains (Krogh Ravna & Terry, 2004; POWELL, 1985).

Individual EMP point analyses derived from cores to rims of the garnets from the boudin samples demonstrate a progressive increase in $Fe/(Mg + Fe^{2+})$, consistent with re-equilibration during cooling (Bryhni & Griffin, 1971; E. Krogh, 1982). These garnets are coarse and anhedral, containing minor amphibole, epidote and plagioclase inclusions confined to the core with homogenous and inclusion poor rims. These textural characteristics contradict the findings in the mineral chemistry and may reflect the prograde metamorphic history from early amphibolite to eclogite stage (Cuthbert et al., 2000; E. Krogh, 1982). Continuous compositional zoning profiles should be obtained to reassess whether these garnets record evidence of the prograde stage.

According to (Cuthbert et al., 2000; Alice Wain, 1997) UHP garnets differ from HP garnets by exhibiting anhedral shapes, having compositionally unzoned profiles and few inclusions. Prograde garnets containing coesite, thereby demonstrating UHP conditions have been observed locally at Vetrhuset and Årsheimneset in the WGR(Cuthbert et al., 2000; Alice Wain, 1997) . This simplified HP and UHP garnet division, can therefore not be applied to exclude UHP conditions for eclogites that seem to have prograde garnet textures.

The chemical attributes of the layered eclogite samples (37560 and 37598) are characterized by intermediate Mg (Xprp = 42%) and $Fe^{2+}/(Mg + Fe^{2+}) = 0.02 – 0.08$ for pyroxene in sample 37598, indicating that these samples experienced slightly lower temperatures than the boudin samples. Garnets in these grain are virtually unzoned, with similar to a slightly decreasing $Fe/(Mg + Fe^{2+})$ ratio from core to rim. Exhibiting subhedral and flattened shapes, these garnets are generally inclusion poor, containing rare rutile, omphacite and one phengitic white mica. These characteristics are similar to the UHP definition by, (Alice Wain, 1997) though coesite remains elusive. According to latest P-T estimates calculated by Jared Butler and Mike Terry using garnet compositions and pyroxene compositions from this sample and an assumed phengite composition, UHP conditions seem highly likely.

6.2.3 Granulite stage

Eclogites are known to be prone to revert to lower pressure assemblages during decompression and exhumation. Near Averøya both eclogites and gneisses record textures and assemblages related to this process. The overprinting mineral assemblages in the eclogites consist of varying amounts of plagioclase + clinopyroxene + amphibole + ilmenite + biotite + calcite + magnetite.

Equation 6.2-2 Garnet + phengite → biotite + quartz

One of the earliest breakdown reactions from (U)HP eclogite metamorphism in the study area is shown in the layered eclogite sample 37598 and involves the breakdown of high pressure phengite according to equation 6.2-2. This is a fluid conservative reaction, which makes the assemblage phengite + garnet + clinopyroxene a suitable geobarometer(Krogh Ravna & Terry, 2004; Ravna & Roux, 2006) coupled with the Fe-Mg clinopyroxene + garnet thermometer (POWELL, 1985). There is only one confirmed grain in this sample situated as an inclusion within a garnet and strongly overprinted by biotite at the edges. Both the phengite and the enclosing biotite are enriched in Ti, which could be a result of contamination of the analyses from surrounding rutile or as (Auzanneau et al., 2010) discovered that Ti-rich phengite can be stable at UHP conditions recording a pressure of 3Gpa and T = 900°C. Inclusions of phengite within garnets have also been observed in sample 37601, the garnet + biotite gneiss, where the high abundance of biotite + plagioclase in the matrix could be products after phengite.

Equation 6.2-3: Kyanite + omphacite + garnet → plagioclase + corundum + plagioclase ± spinel

Thin section 37598 also contains one singular kyanite grain bordering a garnet on one side and a relict omphacite matrix on the other side. Because of the extremely fine-grained nature of these intergrowths it was hard to obtain good compositional analyses of the minerals. The symplectite appears to contain plagioclase + corundum + sapphirine + spinel.

Equation 6.2-4: Garnet + Rutile → ilmenite

Another HP mineral that starts breaking down post-eclogite facies conditions is rutile. The most well preserved rutile grains have been found in the boudin samples and the homogenous-layered eclogites. In the heterogeneous samples these rutiles are commonly overprinted by ilmenite (equation 6.2-4)(Korneliussen et al., 2000). Rutile locally occurs both in garnet amphibole gneiss

and garnet-rich gneisses. This can be explained by extraction of FeO from garnet during decompression and reaction with rutile (per com., P. Robinson).

Equation 6.2-5: Mg, Fe, Ca Garnet + Quartz → Plagioclase + Ca-pyroxene ± Amphibole ± Orthopyroxene

A moat and necklace texture occurs locally within both boudin- and layered eclogite samples 37555, 37560, 37564 and 37565. Based on the occurrence of symplectite S2 and S3 in these samples (described in the following paragraph) this reaction is thought to occur at the granulite to early amphibolite stage of overprinting. Quartz must be present in the protolith either interstitially as veins or beds for this reaction to occur during exhumation. Although the exact reaction remains poorly understood, the study by (P. Robinson, Daczko, N., Krogh, T.E. & Hollocher, K, 2008) suggests that pervasive diffusion of Na from omphacite through the matrix plays an important role.

Equation 6.2-6: Omphacite + Quartz → Ca pyroxene + plagioclase ± amphibole

Equation 6.2-7: Omphacite + garnet → plagioclase + amphibole ± magnetite

Four stages of symplectites replacing omphacite during decompression with either constant or decreasing temperature and continued re-equilibration according to equation 6.2-6 and 6.2-7 (Butler et al., 2012) are variably recorded in the samples at Averøya and shown in fig 6.2.1. Symplectite S1 and S2 are exsolution symplectites, developing as lamellar intergrowths at grain boundaries between two grains with similar chemistry and with different orientations described previously in (Joanny et al., 1991; Passchier & Trouw, 2005). Symplectites S3 and S4 represent the majority of the symplectites in the samples from Averøya and have developed a globular and graphic shape, caused by grain boundary reduction. Temperature and pressure estimates can only be obtained from the lamellar S1 and S2 symplectites(Joanny et al., 1991).

Symplectite S1 are only recorded in sample 37559 and 37600 forming as medium sized lamellar intergrowths along grain boundaries (figure 6.2.1 A). Chemical compositions of the host yields Xjd of 15-20 % in the host omphacite and Xjd of 2-10% in the symplectite and Xan = 30-40%. Pale, yellow amphibole symplectites also occur along with the plagioclase and Ca pyroxene lamellas, these record the lowest $Fe/(Mg + Fe^{2+}) = 0.5 - 0.12$ of all samples. Based on the shape

and descriptions of these symplectites this thesis suggests that these correspond to type S1 or S2 described by (Joanny et al., 1991).

Thinner lamellas characterized symplectite S2, which was only witnessed in sample 37563 in the layered eclogite at Visnes (figure 6.2.1 B). The predominantly amphibole enriched matrix combined with interstitial garnet enveloped by amphibole + plagioclase symplectites (equation 6.2-7) attest to final stages of complete amphibolitization (Hernes, 1954). A few isolated relict omphacite grains contain lamellar symplectites that permeate the grains, becoming progressively more fine-grained towards the grain boundaries. In addition to the phases in equation 6.2.6, orthopyroxene occur locally as an additional symplectite phase in the relict omphacite. This

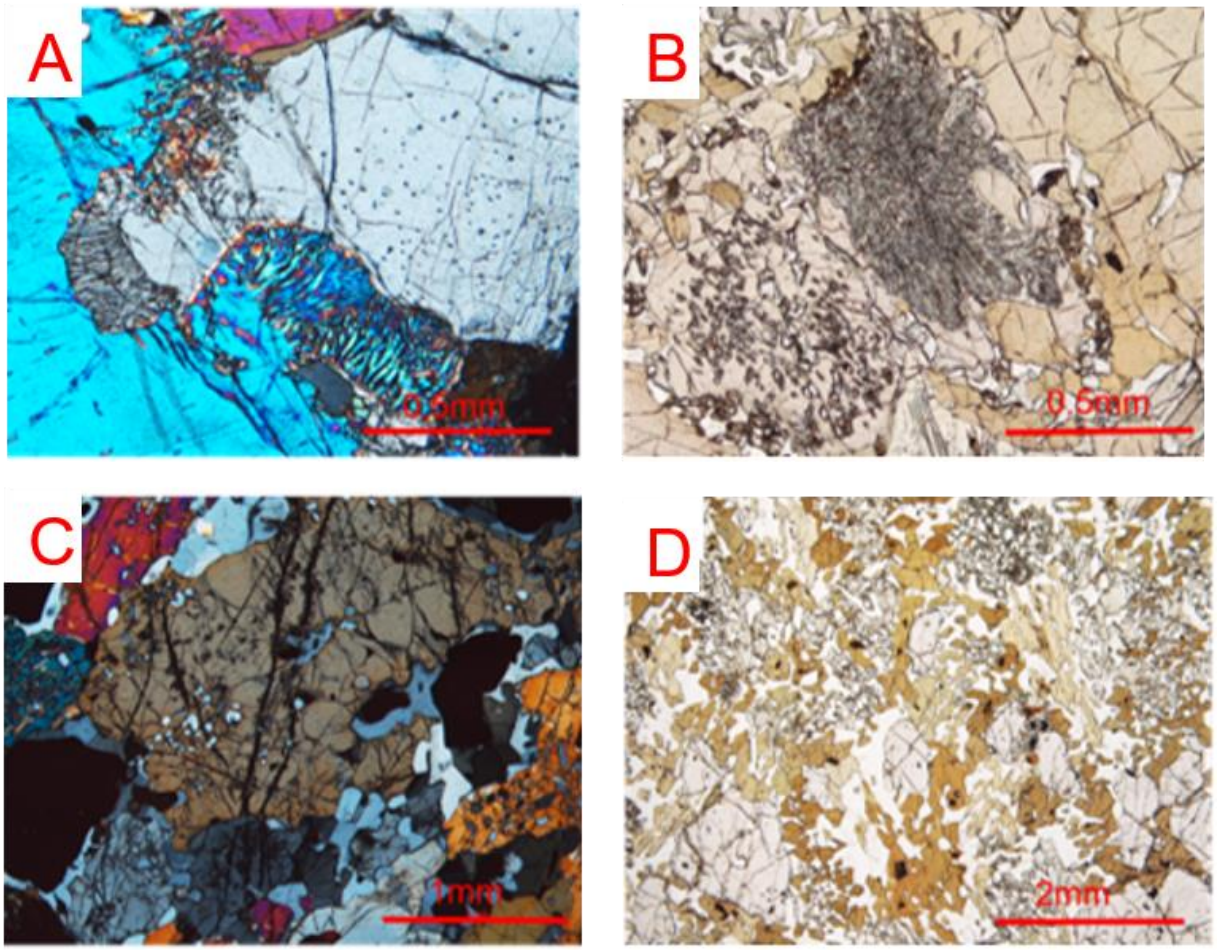

Figure 6.2.1: PP and XP microphotographs showing the symplectite evolution in the Averøya eclogite from lamellar intergrowths in A) S1 in sample 37600 and B) S2 in sample 37563 and globular symplectites as C) S3 in sample 37566 and D) S4 in sample 37557

symplectite has thinner lamellar width than S1, indicating that sample 37563 has become exhumed more slowly than the boudin samples 37559 and 37600 (Joanny et al., 1991).

The third symplectite stage or S3, consists of rod shaped inclusions locally within omphacite occurring in the homogenously layered eclogites (figure 6.2.1 C). These symplectites record compositions of Xjd = 20-35% for the host omphacite with a corresponding Xjd = 5- 20% in the pyroxene symplectite and Xan = 20-30 % for the plagioclase symplectites. Many of the layered eclogite samples have both these symplectites and development of coarser symplectites S4 occurring in the same sample. This could explain the inconsistent spread of the chemical compositions of pyroxene in figure 5.3.2 C. Rare amphibole symplectites show slightly higher $Fe/(Mg + Fe^{2+}) = 0.1 -0.19$ than the boudin samples.

The final stage, S4, is commonly found in the heterogeneous layered eclogites and is characterized by complete eradication of any original grain boundaries by coarse graphic symplectites in the matrix, typically with a dusty overprint. Because of the high amounts of amphibole occurring within these samples a transition into amphibolite stage seems indicated. Although there are no analyses from samples from this stage in this study, the study by (P. Robinson, Daczko, N., Krogh, T.E. & Hollocher, K, 2008) provided chemical compositions from samples at the quarry locality on Averøya. Host pyroxene compositions yields Xjd = 38%, with a corresponding symplectite of Xjd = 11% and Xan = 32% (P. Robinson, Daczko, N., Krogh, T.E. & Hollocher, K, 2008). Amphibole is considerately more abundant these samples as coarser pale brownish grains. There are however no analyses from the amphibole in the retrogressed layered eclogites that can be compared with former amphibole symplectite compositions.

Equation 6.2-8: Fe3+ bearing epidote + minor FeO + CO2 = Calcite + Anorthite + Magnetite + H20

All the gneiss samples show traces of epidote, which is a hydrous mineral that can be stable in some rocks under HP and UHP conditions eclogite conditions (Terry et al., 2000). Isolated grains of epidote in these samples are typically surrounded by small grains of magnetite and intergrowths of Ca plagioclase with calcite. This reaction, shown in Equation 6.2-9, probably occurred during decompression, where the FeO might come from garnet decomposition (per com. P. Robinson).

6.2.4 Amphibolite stage

The main mineral assemblage during this stage consists of epidote + K-feldspar + quartz + plagioclase + biotite + amphibole + titanite + hematite + ilmenite ± rutile ± clinopyroxene. These minerals are all present to a varying extent in undifferentiated garnet + amphibole gneiss samples 37558, 37591, 37592, 37594, 37597, 37601, 37602 and 37698 and also in the garnet amphibolite samples 37591, 37699 and 37700. With the exception of a few garnet gneiss samples, amphibole commonly occurs as a part of the main mineral assemblage in these samples. Here amphibole typically exhibit subhedral shapes and a strong green color, with a $Fe/(Mg + Fe^{2+}) = 0.27$. One of the most easily discernable differences in the gneiss samples from the eclogites, is that all the main minerals show higher $Fe/(Mg + Fe^{2+})$ (NCFMASH ternary diagram in appendix C). This is presumably due to differences in the chemical compositions of the protolith.

One of the main ongoing debates concerning the garnet and amphibole gneisses relates to whether they have experienced the same HP – UHP P-T conditions as the adjacent eclogites (D. A. Carswell & Cuthbert, 2003). Prograde amphibole-stage mineral assemblages are typically identical to post-eclogite amphibole retrograded assemblages, so the solution to the problem would be to identify textures or minerals that can prove prior eclogite facies conditions.

Most studies favors “in situ” eclogite formation (D. Carswell et al., 2003; Medaris & Carswell, 1990) which means that the eclogite and the surrounding host quartzo-feldspathic gneiss, garnet amphibolite and/or garnet peridotite also experienced HP-UHP conditions. These studies argue that incomplete transformation of metagabbros to eclogites and prograde zoned garnets from amphibole to eclogite stage in eclogites suggest high P and low T conditions formation in the crust. Absence of HP-UHP textures in the host rocks has been attributed to effective differential retrogradation partitioned between the different rock types. Because mafic eclogite mineral assemblages are structurally more competent than ductile gneissose rock types, it is widely believed that the latter have experienced more pervasive amphibole stage reworking, thereby obliterating the HP-UHP textures (D. Carswell et al., 2003). Further reinforcing this theory, at least locally, was the discovery of preserved UHP assemblages in schists and gneisses on various localities on Stadlandet (Alice Wain, 1997; AL Wain et al., 2001)

6.3. Summary of the geologic evolution of the Averøya eclogite

Based on all textural, compositional and structural evidence presented in the previous section, a complete evolutionary model through subduction to exhumation can be proposed for the Averøya layered eclogite. The exact ordering of the individual stages have a degree of uncertainty, mainly due to a lack of overprinting relationships in the field and geochronological data. The summary of the evolutionary history relies partly on similar models in different parts of the WGR like Vårdalsneset eclogite (Engvik & Andersen, 2000) and the Harøya eclogite (Butler et al., 2012).

1. Prograde eclogite stage was recorded in partially eclogitized gabbro and possible prograde garnet in some of the eclogite samples.
2. Peak eclogite stage characterized by UHP source conditions from phengite + garnet geothermobarometer, estimating P = 3GPa ± 0.7GPa and T = 800 ± 100 °C (M. Terry and J. Butler, 06.2017). At Averøya this peak UHP – conditions should have occurred around 415 MA (T. E. Krogh et al., 2011).
3. In position of a late subduction to early exhumation eclogite facies fabric, displaying NW - N trending lineations and folds (Terry & Robinson, 2004).
4. Granulite stage: Formation of various symplectites and textures described in 6.2.3, continuing to amphibolite facies conditions. The growth of a garnet and amphibole assemblage have been dated to 410 Ma (T. E. Krogh et al., 2011)
5. Amphibolite stage: Development of the mineral assemblages and textures described in 6.2.4, locally dated at Tøvika to have occurred 395 Ma(T. E. Krogh et al., 2011). This stage is associated with strong NE – SW trending foliations and sub horizontal fold axes (or earlier), accompanied by sinistral or top to the SW sense of shear. A local sinistral shear zone could presumably have played a part in the exhumation of the layered eclogite and/or the other rock types in the Blåhø unit. The separation of the boudin eclogites from the main eclogite body remains unknown, but likely to have occurred at some point during the amphibolite stage.
6. Late crosscutting brittle features in predominantly the layered eclogite and the garnet and amphibole gneiss. This include tensile veins, conjugate fractures and normal faults.

Chapter 7 - Conclusion

This thesis presents the results of extensive geological mapping, coupled with detailed descriptions of petrographic -, geochemical- and magnetic attributes of the four main rock types located on Averøya in the WGR. These include granodioritic to tonalitic migmatite gneiss assigned to the Baltic Basement unit and garnet and amphibole gneiss, garnet amphibolite and layered eclogite assigned to the Blåhø unit. Although it seems likely that the boudin eclogite comes from the main layered eclogite body, it remains inconclusive. The majority of these boudin eclogites have been found in either the garnet amphibolite or the garnet and amphibole gneiss, with only two confirmed occurrences in the Baltic basement unit.

New boundaries have been inferred and interpolated on the map through field work and aided by a magnetic anomaly map. Structural information shows that some of the foliations are parallel to the unit boundaries, whereas others are consistent with the late ENE – WSW trends. Both early eclogite facies and later amphibolite facies structures have been observed in the study area. The resulting map in figure 6.1.2, with corresponding cross sections in figure 6.1.3 shows the interpreted shape of the layered eclogite and its place in the local tectonostratigraphic order.

The second focus of this thesis was to identify common mineral assemblages and textures in both eclogite samples and in the surrounding rocks. High pressure minerals kyanite and relict phengite were positively identified, though coesite remains unconfirmed. The phengite – garnet – pyroxene geobarometer was applied to estimate P-T conditions of 3GPa and 800 ± 100 °C, confirming peak UHP eclogite conditions.

The textures in the thin sections record evidence of the local metamorphic history and in the combination with mineral analyses a complete prograde eclogite-, peak eclogite-, granulite- and amphibolite stage model have been suggested. This model was implemented with the available structural information to propose a preliminary model for the geologic evolution for the Averøya eclogite in chapter 6.3. There are still many aspects of the geological history that remains uncertain, this model could prove valuable for further efforts to unravel the geological history in the study area.

Chapter 8 - Future work

There are a range of investigations that could conducted to increase the knowledge of the geological history in the area. Additional geological mapping should be carried out to further increase the accuracy of geological boundaries between basement rocks and the overlying nappe units. Much of this will depend on greater sophistication in field and laboratory identification of tectonostratigraphic units and their histories, in this case between the Blåhø unit and Baltican basement unit. With the possibility of a semi-continous zone of more magnetic material enveloping the main layered eclogite on Averøya, a higher resolution aeromagnetic map might provide better means of inferring the boundaries of the body.

There are numerous thermometers and barometers that might be applied to reconstruct a full P-T path for the Averøya eclogite. The majority of these methods have been explained in (Krogh Ravna & Terry, 2004) where the following barometers and thermometers can be applied for the individual stages:

1. Pre eclogite stage: In (Ravna & Roux, 2006) the amphibole stage inclusions recorded in cores of garnet were used to determine P-T estimates by applying the Mg-Fe thermometer of hornblende and garnet (POWELL, 1985)coupled with the plagioclase – hornblende and garnet barometer (Kohn & Spear, 1990).
2. Eclogite stage: More time should be spent searching for phengite and/or coesite to obtain more dependable peak P-T estimates.
3. Granulite- /amphibole stage: By applying the method devised by (Joanny et al., 1991), P-T estimates can be obtained from the width of lamellar symplectites according to the growth law, $L = A - B/T$. A higher temperature thereby yields a corresponding coarser symplectite.
4. It would be interesting to apply the phengite – garnet – biotite geothermobarometer to estimate P-T conditions in the garnet and bioitie gneiss, to be compared with results from eclogites

Conclusion

Geochronology

1. Zircons were found locally in garnets in the boudin eclogite sample 37559, which could possibly be dated (U-Pb method).
2. Attempts should be made to date the garnet and amphibole gneiss and the garnet amphibolite to correlate ages with the eclogite formation.

References

Andersen, T. B., Osmundsen, P. T., & Jolivet, L. (1994). Deep crustal fabrics and a model for the extensional collapse of the southwest Norwegian Caledonides. *Journal of Structural Geology, 16*(9), 1191-1203.

Austrheim, H., Corfu, F., Bryhni, I., & Andersen, T. B. (2003). The Proterozoic Hustad igneous complex: a low strain enclave with a key to the history of the Western Gneiss Region of Norway. *Precambrian Research, 120*(1), 149-175.

Auzanneau, E., Schmidt, M., Vielzeuf, D., & Connolly, J. D. (2010). Titanium in phengite: a geobarometer for high temperature eclogites. *Contributions to Mineralogy and Petrology, 159*(1), 1-24.

Brueckner, H. K., Van Roermund, H. L., & Pearson, N. J. (2004). An Archean (?) to Paleozoic evolution for a garnet peridotite lens with sub-Baltic shield affinity within the Seve Nappe Complex of Jämtland, Sweden, Central Scandinavian Caledonides. *Journal of Petrology, 45*(2), 415-437.

Bryhni, I., & Griffin, W. (1971). Zoning in eclogite garnets from Nordfjord, West Norway. *Contributions to Mineralogy and Petrology, 32*(2), 112-125.

Bucher, K., & Grapes, R. (2009). The eclogite-facies Allalin Gabbro of the Zermatt–Saas ophiolite, Western Alps: a record of subduction zone hydration. *Journal of Petrology*, egp035.

Butler, J. P., JAMIESON, R., STEENKAMP, H., & ROBINSON, P. (2012). Discovery of coesite–eclogite from the Nordøyane UHP domain, Western Gneiss Region, Norway: field relations, metamorphic history, and tectonic significance.

Carswell, D., Cuthbert, S., Krabbendam, M., Medaris Jr, L., Brueckner, H., og Romsdal, M., & og Fjordane, S. (2003). Guidebook to the Field Excursions in the Nordfjord—Stadlandet—Almklovdalen Area. *Geological Survey of Norway, Trondheim*, 137.

Carswell, D. A., & Cuthbert, S. J. (2003). Ultrahigh pressure metamorphism in the Western Gneiss Region of Norway. *EMU Notes in Mineralogy, 5*, 51-73.

Coleman, R., Lee, D., Beatty, L., & Brannock, W. W. (1965). Eclogites and eclogites: their differences and similarities. *Geological Society of America Bulletin, 76*(5), 483-508.

Corfu, F. (1980). U・Pb and Rb・Sr systematics in a polyorogenic segment of the Precambrian shield, central southern Norway. *Lithos, 13*(4), 305-323.

Corfu, F., Gasser, D., & Chew, D. M. (2014). *New perspectives on the Caledonides of Scandinavia and related areas*.

Cuthbert, S., Carswell, D., Krogh-Ravna, E., & Wain, A. (2000). Eclogites and eclogites in the Western Gneiss region, Norwegian Caledonides. *Lithos, 52*(1), 165-195.

Deer, W., Howie, R., & Zussman, J. (1982). Rock-forming minerals, Orthosilicates, 1A: Longman, New York.

Dentith, M., & Mudge, S. T. (2014). *Geophysics for the mineral exploration geoscientist*: Cambridge University Press.

Engvik, A., & Andersen, T. (2000). Evolution of Caledonian deformation fabrics under eclogite and amphibolite facies at Vardalsneset, Western Gneiss Region, Norway. *Journal of Metamorphic Geology, 18*(3), 241-258.

Engvik, A., Austrheim, H., & Erambert, M. (2001). Interaction between fluid flow, fracturing and mineral growth during eclogitization, an example from the Sunnfjord area, Western Gneiss Region, Norway. *Lithos, 57*(2), 111-141.

Eskola, P. (1915). *Om sambandet mellan kemisk och mineralogisk sammansättning hos Orijärvitraktens metamorfa bergarter*: Geologiska Kommissionen.

Eskola, P. (1920). The mineral facies of rocks.

References

Eskola, P. (1921). *On the eclogites of Norway*: Рипол Классик.

Essex, R., Gromet, L., ANDRÉASSON, P. G., & Albrecht, L. (1997). Early Ordovician U-Pb metamorphic ages of the eclogite-bearing Seve nappes, Northern Scandinavian Caledonides. *Journal of Metamorphic Geology, 15*(5), 665-676.

Fettes, D. J., Desmons, J., & Árkai, P. (2007). *Metamorphic rocks: a classification and glossary of terms: recommendations of the International Union of Geological Sciences Subcommission on the Systematics of Metamorphic Rocks*: Cambridge Univ Pr.

Fossen, H. (2000). Extensional tectonics in the Caledonides: Synorogenic or postorogenic? *Tectonics, 19*(2), 213-224.

Fossen, H. (2016). *Structural geology*: Cambridge University Press.

Fossen, H., & Rykkelid, E. (1992). Postcollisional extension of the Caledonide orogen in Scandinavia: Structural expressions and tectonic significance. *Geology, 20*(8), 737-740.

Gee, D. G. (1980). Basement-cover relationships in the central Scandinavian Caledonides. *GFF, 102*(4), 455-474.

Gordon, S. M., Whitney, D. L., Teyssier, C., Fossen, H., & Kylander-Clark, A. (2016). Geochronology and geochemistry of zircon from the northern Western Gneiss Region: Insights into the Caledonian tectonic history of western Norway. *Lithos, 246*, 134-148.

Hacker, B. R., Andersen, T. B., Johnston, S., Kylander-Clark, A. R., Peterman, E. M., Walsh, E. O., & Young, D. (2010). High-temperature deformation during continental-margin subduction & exhumation: The ultrahigh-pressure Western Gneiss Region of Norway. *Tectonophysics, 480*(1), 149-171.

Hacker, B. R., & Gans, P. B. (2005). Continental collisions and the creation of ultrahigh-pressure terranes: Petrology and thermochronology of nappes in the central Scandinavian Caledonides. *Geological Society of America Bulletin, 117*(1-2), 117-134.

Hernes, I. (1954). Eclogite-amphibolite on the Molde peninsula, Southern Norway. *Norsk geol. tidsskr, 33*, 163-184.

Hollocher, K. (2014). *A Pictorial Guide to Metamorphic Rocks in the Field*: CRC Press.

Hollocher, K., Robinson, P., Kennedy, C., & Walsh, E. (2014). Metamorphosed cumulate gabbros from the Støren Group of the Upper Allochthon, northern Western Gneiss Region, Norway: petrology and metamorphic record. *Norwegian Journal of Geology/Norsk Geologisk Forening, 94*(4).

Hollocher, K., Robinson, P., Terry, M., & Walsh, E. (2007). Application of major-and trace-element geochemistry to refine U-Pb zircon, and Sm/Nd or Lu/Hf sampling targets for geochronology of HP and UHP eclogites, Western Gneiss Region, Norway. *American mineralogist, 92*(11-12), 1919-1924.

Joanny, V., van Roermund, H., & Lardeaux, J. M. (1991). The clinopyroxene/plagioclase symplectite in retrograde eclogites: a potential geothermobarometer. *Geologische Rundschau, 80*(2), 303-320.

Journel, A. G., & Huijbregts, C. J. (1978). *Mining geostatistics*: Academic press.

Kohn, M. J., & Spear, F. S. (1990). Two new geobarometers for garnet amphibolites, with applications to southeastern Vermont. *American mineralogist, 75*(1-2), 89-96.

Korneliussen, A., McLIMANS, R., Braathen, A., Erambert, M., Lutro, O., & Ragnhildstveit, J. (2000). Rutile in eclogites as a mineral resource in the Sunnfjord region, western Norway. *NORGES GEOLOGISKE UNDERSOKELSE, 436*, 39-48.

Krabbendam, M., & Dewey, J. F. (1998). Exhumation of UHP rocks by

References

transtension in the Western Gneiss Region, Scandinavian Caledonides. *Geological Society, London, Special Publications, 135*(1), 159-181.

Krill, A. (1980). Tectonics of the Oppdal area. *Gff meeting proceedings, 102*(4), 523-530.

Krogh, E. (1982). Metamorphic evolution of Norwegian country-rock eclogites, as deduced from mineral inclusions and compositional zoning in garnets. *Lithos, 15*(4), 305-321.

Krogh Ravna, E., & Terry, M. P. (2004). Geothermobarometry of UHP and HP eclogites and schists–an evaluation of equilibria among garnet–clinopyroxene–kyanite–phengite–coesite/quartz. *Journal of Metamorphic Geology, 22*(6), 579-592.

Krogh, T. E., Kamo, S. L., Robinson, P., Terry, M. P., & Kwok, K. (2011). U–Pb zircon geochronology of eclogites from the Scandian Orogen, northern Western Gneiss Region, Norway: 14–20 million years between eclogite crystallization and return to amphibolite-facies conditions1. *Can. J. Earth Sci, 48*, 441-472.

Kylander-Clark, A., Hacker, B., & Mattinson, J. (2008). Slow exhumation of UHP terranes: titanite and rutile ages of the Western Gneiss Region, Norway. *Earth and Planetary Science Letters, 272*(3), 531-540.

Labrousse, L., Jolivet, L., Andersen, T., Agard, P., Hébert, R., Maluski, H., & Schärer, U. (2004). Pressure-temperature-time deformation history of the exhumation of ultra-high pressure rocks in the Western Gneiss Region, Norway. *Geological Society of America Special Papers, 380*, 155-183.

Lappin, M. A. a. S., D.C. (1978). Mantle equilibrated orthopyroxene pods from the basal gneisses in the Selje district, western Norway. *J. petrol*(19), 530 - 584.

Lutro, O., Robinson, P., & Solli, A. (1997). Proterozoic geology and Scandian overprinting in the Western Gneiss Region. *Norges geologiske undersøkelse, Report, 97*, 86.

McEnroe, S. A., Fabian, K., Robinson, P., Gaina, C., & Brown, L. L. (2009). Crustal magnetism, lamellar magnetism and rocks that remember. *Elements, 5*(4), 241-246.

Medaris, L., & Carswell, D. (1990). Petrogenesis of Mg-Cr garnet peridotites in European metamorphic belts. *Eclogite facies rocks, 260*, 290.

Morimoto, N. (1988). Nomenclature of pyroxenes. *Mineralogy and Petrology, 39*(1), 55-76.

Mørk, M. B. E. (1985). A gabbro to eclogite transition on Flemsøy, Sunnmøre, western Norway. *Chemical Geology, 50*(1-3), 283-310.

Mørk, M. B. E. (1986). Coronite and eclogite formation in olivine gabbro (Western Norway): reaction paths and garnet zoning. *Mineralogical Magazine, 50*(357), 417-426.

Mørk, M. B. E., Kullerud, K., & Stabel, A. (1988). Sm-Nd dating of Seve eclogites, Norrbotten, Sweden—evidence for early Caledonian (505 Ma) subduction. *Contributions to Mineralogy and Petrology, 99*(3), 344-351.

Nabighian, M. N., Grauch, V., Hansen, R., LaFehr, T., Li, Y., Peirce, J., . . . Ruder, M. (2005). The historical development of the magnetic method in exploration. *Geophysics, 70*(6), 33ND-61ND.

Nelson, S. A. (2004). Metamorphic Rocks-Classification, Field Gradients, & Facies. *Tulane University.*

Osmundsen, P., Eide, E., Haabesland, N., Roberts, D., Andersen, T., Kendrick, M., . . . Redfield, T. (2006). Kinematics of the Høybakken detachment zone and the Møre–Trøndelag Fault Complex, central Norway. *Journal of the Geological Society, 163*(2), 303-318.

References

Passchier, C., & Trouw, R. (2005). Microtectonics. vol: Springer, Berlin, Federal Republic of Germany.

Peterman, E. M., Hacker, B. R., & Baxter, E. F. (2009). Phase transformations of continental crust during subduction and exhumation: Western Gneiss Region, Norway. *European Journal of Mineralogy, 21*(6), 1097-1118.

Philpotts, A., & Ague, J. (2009). *Principles of igneous and metamorphic petrology*: Cambridge University Press.

POWELL, R. (1985). Regression diagnostics and robust regression in geothermometer/geobarometer calibration: the garnet-clinopyroxene geothermometer revisited. *Journal of Metamorphic Geology, 3*(3), 231-243.

Ravna, E. K., & Roux, M. (2006). Metamorphic Evolution of the T⊘nsvika Eclogite, Troms⊘ Nappe—Evidence for a New UHPM Province in the Scandinavian Caledonides. *International Geology Review, 48*(10), 861-881.

Renedo, R. N., Nachlas, W. O., Whitney, D. L., Teyssier, C., Piazolo, S., Gordon, S. M., & Fossen, H. (2015). Fabric development during exhumation from ultrahigh-pressure in an eclogite-bearing shear zone, Western Gneiss Region, Norway. *Journal of Structural Geology, 71*, 58-70.

Robinson, P. (1991). The eye of the petrographer, the mind of the petrologist. *American mineralogist, 76*(11-12), 1781-1810.

Robinson, P. (1995). Extension of Trollheimen tectono-stratigraphic sequence in deep synclines near Molde and Brativag, Western Gneiss Region, southern Norway. *Norsk Geologisk Tidsskrift, 75*(4), 181-197.

Robinson, P., Daczko, N., Krogh, T.E. & Hollocher, K. (2008). *Unusual plagioclase moat / pyroxene necklace structure around garnet in a quartz-rich layer of the Averøya eclogite, western Gneiss Region, Norway.* Paper presented at the 33rd International Geological Congress, Oslo, 6-14 August 2008.

Robinson, P., Roberts, D., Gee, D. G., & Solli, A. (2014). A major synmetamorphic Early Devonian thrust and extensional fault system in the Mid Norway Caledonides: relevance to exhumation of HP and UHP rocks. *Geological Society, London, Special Publications, 390*(1), 241-270.

Robinson, P., Terry, M. P., Carswell, D., Van Roermund, H., Krogh, T. E., Root, D., . . . Solli, A. (2003). Tectono-stratigraphic setting, structure, and petrology of HP and UHP metamorphic rocks and garnet peridotites in the Western Gneiss Region, Møre and Romsdal, Norway. *Geological Survey of Norway, Report*(2003.057), 107-113.

Root, D., Hacker, B., Gans, P., Ducea, M. N., Eide, E., & Mosenfelder, J. (2005). Discrete ultrahigh-pressure domains in the Western Gneiss Region, Norway: implications for formation and exhumation. *Journal of Metamorphic Geology, 23*(1), 45-61.

Røhr, T. S., Bingen, B., Robinson, P., & Reddy, S. M. (2013). Geochronology of Paleoproterozoic Augen Gneisses in the Western Gneiss Region, Norway: Evidence for Sveconorwegian Zircon Neocrystallization and Caledonian Zircon Deformation.

Scambelluri, M., Van Roermund, H. L., & Pettke, T. (2010). Mantle wedge peridotites: fossil reservoirs of deep subduction zone processes: inferences from high and ultrahigh-pressure rocks from Bardane (Western Norway) and Ulten (Italian Alps). *Lithos, 120*(1), 186-201.

Smith, D. (1988). A review of the peculiar mineralogy of the “Norwegian coesite-eclogite province”, with crystal-chemical, petrological, geochemical and geodynamical notes and an extensive

References

bibliography. *Eclogites and eclogite-facies rocks, 12*, 1-206.

Smith, D. C. (1984). Coesite in clinopyroxene in the Caledonides and its implications for geodynamics. *Nature, 310*(5979), 641-644.

Smulikowski, W., Desmons, J., & Fettes, D. (2007). *Types, grade and facies of metamorphism*: Cambridge University Press.

Terry, M. P., & Robinson, P. (2003). Evolution of amphibolite-facies structural features and boundary conditions for deformation during exhumation of high- and ultrahigh-pressure rocks, Nordøyane, Western Gneiss Region, Norway. *Tectonics, 22*(4).

Terry, M. P., & Robinson, P. (2004). Geometry of eclogite-facies structural features: Implications for production and exhumation of ultrahigh-pressure and high-pressure rocks, Western Gneiss Region, Norway. *Tectonics, 23*(2).

Terry, M. P., Robinson, P., & Ravna, E. K. (2000). Kyanite eclogite thermobarometry and evidence for thrusting of UHP over HP metamorphic rocks, Nordoyane, Western Gneiss Region, Norway. *American mineralogist, 85*(11/12), 1637-1650.

TUCKER, R. D. (1986). Geology of the Hemnefjord Orkanger area, south central Norway. *Norges geologiske undersøkelse, Report*(404), 1-24.

Tucker, R. D., ROBINSON, P., SOLLI, A., GEE, D. G., THORSNES, T., KROGH, T. E., . . . BICKFORD, M. (2004). Thrusting and extension in the Scandian Hinterland, Norway: New U-Pb ages and tectonostratigraphic evidence. *American journal of science, 304*(6), 477-532.

Turner, F. J. a. V., J. (1960). Igneous and metamorphic petrology. *McGraw Hill New York*, 459.

Vrijmoed, J., Van Roermund, H., & Davies, G. (2006). Evidence for diamond-grade ultra-high pressure metamorphism and fluid interaction in the Svartberget Fe–Ti garnet peridotite–websterite body, Western Gneiss Region, Norway. *Mineralogy and Petrology, 88*(1), 381-405.

Wain, A. (1997). New evidence for coesite in eclogite and gneisses: Defining an ultrahigh-pressure province in the Western Gneiss region of Norway. *Geology, 25*(10), 927-930.

Wain, A., Waters, D., & Austrheim, H. (2001). Metastability of granulites and processes of eclogitisation in the UHP region of western Norway. *Journal of Metamorphic Geology, 19*(5), 609-625.

Walsh, E. O., Hacker, B. R., Gans, P. B., Wong, M. S., & Andersen, T. B. (2013). Crustal exhumation of the Western Gneiss Region UHP terrane, Norway: 40 Ar/39 Ar thermochronology and fault-slip analysis. *Tectonophysics, 608*, 1159-1179.

Winter John, D. (2010). Principles of Igneous and Metamorphic Petrology.

Appendix

Appendix A – Equal area lower hemisphere diagrams and map over kinematic indicators and brittle structures

Appendix B – Thin section XP and PP scanned images and hand sample image.

Appendix C – Mineral chemistry

Appendix

Appendix A, Equal area diagrams, lower hemisphere

F2

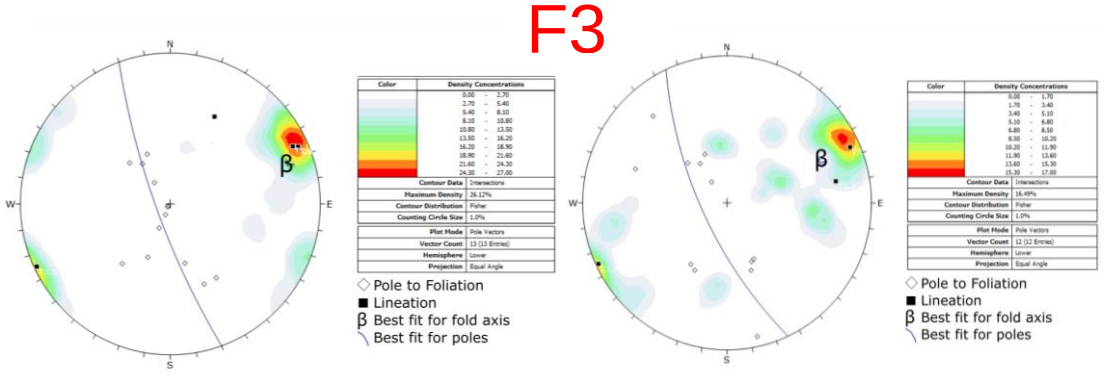

F3

F5

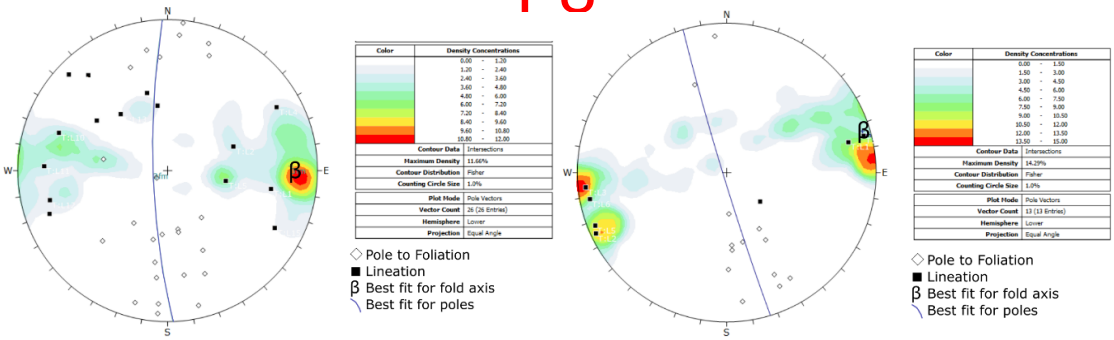

F8

M1

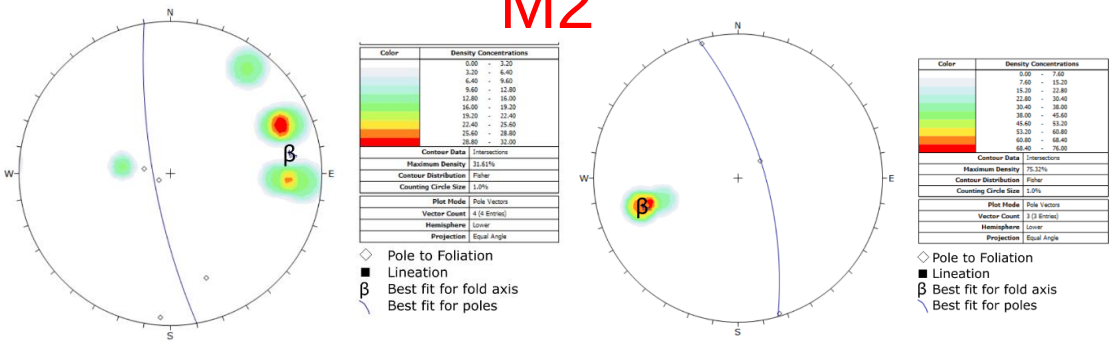

M2

M3

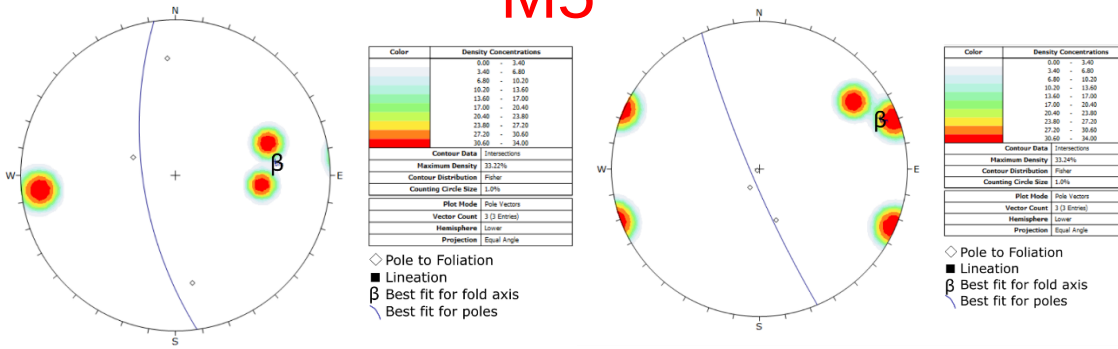

M5

Appendix

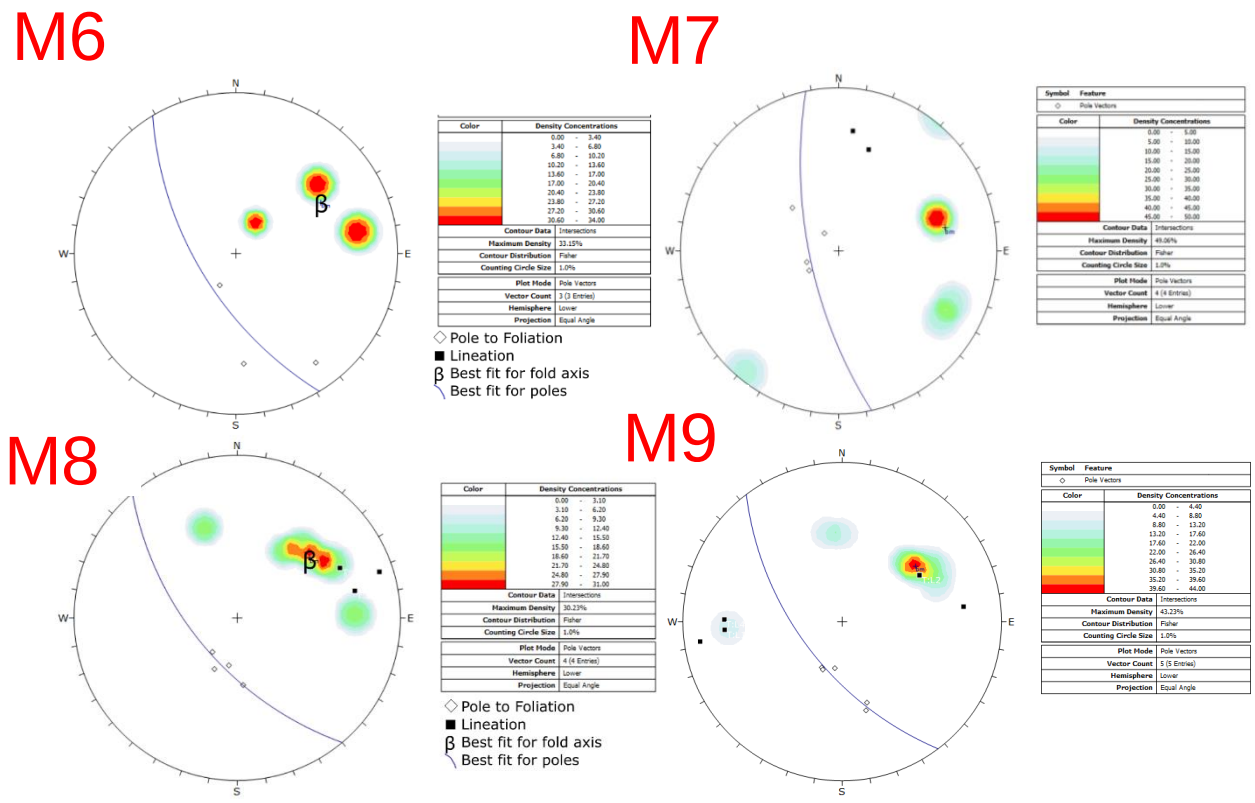

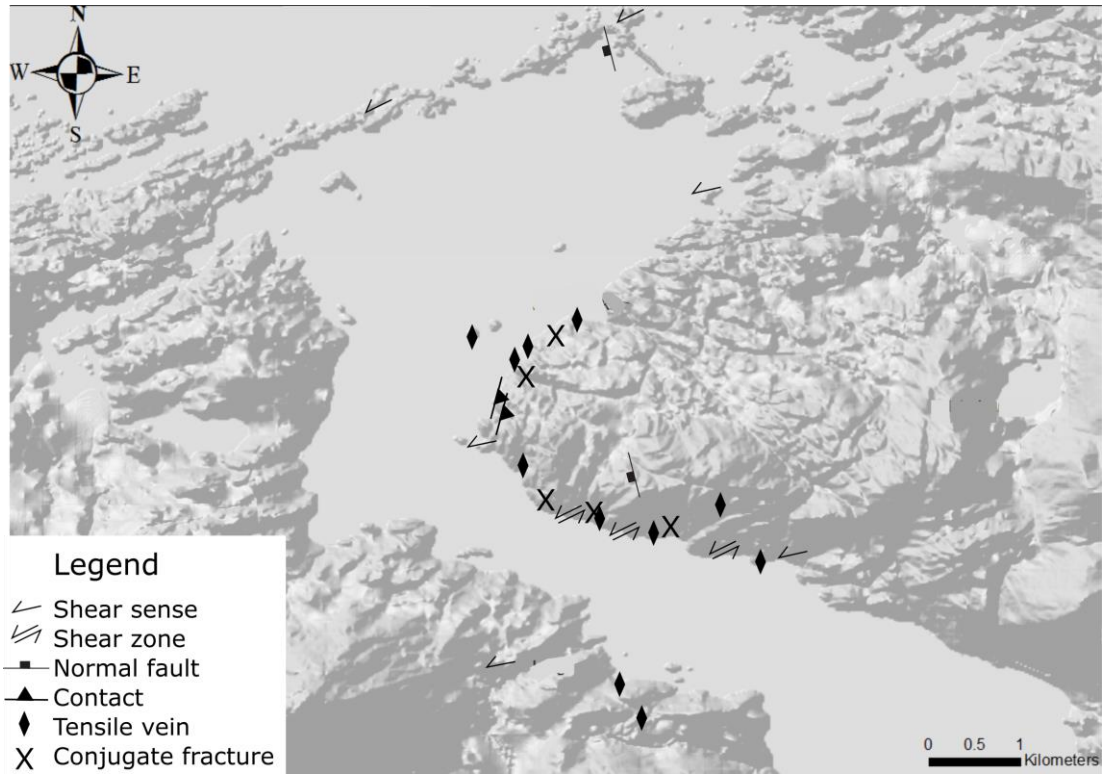

Distribution of kinematic indicators and brittle structures in the study area.

Appendix

Appendix B – Thin Sections

Thin Section – 37559 (B1)

Thin section: 37555 (B2)

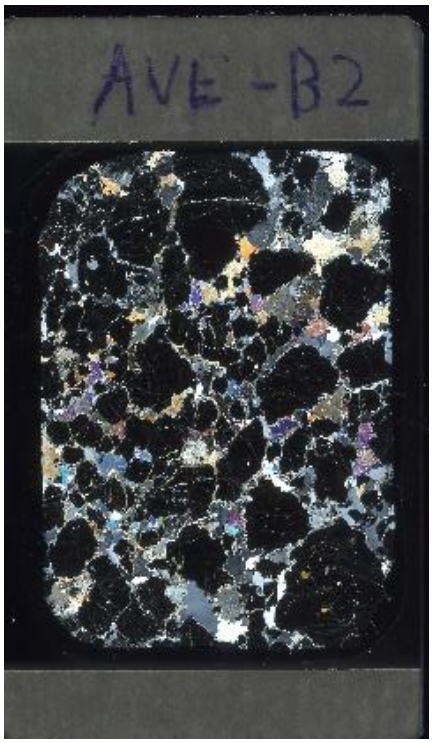

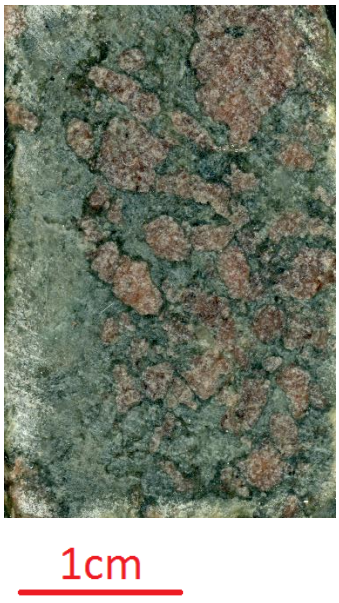

Appendix

Thin Section: 37594 (B3)

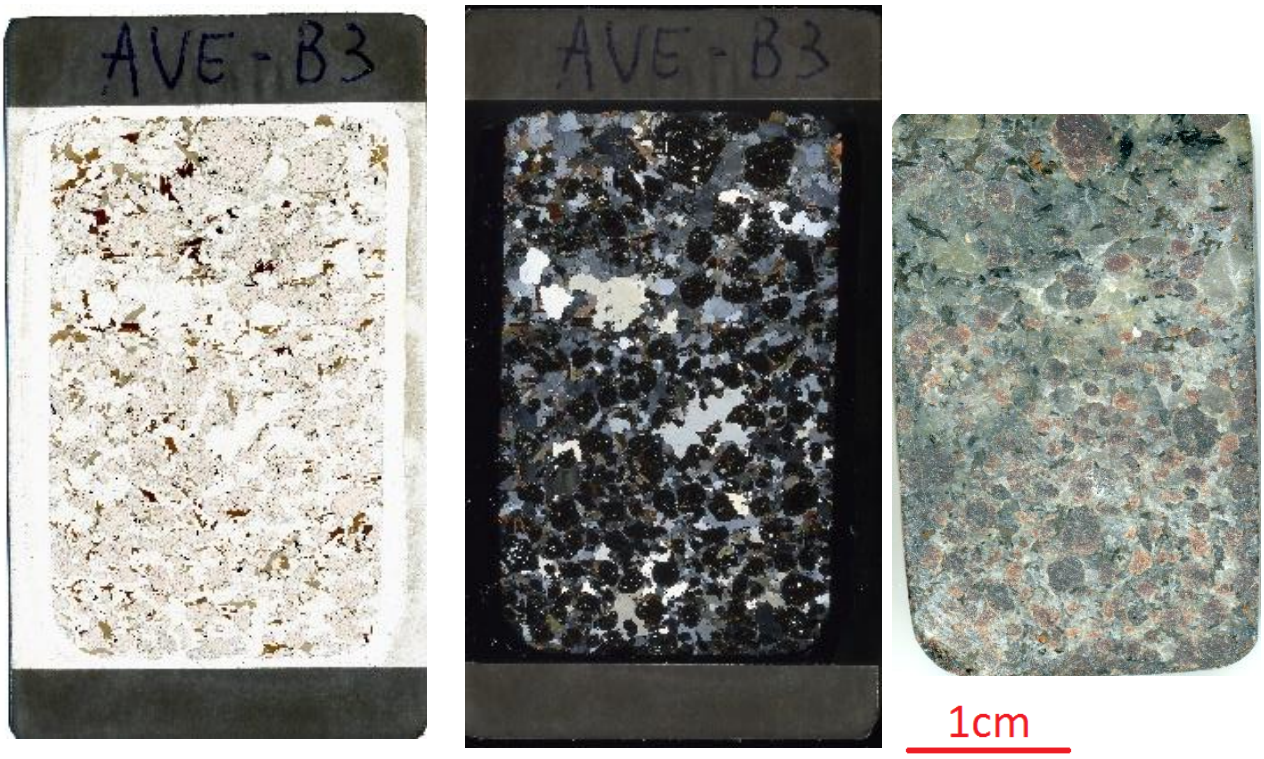

Thin Section: 37595 (B4)

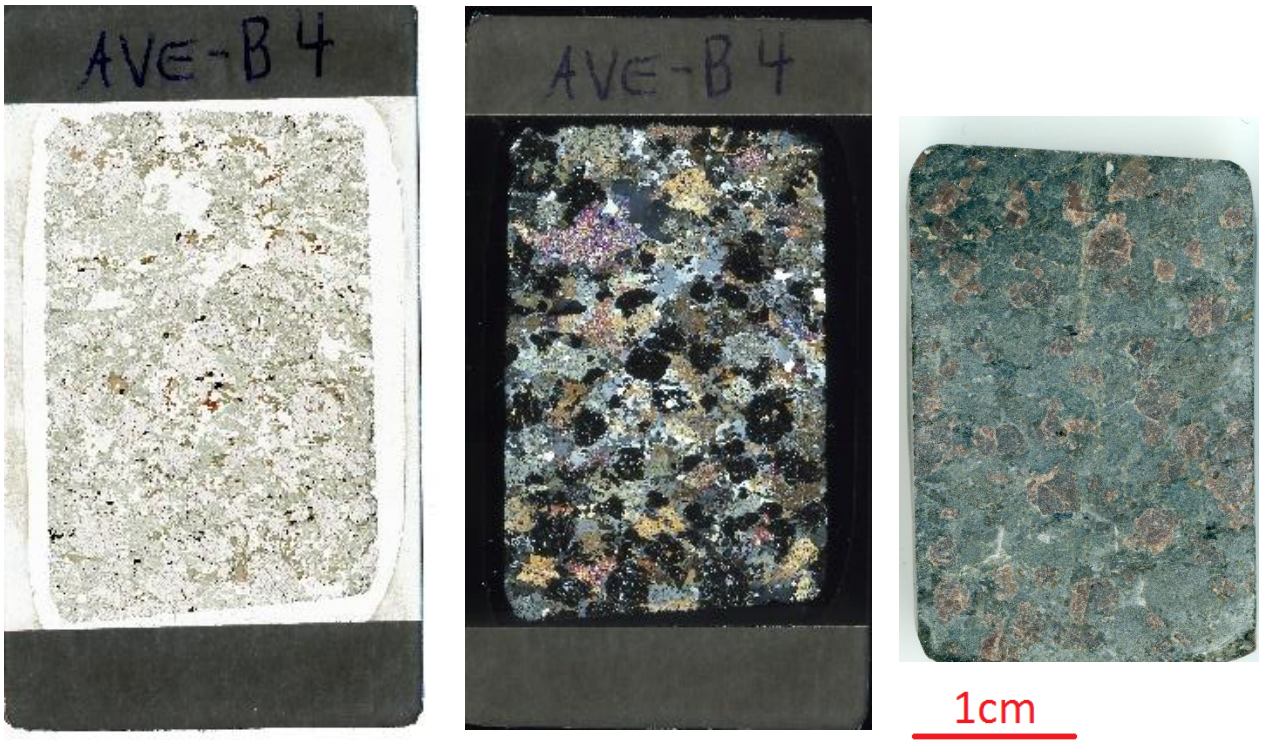

Appendix

Thin section: 37596 (B5)

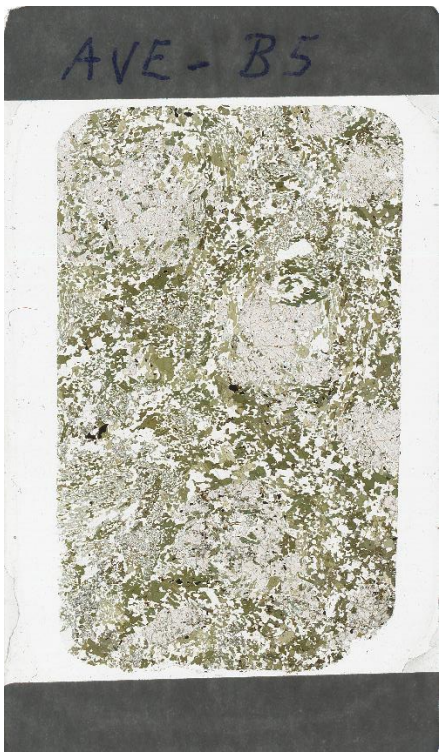

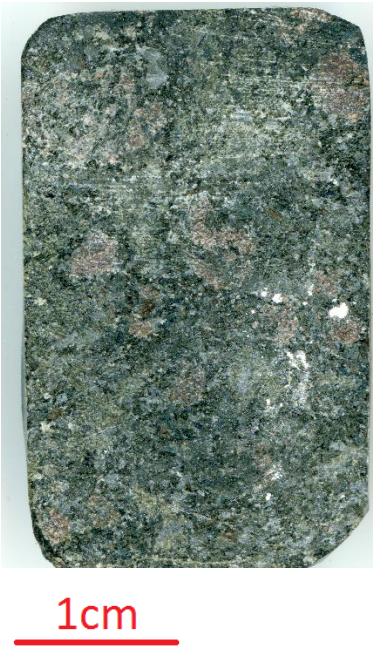

Thin Section: 37599 (B6)

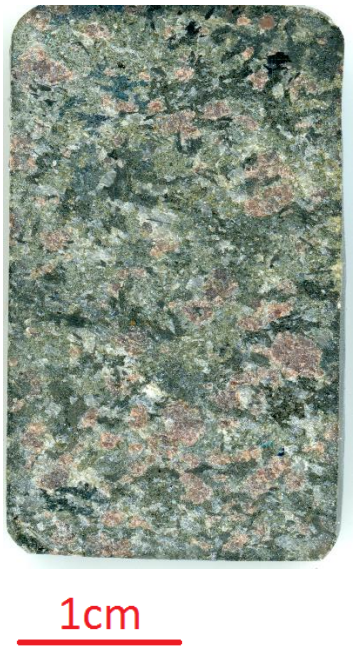

Appendix

Thin Section: 37600 (B7)

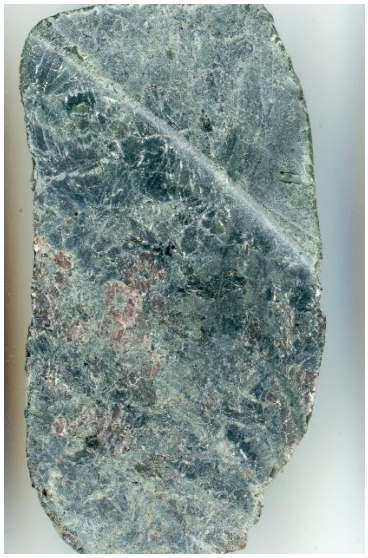

Thin Section: 37556 (E1)

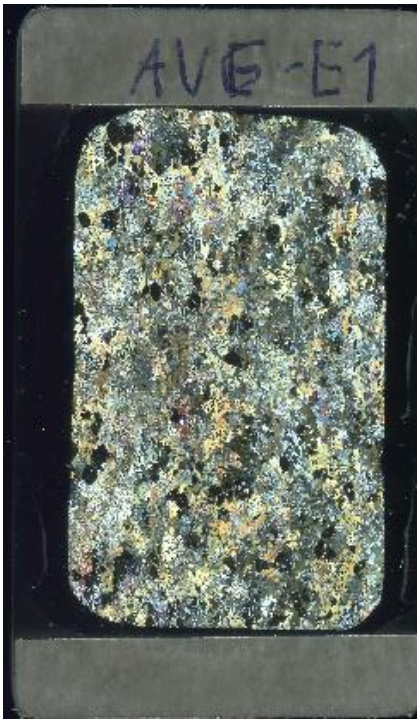

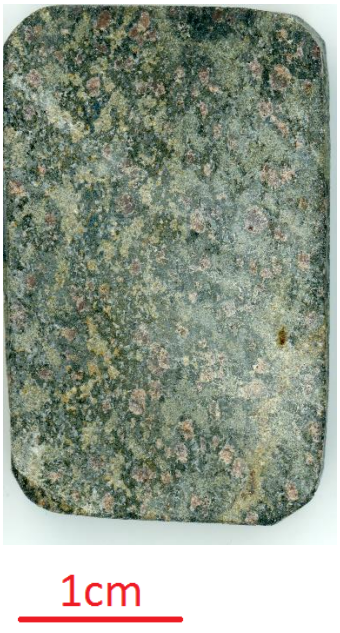

Appendix

Thin Section: 37557 (E2)

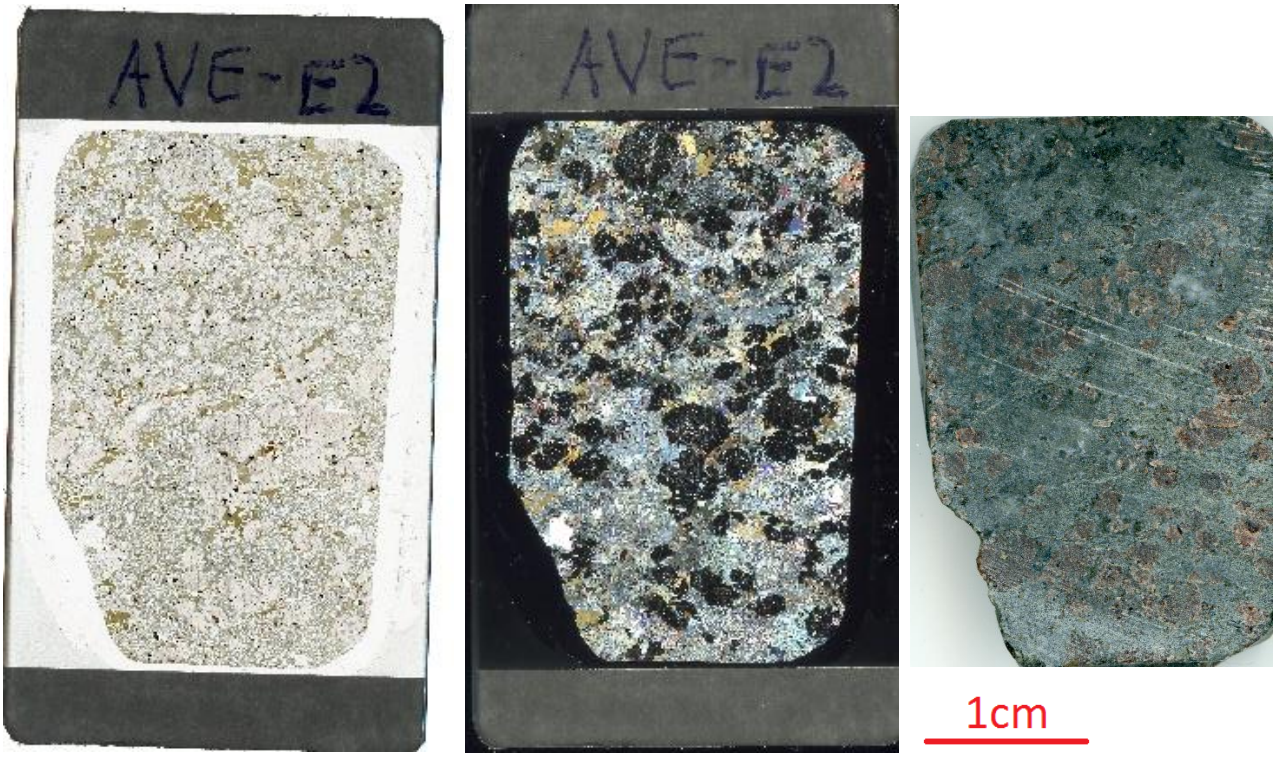

Thin section: 37558 (E3)

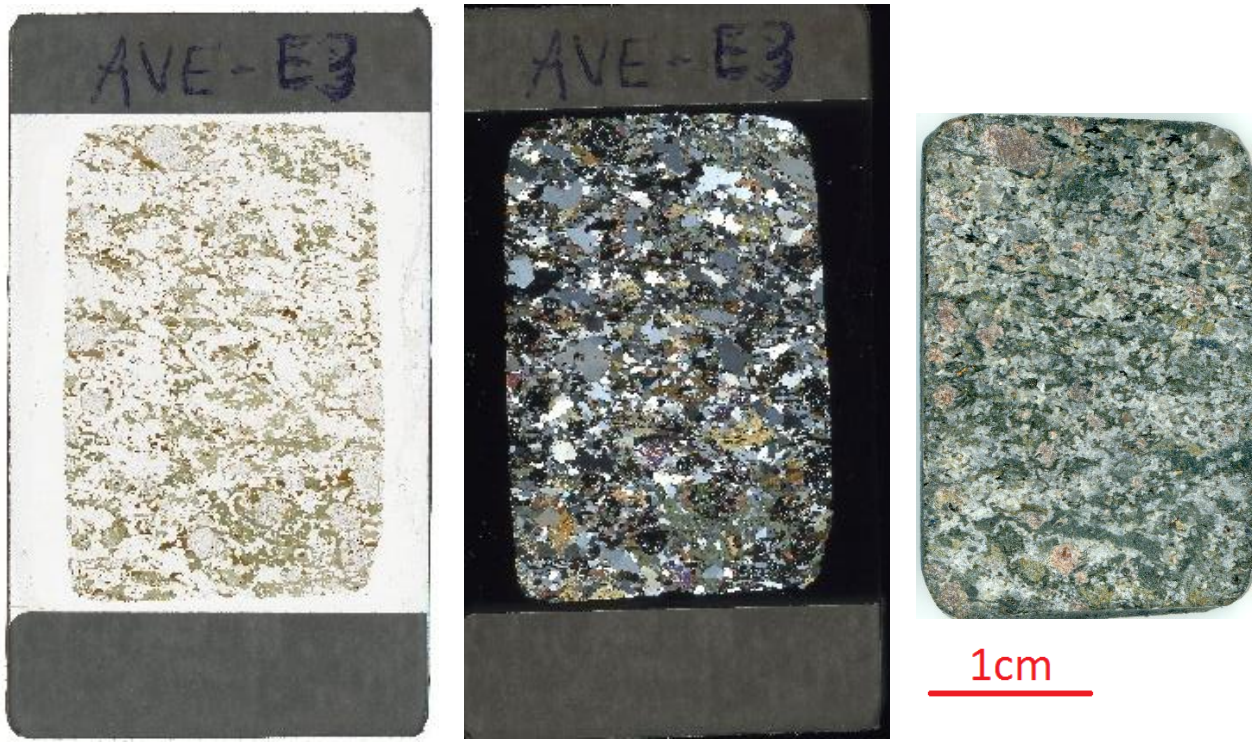

Appendix

Thin section: 37560 (E4)

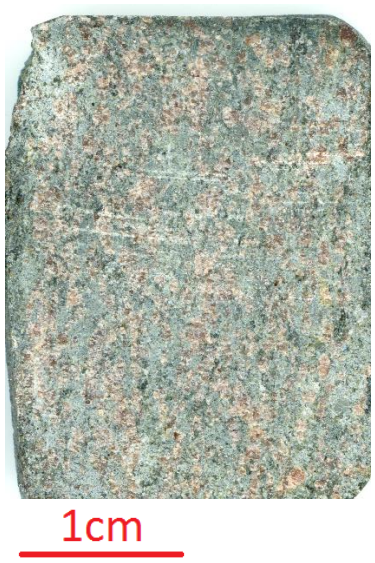

Thin section: 37562 (E5)

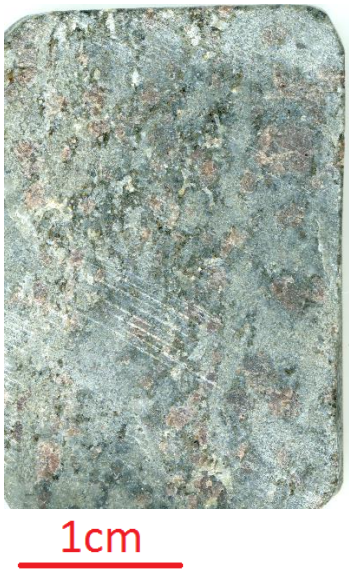

Appendix

Thin section: 37563 (E6)

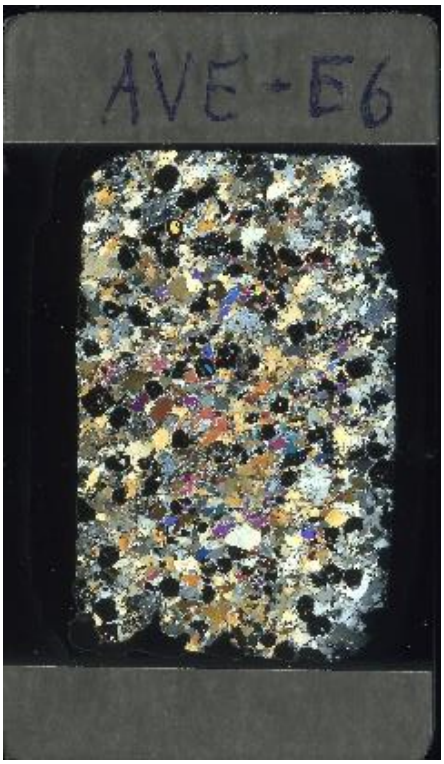

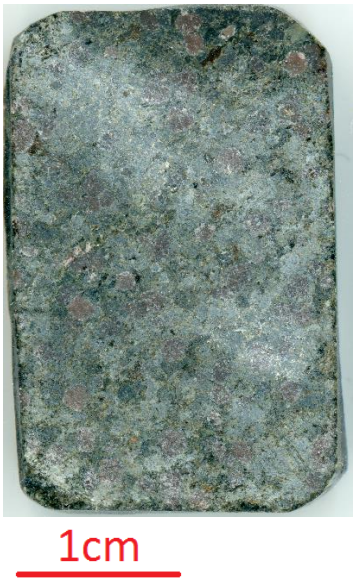

Thin section: 37564 (E7)

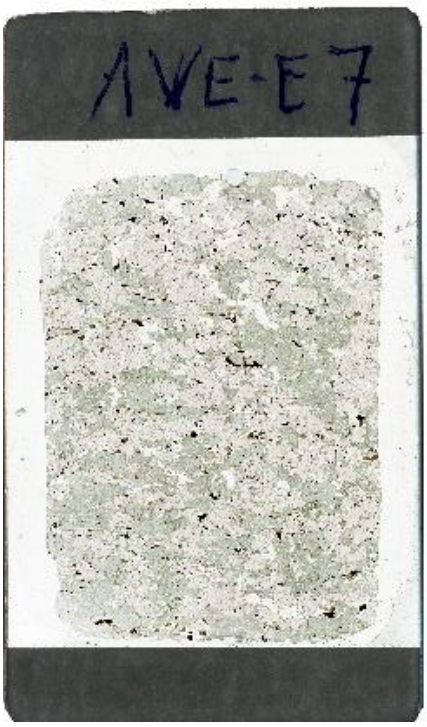

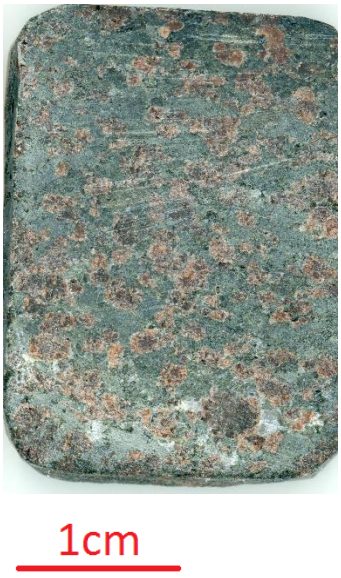

Appendix

Thin section: 37552 (E8)

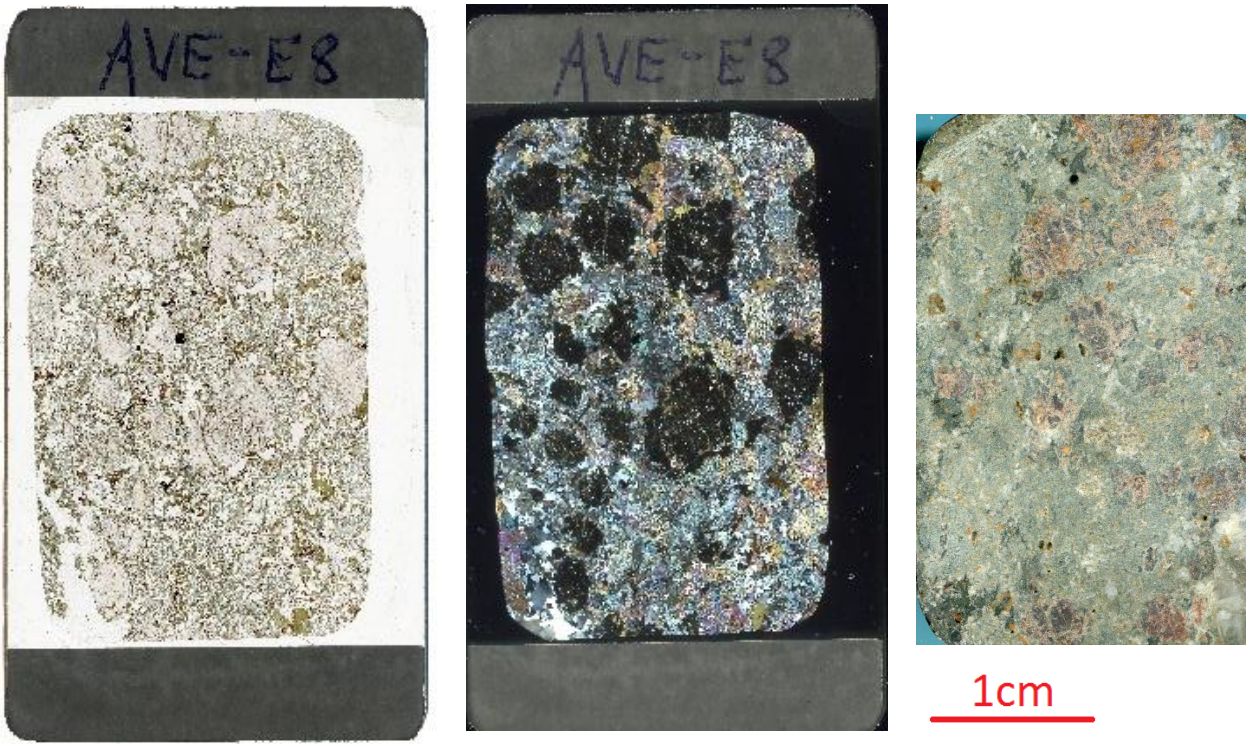

Thin section: 37551 (E9)

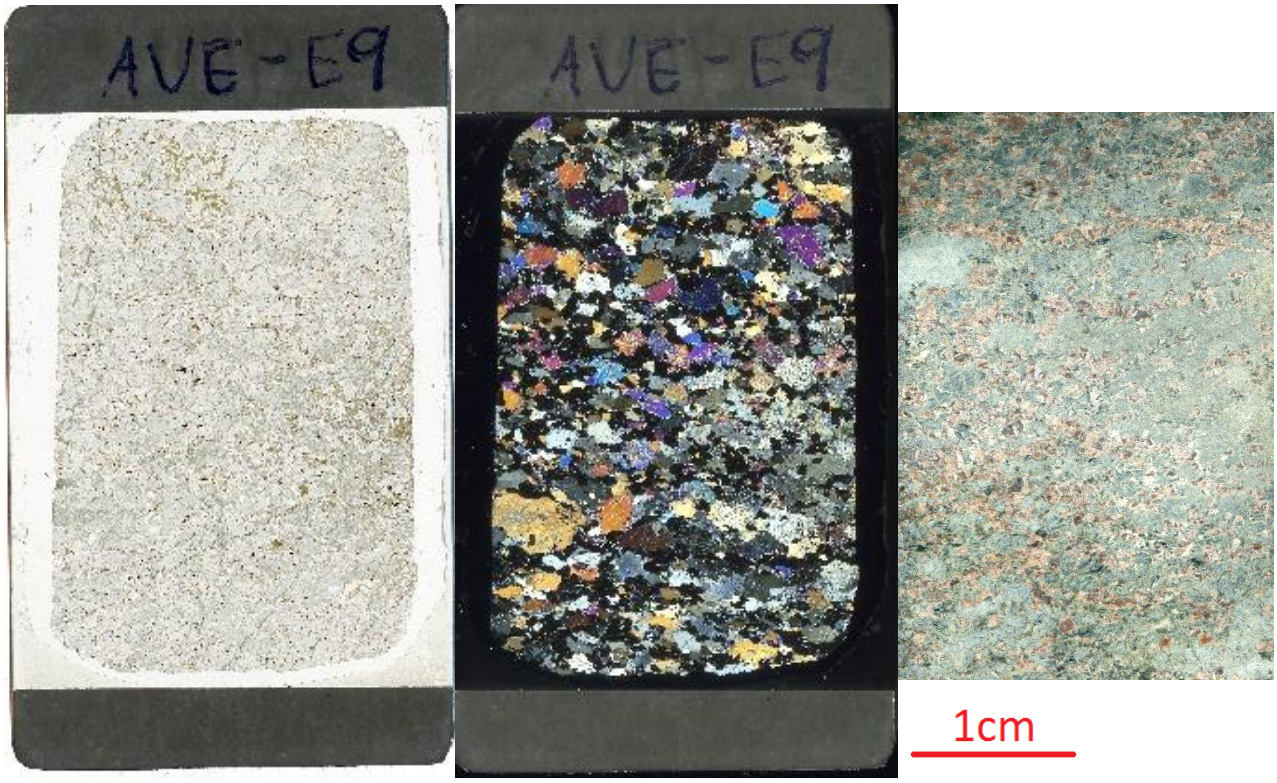

Appendix

Thin section: 37597 (E10)

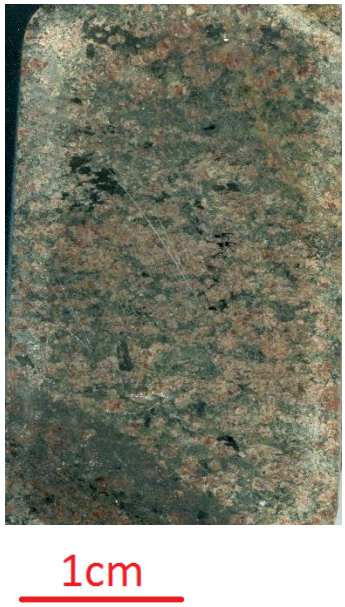

Thin section: 37598 (E11)

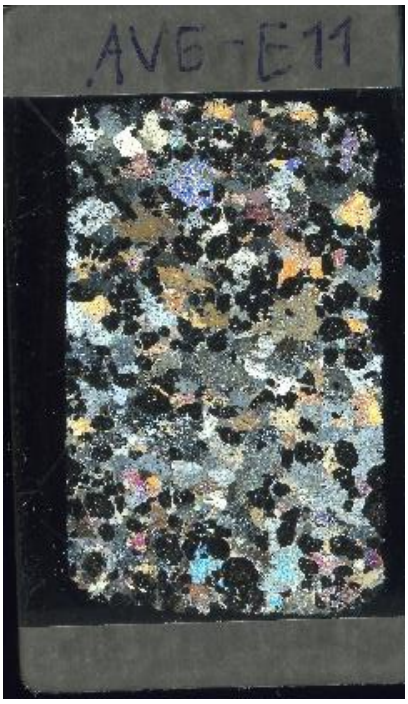

Appendix

Thin section: 37591 (G2)

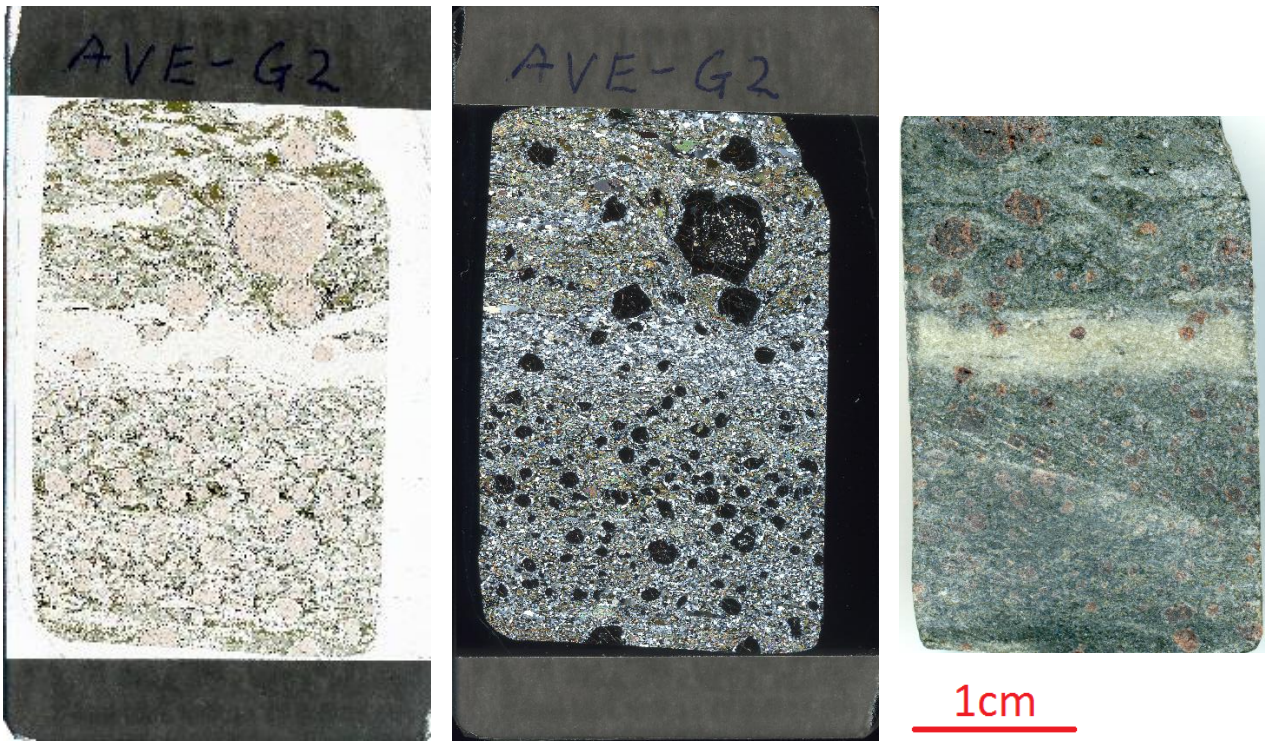

Thin section: 37591 (G3)

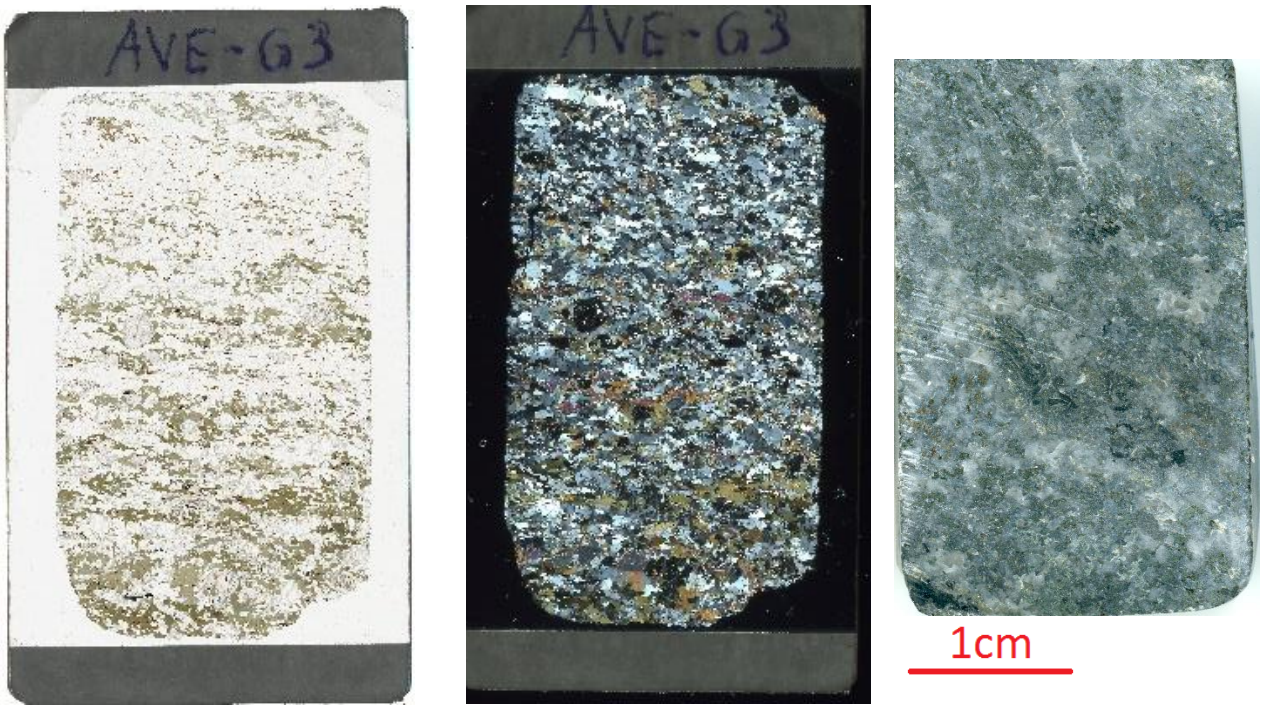

Appendix

Thin section: 37591 (G4)

Thin section: 37601 (G5)

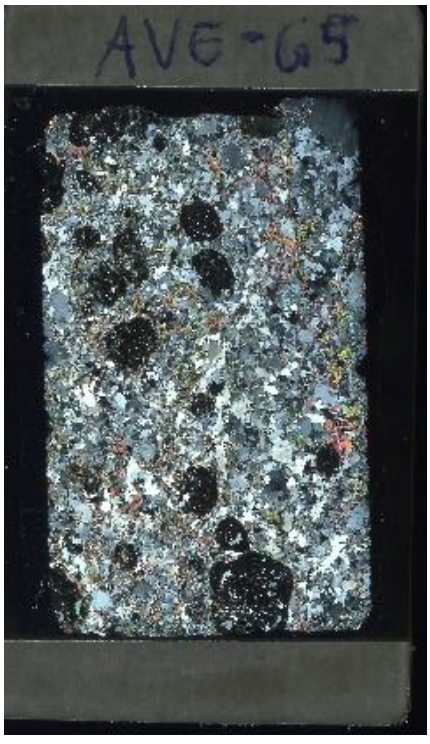

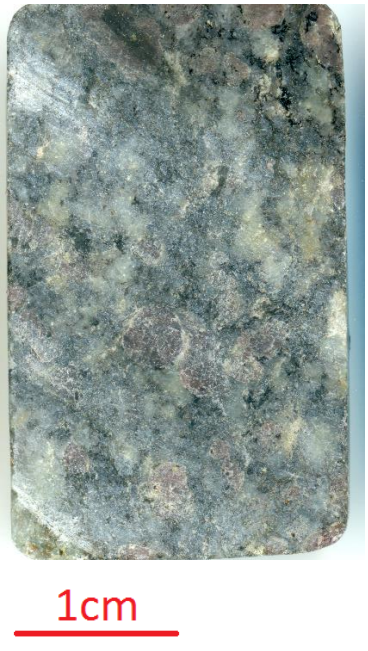

Appendix

Thin section: 37602 (G6)

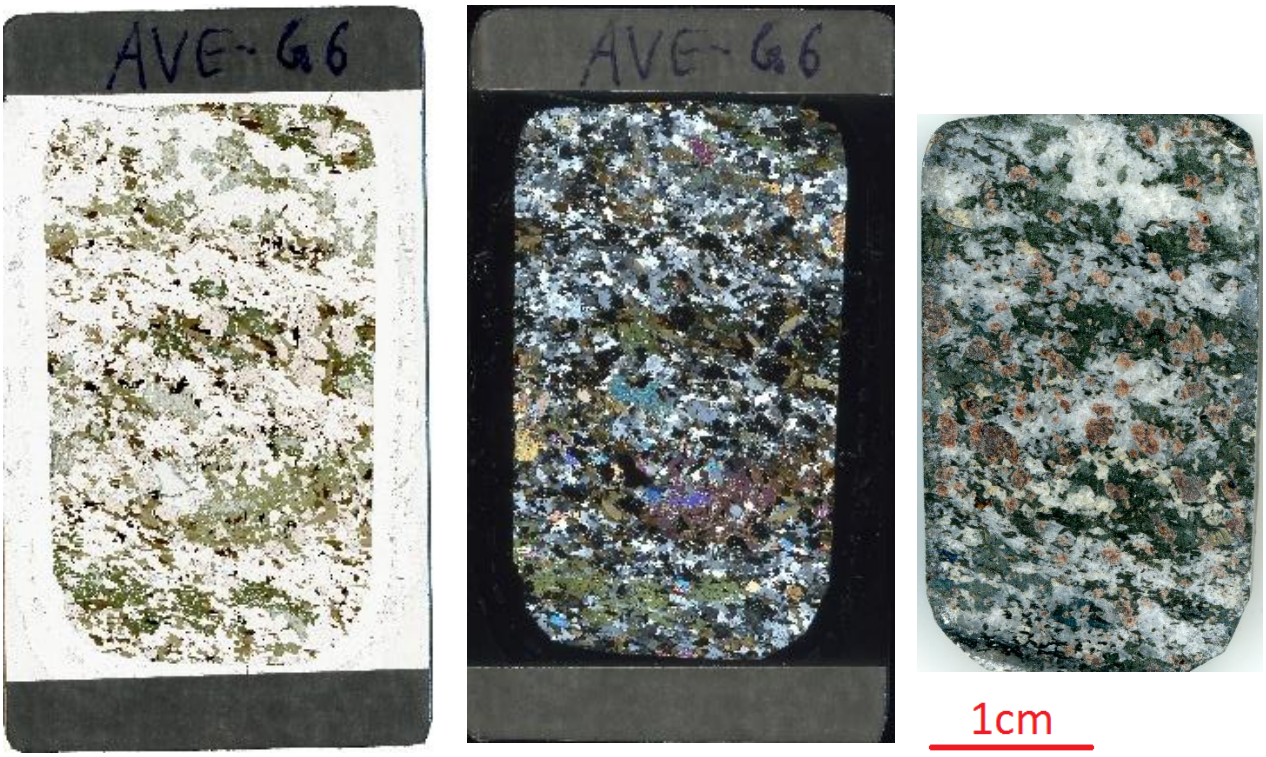

Thin section: 37554 (G1)

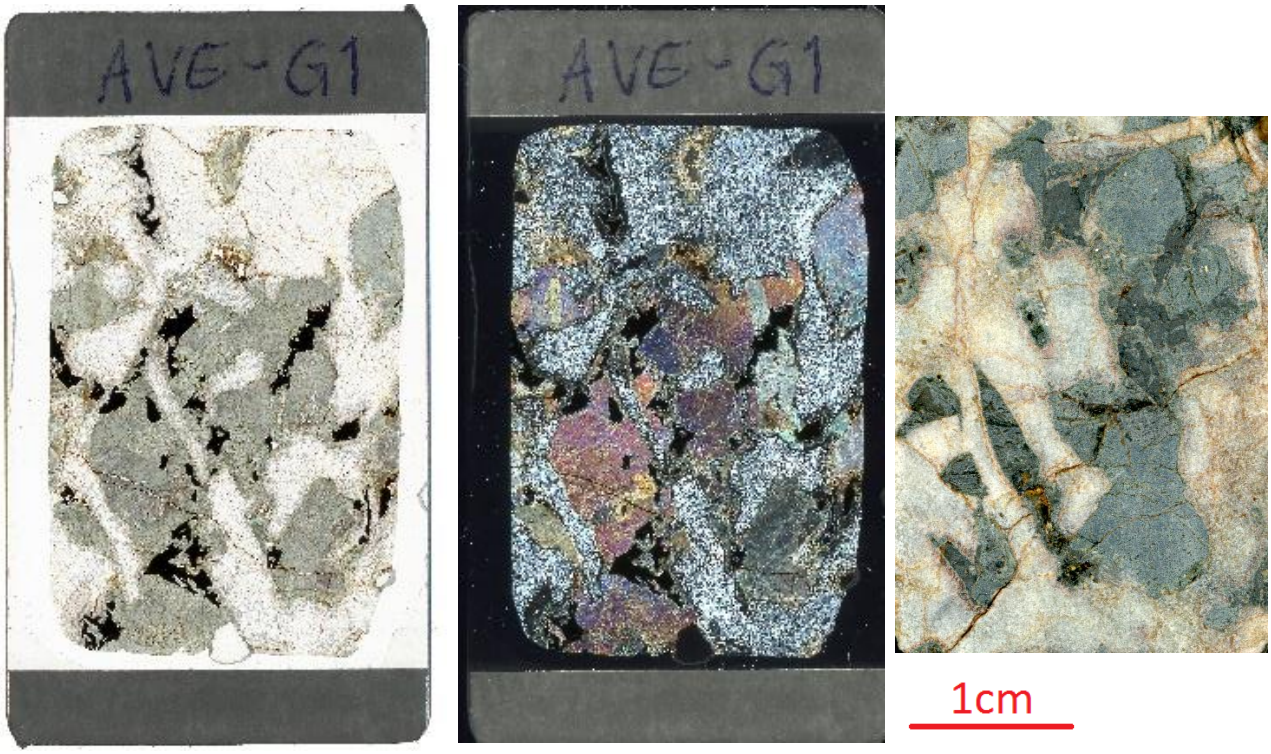

Appendix

Thin section: 37553 (M1)

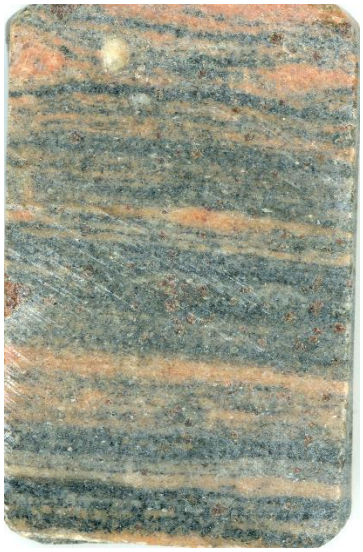

Thin section: 37561 (Q1)

Appendix

Thin section: 37597

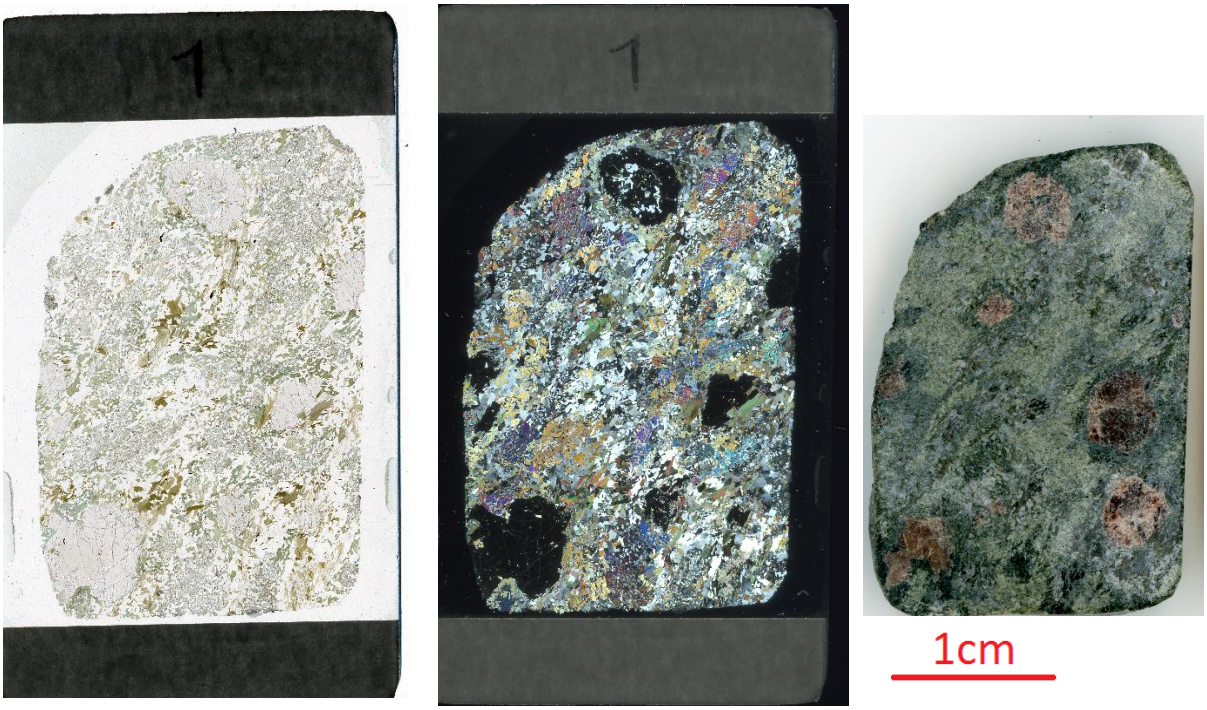

Thin section: 37698

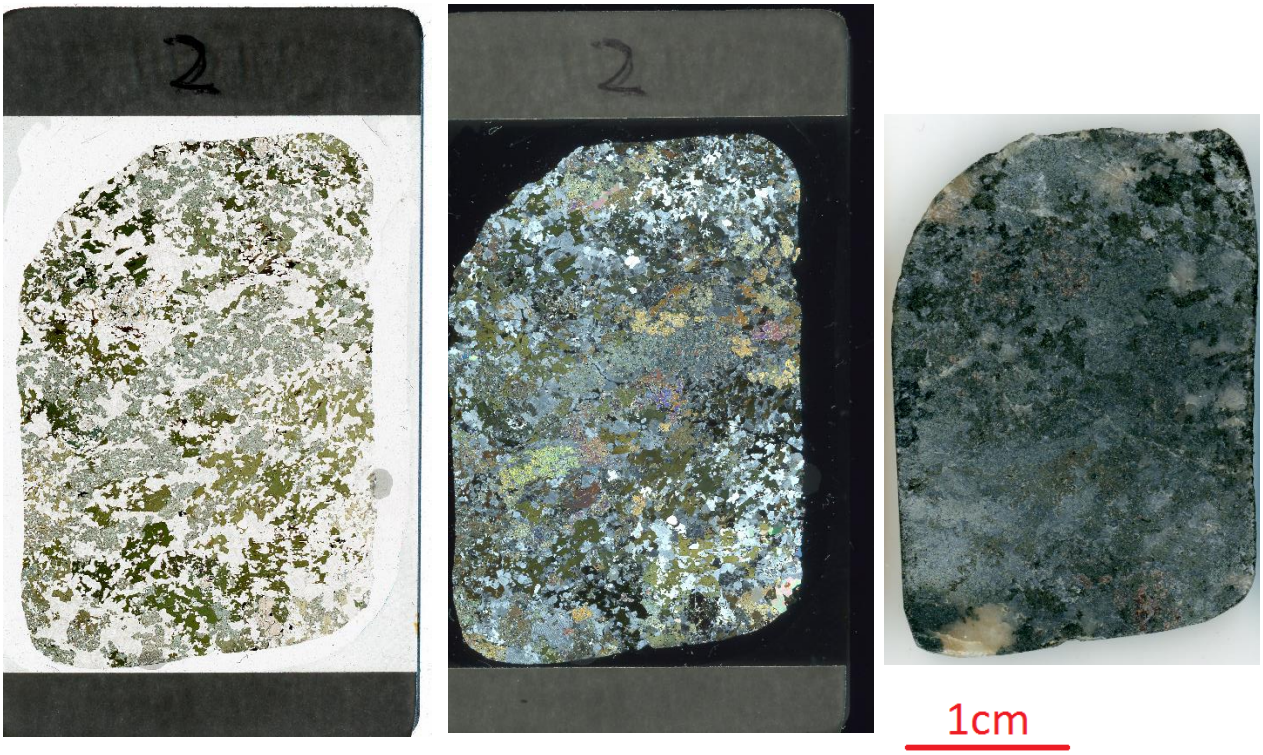

Appendix

Thin section: 37699

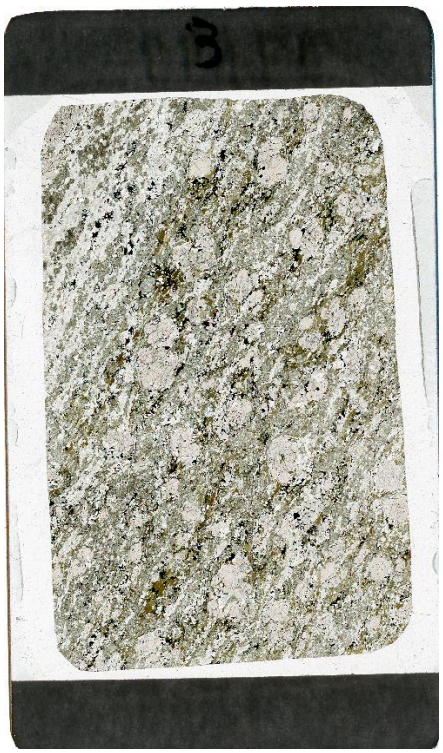

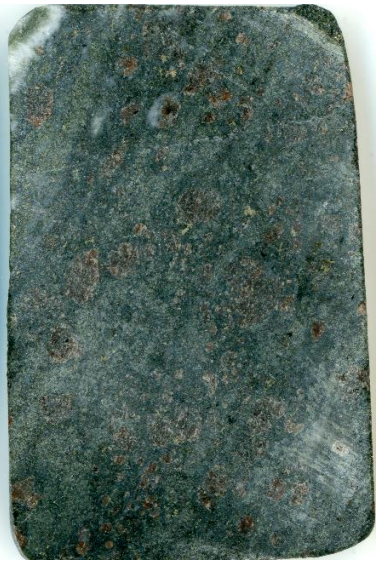

1cm

~~Thin section: 37700~~

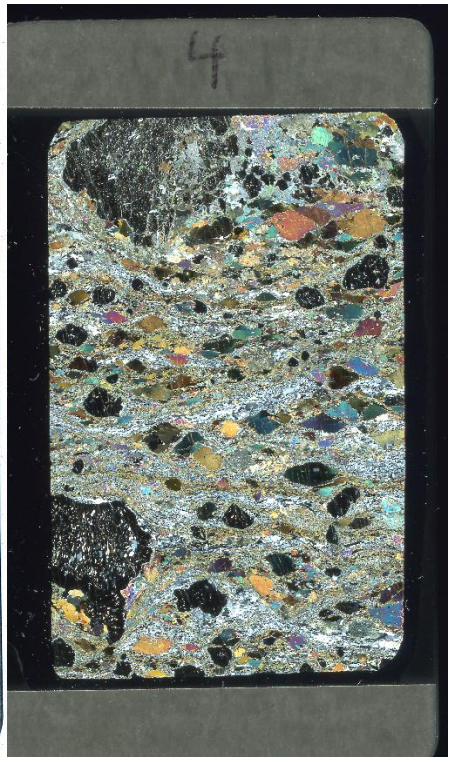

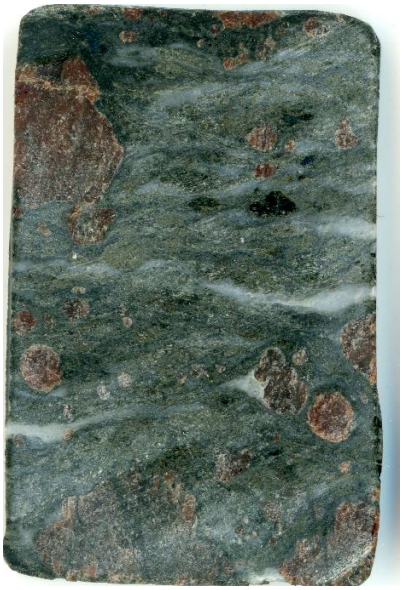

Appendix

Appendix C

	B1.7 epidote	B1.11 quartz	B1.3.5 kyanite	G6.5.10 scapolite	B7.2.6 rutile	G5.1.2 biotite	G5.2.4 phengite	G5.3.8 ox	G5.4.1 apatite	E11.1.3 corundum	E11.1.4 kyanite	E11.1.8 sphene	E4.4.7 Zircon	G1.6.6 biotite
SiO2	37.521	99.995	37.973	42.139	0	37.264	49.382	0.123	0.06	6.559	36.749	2.043	34.213	36.725
Na2O	0	0.036	0.013	1.329	0.012	0.119	0.067	0	0.015	0.856	0.029	0.217	0.027	0.075
SO3	0.025	0.039	0.057	0.075	0	0.036	0.014	0	0.007	0.001	0	0.005	0	0.006
V2O3	0.034	0	0.005	0.075	1.019	0.06	0.097	0.031	0.041	0.034	0.002	0.015	0	0.054
F	0	0.036	0	0	0	0	0.003	0	3.249	0	0	0.015	0	0
Cl	0	0	0	0	0	0.03	0.02	0	41.812	0	0.005	0.03	0	0.01
Cr2O3	0.598	0	0.242	0	0.511	0.001	0.052	0	0.003	0.182	0.164	0.338	0	0
MgO	1.12	0.147	0	10.588	0.029	17.539	1.513	0	0.108	0	0	16.907	0.193	15.978
P2O5	0.192	0.016	0	0.01	0.012	10.253	8.914	0	0.032	0	0.031	0	0.009	9.82
MnO	0	0	0	0.202	0.013	0.04	0.037	0.034	0.02	0.019	0.01	0.079	0	0.053
Al2O3	27.385	0.134	62.573	12.606	0	17.297	30.141	0.167	0.184	91.852	60.341	63.092	0.219	15.371
K2O	0	0.033	0.028	1.602	0.022	0	0	0	54.866	0.485	0	0.229	0.201	0
FeO	3.483	0.131	0.353	17.849	0.045	13.078	1.543	83.15	0.706	0.305	0.284	17.609	0.851	16.039
CaO	20.869	0.113	0	11.253	97.228	1.01	1.458	0	0	0	0	0.003	0.008	2.19
TiO2	0.112	0.003	0.017	1.544	0.708	0.089	0.091	0	0.031	0	0	0	0.169	0.422
BaO	0.011	0	0.118	0.044	0	0	0		0	0	0	0	0	0.038
Total	91.35	100.668	101.379	99.316	99.599	96.808	93.328	83.923	99.764	100.293	97.615	100.575	98.661	96.78

Raw data for chemical analyses of accessory minerals

Appendix

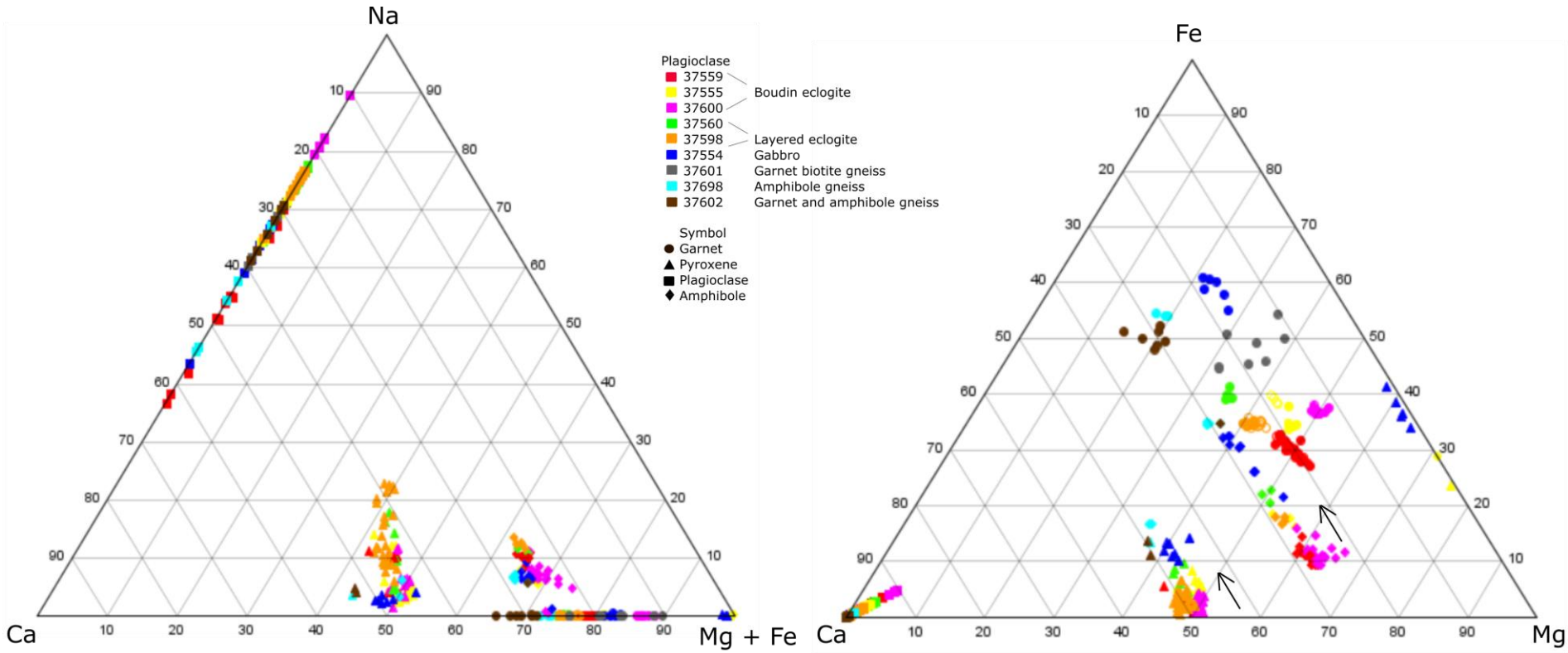

NCFMASH projections, showing first Na – Ca – Mg + Fe and thereafter Fe – Mg – Ca. The main minerals garnet, pyroxene, plagioclase and amphibole have been plotted as kations.